

PROBING HIGH SCALE PHYSICS WITH TOP QUARKS AT THE LARGE HADRON COLLIDER

By

Zhe Dong

A DISSERTATION SUBMITTED IN PARTIAL FULFILLMENT OF THE
REQUIREMENTS FOR THE DEGREE OF

DOCTOR OF PHILOSOPHY

(PHYSICS)

at the

UNIVERSITY OF WISCONSIN – MADISON

2012

Date of final oral examination: 04/25/12

The dissertation is approved by the following members of the Final Oral Committee:

Tao Han, Professor, Physics (Thesis Adviser)

Vernon D. Barger, Professor, Physics

Lisa L. Everett, Associate Professor, Physics

Yibin Pan, Associate Professor, Physics

Tonghai Yang, Professor, Mathematics

Acknowledgements

First of all, I would like to thank my advisor, Professor Tao Han, for his support and invaluable guidance upon my study, life and career decisions throughout my graduate years. His extensive knowledge and experience were crucial to the progress in my research. I am deeply indebted to him.

I would like to thank Prof. Gary Shiu and Prof. Fabio Maltoni for their guidances and collaborations. Their insights and experience were pivotal to the success of my research.

I am grateful to Prof. Vernon D. Barger, Prof. Michael Ramsey-Musolf, Dr. Pavel Fileviez Perez, Dr. Min-xin Huang, Dr. Ian Lewis, Dr. Gui-yu Huang, Dr. Ying-chuan Li, who have been always available for help and sharing their lucid valuable knowledge. Many thanks also go to Linda Dolan, without whom the days in Madison and Pheno Institute won't be so easy and comfortable. Also, thanks to Profs. Lisa L. Everett, Yinbin Pan, Tonghai Yang, who cordially join my thesis defense committee.

I also want to give special thanks to Prof. Alberto Sirlin, who guided me into the field and let me know "a master only masters the knowledge, and only the Master masters the method." Warmly grateful to Prof. Thomas J. Weiler, who has been a good friend and the person I feel greatly indebted.

Finally, I wish to thank my mother, Huijun, my father, Diansheng, grand parents Zhizhou and Meirong, my brother Qian for their love and supports that I have been replying upon.

Contents

Acknowledgements	i
Contents	ii
List of Figures	iv
List of Tables	vii
Abstract	viii
1 Introduction to Standard Model	1
1.1 Electroweak Gauge Theory	2
1.2 Spontaneous Symmetry Breaking	5
1.3 Quantum Chromodynamics	11
2 Beyond the Standard Model	14
2.1 The Problems with the Standard Model	14
2.2 The Minimal Supersymmetric Standard Model	16
2.2.1 Motivation of Supersymmetry	16
2.2.2 Formalism of Supersymmetry	18
2.2.3 The Minimal Supersymmetric Standard Model	22
2.3 Minimal SU(5) Grand Unification	42
2.4 Top Quarks as a Window to High Scale Physics	46

3	String Resonance in $t\bar{t}$ Channel at the LHC	48
3.1	$t\bar{t}$ Production via a String Resonance	52
3.1.1	$n = 1$ Resonances	52
3.1.2	$n = 2$ Resonances	54
3.2	$t\bar{t}$ Final State And String Resonances at the LHC	60
3.2.1	Invariant Mass Distribution of $t\bar{t}$ Events	62
3.2.2	Angular Distribution of $t\bar{t}$ Events	64
3.3	$t\bar{t}g$ Final State And String Resonances at the LHC	66
3.4	Higher String Scale signal	68
3.5	Discussions and Conclusion	69
4	Baryon Number Violating Processes with Top Quarks	72
4.1	Effective operators	73
4.2	Processes	75
4.3	LHC searches	79
4.4	Indirect constraints	82
5	Summary	84
A	Physical Degrees of Freedom Counting for $n = 1$ Resonance	86
B	Complete set of independent operators	90
	Bibliography	94

List of Figures

1	The Higgs potential $V(\phi)$ for $\mu^2 > 0$ (dashed line) and $\mu^2 < 0$ (solid line).	7
2	One loop diagrams contributing to the Higgs squared mass μ^2 , from (a) a Dirac fermion f loop, and (b) a scalar S loop. Adapted from [20]	18
3	Cancellation of anomaly by two higgsinos in the Minimal Supersymmetric Standard Model	24
4	Proton decay $p \rightarrow e^+ \pi^0$ mediated by a sstrange or a sbottom. Adapted from [20]	32
5	$\mu \rightarrow e \gamma$ with contribution from soft supersymmetric breaking terms. Adapted from [20]	38
6	$K - \bar{K}$ mixing with contribution from soft supersymmetric breaking terms.	38
7	Renormalization group evolution of $\alpha_i^{-1}(Q)$, with dashed lines for the Standard Model and solid lines for the MSSM	45
8	The normalized angular distribution of $gg \rightarrow t\bar{t}$ via the exchange of a string resonance for (a) $n = 1$ (top), and (b) $n = 2$ (bottom).	53
9	Total cross section for a string resonance production at the LHC versus it mass scale M_s for (a) $n = 1$ and (b) $n = 2$ (mass $1.4M_s$). Solid curves represent $gg \rightarrow t\bar{t}$. Dashed curves include the top quark decay branching fractions for the semi-leptonic mode $t\bar{t} \rightarrow b\ell\nu, bj j'$.	61

10	Invariant mass distribution of $t\bar{t}$ at the LHC (a) with the c.m. energy 14 TeV, (b) with the c.m. energy 7 TeV. Decay branching fractions with one hadronically and the other leptonically have been included. All channels (All), in the figure, include both string resonance signal (SR) and Standard Model background (SM). The distributions of $J = 2$ and $J = 3$ states are shown for $n = 2$ resonance, respectively.	63
11	Normalized angular distribution of $t\bar{t}$ at the LHC via the string resonance exchange in the peak region $900 - 1100$ GeV for $n = 1$, and in the region $1350 - 1450$ GeV for $n = 2$	64
12	Invariant mass distributions in the $g + g \rightarrow n = 2$ resonance $\rightarrow n = 1$ resonance + $g \rightarrow t\bar{t} + g$ channel. Upper two graphs: $t\bar{t}$ invariant mass signal and the Standard Model background. Lower two graphs: $t\bar{t} + g$ invariant mass signal and the Standard Model background. The summed signal, in the figure, includes the contributions from both $J = 2$ and $J = 3$ resonances.	67
13	(a) The distribution of the minimum separation between any two jets from $t(\bar{t})$ decay ΔR_{jj} . (b) $\Delta R_{jj}^{\text{cut}}$ Efficiency: Peak region cross section percentage versus $\Delta R_{jj}^{\text{cut}}$ of $t\bar{t}$ semi-leptonic decay at the LHC. The energy labels in the legends stand for the resonance masses.	69
14	Energy spectrum of the charged lepton in the SM $t \rightarrow bE^+\nu_E$ (blue curve) and in BNV $t \rightarrow \bar{U} \bar{D} E^+$ top decays.	77

15	Transverse momentum for the charged lepton in the BNV production signal $\bar{t}\mu^+$ (from ud initial state) and in the W^+ +3-jet and $\bar{t}W^+$ backgrounds. Top quarks are decayed hadronically. Selection cuts on the three jets and the muon are given in the text.	81
16	Representative (a) tree-level and (b) two-loop-level diagrams involving the BNV operators given in Eq. (4.2) and leading, in principle, to nucleon decay.	83

List of Tables

1	Weak Quantum Numbers for Fermion Fields	3
2	Chiral supermultiplets of the Minimal Supersymmetric Standard Model.	23
3	Vector supermultiplets of the Minimal Supersymmetric Standard Model.	25
4	The decay widths of $n = 2$ string resonances. All quantities are to be multiplied by the factor $\frac{g^2}{4\pi}M_s$. For the Standard Model, $N = 3$, $N_f = 6$.	58
5	Basic acceptance cuts for $t\bar{t}$ events at the LHC.	62
6	Cross sections (fb) for representative BNV production processes at the LHC, with three different choices of A, B and C , $\sqrt{\hat{s}} < \Lambda = 1$ TeV, $\sqrt{s} = 7$ TeV (14 TeV in parentheses) and CTEQ6L1 PDF [108] (renormalization and factorization scales set at $m_t = 173$ GeV).	79

Abstract

Probing High Scale Physics with Top Quarks at the Large Hadron Collider

Zhe Dong

Under the supervision of Professor Tao Han

With the Large Hadron Collider (LHC) running at TeV scale, we are expecting to find the deviations from the Standard Model in the experiments, and understanding what is the origin of these deviations. Being the heaviest elementary particle observed so far in the experiments with the mass at the electroweak scale, top quark is a powerful probe for new phenomena of high scale physics at the LHC. Therefore, we concentrate on studying the high scale physics phenomena with top quark pair production or decay at the LHC. In this thesis, we study the discovery potential of string resonances decaying to $t\bar{t}$ final state, and examine the possibility of observing baryon-number-violating top-quark production or decay, at the LHC. We point out that string resonances for a string scale below 4 TeV can be detected via the $t\bar{t}$ channel, by reconstructing center-of-mass frame kinematics of the resonances from either the $t\bar{t}$ semi-leptonic decay or recent techniques of identifying highly boosted tops. For the study of baryon-number-violating processes, by a model independent effective approach and focusing on operators with minimal mass-dimension, we find that corresponding effective coefficients could be directly probed at the LHC already with an integrated luminosity of 1 fb^{-1} at 7 TeV, and further constrained with 30 (100) fb^{-1} at 7 (14) TeV.

Chapter 1

Introduction to Standard Model

The Standard Model, which describes the electromagnetic, weak and strong interactions, constitutes one of the most fabulous achievements in the history of particle physics.

Experiments have found all but one of its ingredient particles and confirmed the theory in all directions to a high degree of precision. At CERN, the W^\pm and Z gauge bosons was discovered by UA1 [1] and UA2 Collaborations in 1983 [2]; at Fermilab, the top quark was discovered by CDF [3] and D0 [4] in 1995, and the ν_τ neutrino was discovered by DONUT [5] in 2000. Only the Higgs boson, which is predicted by Standard Model, is still beyond the grasp of experimentalists.

The Standard Model, as a relativistic, renormalizable local quantum field theory, is built on three principles:

- The gauge group is $SU(3)_C \times SU(2)_L \times U(1)_Y$,
- Fermion representations are left-handed doublets and right-handed singlets,
- There is one Higgs doublet, which introduces masses to fermions elegantly without spoiling renormalizability,

together with 21 *a priori* free parameters, which are inserted by hand, including 3 coupling constants, 12 fermion masses, 4 fermion mixing parameters, 1 Higgs mass and 1 independent gauge boson mass.

1.1 Electroweak Gauge Theory

The Standard Model of electroweak interactions [6] is built on the gauge group $SU(2)_L \times U(1)_Y$.

An $SU(2)$ gauge symmetry is applied to left-handed fermion field ψ_L only, where the fermion fields are given by

$$\psi_L = \frac{1}{2}(1 - \gamma_5)\psi, \quad \psi_R = \frac{1}{2}(1 + \gamma_5)\psi. \quad (1.1)$$

The conserved quantum number is *weak isospin* \mathbf{T}_L . An independent $U(1)$ gauge group, whose conserved quantum number is *hypercharge* Y , is introduced to incorporate the electric charge Q and is essential in unifying the weak and electromagnetic interactions in a common gauge structure. The value of the hypercharge Y have been adjusted to satisfy the Gell-Mann-Nishijima formula,

$$Q = T_3 + \frac{Y}{2}. \quad (1.2)$$

Left-handed fermions transform non-trivially under $SU(2)_L \times U(1)_1$, and right-handed fermions are assigned to be $SU(2)$ singlets and transform under $U(1)_Y$ only. Table 1 summarizes the weak quantum numbers for fermion fields.

Remarkably, these hypercharge values satisfy the anomaly conditions, that is the one fermion loop diagrams with three external gauge bosons of the form $U(1)U(1)U(1)$, $U(1)SU(2)SU(2)$, $U(1)SU(2)SU(3)$, all vanish. In addition, the sum of all fermion hypercharges vanishes as well, so that to cancel the mixed gravitational anomaly [7].

The Lagrangian describing the electroweak interactions is

$$\mathcal{L}_{EW} = \mathcal{L}_{gauge} + \mathcal{L}_f, \quad (1.3)$$

	T_3	$Y/2$	Q
ν_{eL}	$\frac{1}{2}$	$-\frac{1}{2}$	0
e_L	$\frac{-1}{2}$	$-\frac{1}{2}$	-1
u_L	$\frac{1}{2}$	$\frac{1}{6}$	$\frac{2}{3}$
d_L	$-\frac{1}{2}$	$\frac{1}{6}$	$-\frac{1}{3}$
e_R	0	-1	-1
u_R	0	$\frac{2}{3}$	$\frac{2}{3}$
d_R	0	$-\frac{1}{3}$	$-\frac{1}{3}$

Table 1: Weak Quantum Numbers for Fermion Fields

where the gauge interaction part is

$$\mathcal{L}_{gauge} = -\frac{1}{4}W_{\mu\nu}^i W^{\mu\nu i} - \frac{1}{4}B_{\mu\nu}B^{\mu\nu}, \quad (1.4)$$

where isotriplet W_μ^i , $i = 1, 2, 3$ and singlet B_μ are the SU(2) and U(1) gauge fields respectively, with field strength tensors

$$B_{\mu\nu} = \partial_\mu B_\nu - \partial_\nu B_\mu, \quad (1.5)$$

$$W_{\mu\nu}^i = \partial_\mu W_\nu^i - \partial_\nu W_\mu^i - g\epsilon_{ijk}W_\mu^j W_\nu^k.$$

The covariant derivative is

$$D_\mu = \partial_\mu + igT_i W_\mu^i + ig'\frac{Y}{2}B_\mu, \quad (1.6)$$

with $g(g')$ being the SU(2)_L (U(1)_Y) coupling. The fermion kinetic terms is

$$\mathcal{L}_f = i\bar{\psi}_j \gamma^\mu D_\mu \psi_j. \quad (1.7)$$

Under the local gauge transformation, these fields transform as:

$$\begin{aligned}
& \text{SU}(2)_L & \text{U}(1)_Y \\
& \psi_L \rightarrow [1 - igT_i\alpha^i(x)]\psi_L & \psi_L \rightarrow [1 - ig'\frac{1}{2}Y\beta(x)]\psi_L \\
& \psi_R \rightarrow \psi_R & \psi_R \rightarrow [1 - ig'\frac{1}{2}Y\beta(x)]\psi_R \\
& W_\mu^i \rightarrow W_\mu^i + \partial_\mu\alpha^i(x) + g\epsilon_{ijk}\alpha(x)^jW_\mu^k & W_\mu^i \rightarrow W_\mu^i \\
& B_\mu \rightarrow B_\mu & B_\mu \rightarrow B_\mu + \partial_\mu\beta(x)
\end{aligned} \tag{1.8}$$

This Lagrangian defined above is invariant under the infinitesimal local gauge transformations for $\text{SU}(2)_L$ and $\text{U}(1)_Y$ independently.

The weak isospin operators \mathbf{T}_L obey the commutation relation $[T_a, T_b] = i\epsilon_{abc}T_c$ and can be represented in terms of the Pauli matrices by $T_a = \tau_a/2$.

In the adjoint representation, the $\text{SU}(2)_L$ massless gauge fields form a weak isospin triplet with the charged fields being defined by $W_\mu^\pm = (W_1 \mp iW_2)_\mu/\sqrt{2}$, and the isospin raising and lowering operators are of the form $T_L^\pm = (T_{L1} \pm iT_{L2})/\sqrt{2}$. The neutral component of \mathbf{W} mixes with the abelian gauge field B_μ to form the physical states

$$\begin{aligned}
Z_\mu &= W_\mu^3 \cos \theta_w + B_\mu \sin \theta_w, \\
A_\mu &= B_\mu \cos \theta_w - W_\mu^3 \sin \theta_w,
\end{aligned} \tag{1.9}$$

where θ_w is the weak mixing angle, or rather Weinberg angle, which is related with the $\text{SU}(2)_L$, $\text{U}(1)_Y$ coupling strengths by $\tan \theta_w = g'/g$.

In order to obtain Quantum Electrodynamics (QED) the massless A_μ is identified

with the photon and $e \equiv g \sin \theta_w$. The QED, weak charged and neutral currents become:

$$\begin{aligned} J_\mu^{em} &= \bar{\psi} \gamma_\mu Q \psi, \\ J_\mu^{CC} &= \bar{\psi} \gamma_\mu T_L^\pm \psi, \\ J_\mu^{NC} &= \bar{\psi} (T_{3L} - x_w Q) \psi, \end{aligned} \tag{1.10}$$

with the interaction of gauge bosons with any fermion field ψ arising from $i\bar{\psi}\gamma^\mu D_\mu\psi$ being

$$\mathcal{L} = -e J_\mu^{em} A^\mu - \frac{g}{\sqrt{2}} J_\mu^{CC} W^\mu - g_Z J_\mu^{NC} Z^\mu. \tag{1.11}$$

Here, $x_w \equiv \sin^2 \theta_w$, $g_Z \equiv g/\cos \theta_w$ and the T_L^\pm act only on the left-handed isodoublets ψ_L , and vanish on ψ_R .

At this stage, all fields are massless, and all gauge couplings respect chirality, *i.e.* left and right-handed fermions evolve separately. There remains to generate the masses for fermions, and rewrite the currents in terms of mass (flavor) eigenstates rather than weak eigenstates, as showed above. Also, massless gauge bosons are not acceptable for the weak interactions, which are known to be short-ranged. Masses can be introduced elegantly without spoiling renormalizability [8] by spontaneous symmetry breaking [9]. The idea is that the lowest energy (vacuum) state does not respect the gauge symmetry and induces effective masses for particles propagating through it [10].

1.2 Spontaneous Symmetry Breaking

The gauge invariance, and therefore renormalizability, forbids any mass terms for gauge bosons and for chiral fermions. A neat solution is that masses for the non-abelian gauge

fields and fermions are generated by the Higgs Mechanism [9] via spontaneous symmetry breaking (SSB) which preserves the renormalizability [8] of the gauge theory.

In the Standard Model, an $SU(2)$ iso-doublet spin zero field with $U(1)$ charge $Y_\phi/2 = 1/2$ is introduced:

$$\Phi = \begin{pmatrix} \phi^+ \\ \phi^0 \end{pmatrix}, \quad (1.12)$$

where ϕ^+ and ϕ^0 are complex scale fields.

The Lagrangian is augmented by a potential

$$\mathcal{L}_\Phi = (D_\mu \Phi)^\dagger D^\mu \Phi - V(\Phi), \quad (1.13)$$

wherein the first term gives masses to gauge bosons after the SSB, with latter term being scalar potential to generate the SSB. The combination of $SU(2)_L \times U(1)_Y$ invariance and renormalizability restricts $V(\Phi)$ to the form [11]

$$V(\Phi) = \mu^2 \Phi^\dagger \Phi + \lambda (\Phi^\dagger \Phi)^2. \quad (1.14)$$

The complex Higgs doublet can also be rewritten in a Hermitian basis as

$$\Phi = \begin{pmatrix} \phi^+ \\ \phi^0 \end{pmatrix} = \frac{1}{\sqrt{2}} \begin{pmatrix} \phi_1 - i\phi_2 \\ \phi_3 - i\phi_4 \end{pmatrix}, \quad (1.15)$$

where $\phi_i = \phi_i^\dagger$ are four Hermitian fields. The scalar potential, under this basis, becomes,

$$V(\Phi) = \frac{1}{2} \mu^2 \left(\sum_{i=1}^4 \phi_i^2 \right) + \frac{1}{4} \lambda \left(\sum_{i=1}^4 \phi_i^2 \right)^2, \quad (1.16)$$

which is invariant under $O(4)$. Without loss of generality we can choose the axis so that the only component with non-zero vacuum expectation value (vev) is $\langle 0 | \phi_3 | 0 \rangle = \nu$.

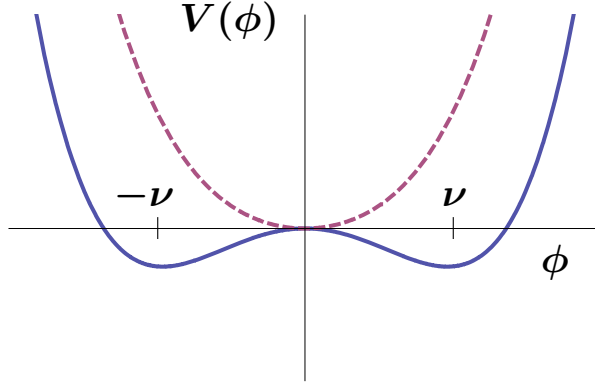


Figure 1: The Higgs potential $V(\phi)$ for $\mu^2 > 0$ (dashed line) and $\mu^2 < 0$ (solid line).

Thus,

$$\langle 0|\Phi|0\rangle = \frac{1}{\sqrt{2}} \begin{pmatrix} 0 \\ v \end{pmatrix}, \quad V(\phi) \rightarrow V(v) = \frac{1}{2}\mu^2 v^2 + \frac{1}{4}\lambda v^4. \quad (1.17)$$

With $\mu^2 > 0$, the minimum of $V(v)$ is at $v = 0$. $SU(2) \times U(1)$ is unbroken at the minimum. With $\mu^2 < 0$, the $v = 0$ point is unstable, and the minimum occurs at $v = (-\mu^2/\lambda)^{1/2}$ as illustrated in Fig. 1. The non-vanishing vev selects a preferred direction in $SU(2)_L \times U(1)_Y$ space and $SU(2)_L \times U(1)_Y$ group is spontaneously broken to the $U(1)_{em}$ subgroup.

To quantize the Higgs field around the classical vacuum, one can introduce the Kibble parametrization [12]:

$$\Phi(x) = \exp\left(\frac{i\xi \cdot \tau}{2v}\right) \begin{pmatrix} 0 \\ (v + H(x))/\sqrt{2} \end{pmatrix}, \quad (1.18)$$

where $H(x)$ is a Hermitian field with no vev, and turns out to be the physical Higgs field. ξ_i ($i = 1, 2, 3$) are the three massless pseudoscalar Nambu-Goldstone bosons [13]

generated by the spontaneous symmetry breaking, and the phase factor could be removed by an $SU(2)_L$ gauge transformation, as in *unitary* gauge:

$$\Phi(x) = \frac{1}{\sqrt{2}} \begin{pmatrix} 0 \\ (v + H(x))/\sqrt{2} \end{pmatrix}. \quad (1.19)$$

In this gauge, the Nambu-Goldstone bosons are eaten by the gauge field into the longitudinal modes of the massive gauge bosons corresponding to the broken symmetry, W^\pm and Z .

Covariant derivative on iso-doublet scalar field takes simple form in unitary gauge:

$$D_\mu \Phi = \frac{1}{\sqrt{2}} \begin{pmatrix} \frac{i}{\sqrt{2}} g W_\mu^+ (v + H) \\ \partial_\mu H - \frac{i}{\sqrt{2}} g_Z Z_\mu (v + H) \end{pmatrix}. \quad (1.20)$$

Then the Higgs potential becomes:

$$\begin{aligned} \mathcal{L}_\Phi &= \frac{1}{4} g^2 W^{+\mu} W_\mu^- (v + H)^2 + \frac{1}{8} g_Z^2 Z^\mu Z_\mu (v + H)^2 + \frac{1}{2} (\partial_\mu H)^2 - V(\Phi) \\ &= M_W^2 W^{+\mu} W_\mu^- \left(1 + \frac{H}{v}\right)^2 + \frac{1}{2} M_Z^2 Z^\mu Z_\mu \left(1 + \frac{H}{v}\right)^2 + \frac{1}{2} (\partial_\mu H)^2 - V(\Phi), \end{aligned} \quad (1.21)$$

which provides the W and Z boson masses

$$M_W = \frac{gv}{2}, \quad M_Z = \frac{g_Z v}{2} = \frac{M_W}{\cos \theta_w},$$

and leaves photon massless.

The scalar potential in unitary gauge takes the form:

$$V(\Phi) = -\frac{1}{2} (-2\mu)^2 H^2 + \frac{1}{4} \mu^2 v^2 \left[-1 + 4 \frac{H^3}{v^3} + \frac{H^4}{v^4} \right]. \quad (1.22)$$

The first term shows that a physical Higgs boson has a tree-level mass

$$M_H = \sqrt{-2\mu^2}, \quad (1.23)$$

and the second term is a constant $-\mu^2 v^2/4$, reflecting the fact $V < 0$ at the minimum. The third and fourth terms introduce cubic and quartic interaction of Higgs scalar. Such a constant term seems has no significance for micro-scopic physics in absence of gravity, but since cosmological constant could be viewed as the vacuum energy, it is of great importance when the theory includes gravity as an ingredient, and will give an opposite sign and much bigger cosmological constant than the observed one. This intimates a sign for new physics beyond standard model.

After SSB, the fermion masses are generated by the Yukawa coupling between the Higgs double and the fermions. The Yukawa interaction Lagrangian can be expressed as

$$\mathcal{L}_{Yuk} = -\lambda_{e_k} \bar{L}_{L_k} \Phi e_{R_k} - \lambda_{u_{jk}} \bar{Q}_{L_j} \tilde{\Phi} u_{R_k} - \lambda_{d_{jk}} \bar{Q}_{L_j} \Phi d_{R_k} + h.c., \quad (1.24)$$

where the $SU(2)_L$ left-handed doublets for leptons and quarks are written as

$$L_{L_k} = \frac{1}{2}(1 - \gamma_5) \begin{pmatrix} \nu_k \\ e_k \end{pmatrix}, \quad Q_{L_k} = \frac{1}{2}(1 - \gamma_5) \begin{pmatrix} u_k \\ d_k \end{pmatrix}, \quad (1.25)$$

and the right-handed singlets for lepton, and up-type and down-type quarks as

$$e_{R_k} = \frac{1}{2}(1 + \gamma_5)e, \quad u_{R_k} = \frac{1}{2}(1 + \gamma_5)u, \quad d_{R_k} = \frac{1}{2}(1 + \gamma_5)d, \quad (1.26)$$

with $k = 1, 2, 3$ as the generation index. One needs Higgs field with $y = +1/2$ to give masses to the down-type quarks and leptons, and $y = -1/2$ to the up-type quarks. Φ^\dagger has $y = -1/2$, but transforms as $\mathbf{2}^*$ in $SU(2)$ rather than $\mathbf{2}$. So one has to introduce "tilde trick" by relating the $\mathbf{2}^*$ representation with $\mathbf{2}$ by a similarity transform,

$$\tilde{\Phi} = i\tau^2 \Phi^\dagger = \begin{pmatrix} \phi^{0\dagger} \\ -\phi^- \end{pmatrix}, \quad (1.27)$$

which transforms as **2** and is of $y = -1/2$.

For simplicity, we will only discuss the Yukawa interaction related up-type quark, and one can generalize it for the other fermions. Under the unitary gauge, the Yukawa interaction becomes

$$\begin{aligned}\mathcal{L}_{Yuk} &= - \sum_{i,j=1}^3 \lambda_{ij}^u \bar{u}_{iL}^0 u_{jR}^0 \left(\frac{v+H}{2} \right) + h.c. , \\ &= \bar{\mathbf{u}}_L^0 \mathbf{M}^u \mathbf{u}_R^0 \left(1 + \frac{H}{v} \right) .\end{aligned}\tag{1.28}$$

The subscript 0 stands for the field being in weak eigenstates, and \mathbf{M}^u is a 3×3 fermion mass matrix,

$$\mathbf{M}^u = \frac{\boldsymbol{\lambda}^u v}{\sqrt{2}} ,\tag{1.29}$$

which is induced by SSB. The second term specifies the fermion-fermion-Higgs Yukawa coupling, while the first term gives the masses to fermion.

However, \mathbf{M} is neither diagonal nor symmetric in weak eigenstates. To identify the fermion physical masses, one has to diagonalize \mathbf{M} by introducing unitary transformations,

$$\mathbf{M}_D^u = \mathcal{U}_L^{u\dagger} \mathbf{M}^u \mathcal{U}_R^u = \begin{pmatrix} m_u & 0 & 0 \\ 0 & m_c & 0 \\ 0 & 0 & m_t \end{pmatrix} ,\tag{1.30}$$

where \mathcal{U}_L^u and \mathcal{U}_R^u are the unitary transformation matrices for left-handed and right-handed up-type fermion fields, respectively. Correspondingly, the mass (flavor) eigenstate fermion fields are defined by

$$\mathbf{u}_L = \mathcal{U}_L^{u\dagger} \mathbf{u}_L^0 = (u_L \ c_L \ t_L)^T , \quad \mathbf{u}_R = \mathcal{U}_R^{u\dagger} \mathbf{u}_R^0 .\tag{1.31}$$

Diagonalization of the masses in the quark sector introduces the weak mixing, or Cabibbo-Kobayashi-Maskawa (CKM) matrix [14], which then appears in the hadronic weak

charged current as

$$\begin{aligned}
J_W^{\mu\dagger} &= \sum_{i=0}^3 [\bar{\nu}_i^0 \gamma^\mu (1 - \gamma^5) e_m^0 + \bar{\mu}_i^0 \gamma^\mu (1 - \gamma^5) d_m^0] \\
&= (\bar{\nu}_e \bar{\nu}_\mu \bar{\nu}_\tau) \gamma^\mu (1 - \gamma^5) V_l \begin{pmatrix} e^- \\ \mu^- \\ \tau^- \end{pmatrix} + (\bar{u} \bar{c} \bar{t}) \gamma^\mu (1 - \gamma^5) V_q \begin{pmatrix} d \\ s \\ b \end{pmatrix}, \quad (1.32)
\end{aligned}$$

with the Lagrangian written as in (1.11). The miss match between up and down-type quark unitary transformation give rise to the presence of 3×3 CKM matrix $V_q \equiv A_L^{u\dagger} A_L^d$. V_l is the leptonic mixing matrix, which is crucial for describing neutrino oscillations, but for the Standard Model, where neutrinos are assumed to be massless, V_l could be effectively set to be I . After diagonalization, the coupling strength of the physical Higgs boson to the i th fermion is $m_i/v = gm_i/2M_W$, *i.e.* other than top quark, the coupling is very weak.

1.3 Quantum Chromodynamics

The strong interactions sector of the Standard Model, Quantum Chromodynamics [15] (QCD), which is a local non-abelian gauge theory based on SU(3) group with internal symmetry called *color*. The QCD theory consists of six fermions, *quarks*, and eight massless gauge bosons, *gluons*, corresponding to the eight generators of the SU(3) color group. Each quark flavor, carrying one color index, is a color triplet in the fundamental representation **3** of SU(3)_C, and the gluons lie in the adjoint representation **8**, each of which carries two color indices. All other particles in the Standard Model are color singlets and discharged from strong interactions.

The QCD Lagrangian may be written as

$$\mathcal{L}_{QCD} = -\frac{1}{4}F_a^{\mu\nu}F_{a\mu\nu} + \bar{\psi}_i(i\gamma_\mu D_{ij}^\mu - M_{ij})\psi_j, \quad (1.33)$$

with the field strength tensor for gluon field $G_a^\mu, a = 1, \dots, 8$ written as

$$F_a^{\mu\nu} = \partial^\mu G_a^\nu - \partial^\nu G_a^\mu + g_s f_{abc} G_b^\mu G_c^\nu \quad (1.34)$$

and the covariant derivative being

$$D_{ij}^\mu = \partial^\mu \delta_{ij} - ig_s (T_a)_{ij} G_a^\mu.$$

Here g_s represents the strong coupling constant and the indices are summed over color with $a = 1, \dots, 8$ and $i = 1, 2, 3$. T_a and f_{abc} are the SU(3) generators and structure constants, respectively, which obey the commutation relation

$$[T_a, T_b] = if_{abc} T_c. \quad (1.35)$$

The generators are related to the 3×3 Gell-Mann matrices [17] by $T_a = \lambda_a/2$. The QCD lagrangian is invariant under local gauge transformations

$$\begin{aligned} \phi(x) &\rightarrow \exp(ig_s \alpha_a(x) T_a) \phi(x) \\ G_a^\mu(x) &\rightarrow G_a^\mu(x) + \partial^\mu \alpha_a(x) + g_s f_{abc} \alpha_b(x) G_c^\mu(x). \end{aligned} \quad (1.36)$$

Note that in the limit of equal mass quarks, the QCD Lagrangian possesses a global SU(3)_f flavor symmetry, and in the limit of massless quarks an SU(3)_L × SU(3)_R chiral symmetry is present. SU(3) gauge invariance ensures that the gluons are massless. As noticed in previous section, the quark masses are generated by spontaneous symmetry breaking.

The QCD is drastically different from the standard electroweak theory in two aspects: The first is having gluon self-interaction, which is due to the non-abelian nature of the theory and introduced by triple and quartic gluon vertex. Secondly, QCD has the property of asymptotic freedom [16], *i.e.*, the running coupling becomes weak at high energy scale, or rather, short distance, while at low energy or large distance the theory is strongly coupled, which leads to the confinement of quarks and gluons. The asymptotic freedom is crucial when one tries to apply the perturbation theory in QCD calculation for high energy scattering processes. To see this, by renormalization group equation, under one-loop correction, the strong coupling constant g_s is running as a function of energy Q^2

$$\alpha_s(Q^2) \equiv \frac{g_s^2(Q^2)}{4\pi} = \frac{12\pi}{(33 - 2n_f) \ln(Q^2/\Lambda^2)}, \quad (1.37)$$

where n_f is the number of fermion flavors, and Λ is the infrared energy scale cut to be determined by experiments. One can see that as $Q^2 \rightarrow \infty$, $\alpha_s \rightarrow 0$, where quarks and gluons are deconfined, which is the reason why we call it asymptotic free.

Chapter 2

Beyond the Standard Model

2.1 The Problems with the Standard Model

The Standard Model has been a very successful theory at the energy up to weak scale, since it explains nearly all particle physics experiments with extremely high precision. However there are some reasons letting us believe that it is not the whole story, and should be regard as the effective theory of some deeper one at the energy scale that our current collider experiments have been probed.

In the previous section, we present the Standard Model as a theory with gauge group $SU(3)_C \times SU(2)_L \times U(1)_Y$ describing strong, weak, and electromagnetic interactions. Yet this is far from a real unified picture, since each of the three gauge groups has its own coupling and strength. One may obviously ask whether we could find a theory which could unify those three different gauge groups into a single one.

The mass of the W-boson, which is acquired via the Higgs mechanism and proportional to the Higgs mass, has been experimentally determined to be of the order of 80 GeV. But the Higgs mass receives large radiative corrections that are quadratically divergent. In order to have a feasible perturbation theory describing the experiments, these divergencies have to be cancelled by hand in every order, which is fine tuning. Such an accidental cancellations appears miraculous, and raise the question whether

there is another mechanism to stabilize weak scale physics.

The Standard Model has a lot of free parameters built in, such as the masses of quarks and leptons, the weak mixing angles, and CKM matrix. Hence, what is the origin of the observed pattern of fermion masses and mixings? The model provides a description of these quantities but would make equally good sense regardless of what values these couplings take in case of perturbation theory valid. This is the so-called flavor problem of the Standard Model.

One could list a long table of theoretical problems with the Standard Model, albeit it is experimentally successful. Based on the imperfection of the Standard Model at the higher scale, physicists tried to build models beyond it in many directions, including:

- grand unification theory ,
- theories based on Left-Right symmetric gauge groups ,
- theories with extra $U(1)'$ or other extended gauge groups ,
- theories extra Higgs-bosons ,
- technicolor theory ,
- extra-dimension theories ,
- supersymmetry and supergravity ,
- string theory .

Here, we don't have space to introduction all of them. In next section, we will introduce the minimal supersymmetric standard model, and in section 2.3, the brief idea about the grand unification theory.

2.2 The Minimal Supersymmetric Standard Model

There might be tens of reasons why we pursue the supersymmetry models as we step forward beyond the Standard Model.

- The supersymmetry is mathematical beauty;
- Unification of the gauge couplings at the scale $M_U \approx 10^{16}$ GeV;
- Having a light Higgs and easy agreement with the precision electroweak measurements;
- The lightest supersymmetric partner could be a good candidate for the cold dark matter particle;
- The last and maybe the most important one, the model could solve the *gauge hierarchy problem*.

Before scrutinizing the minimal supersymmetric standard model (MSSM), we will briefly introduce the motivation and the formalism of the supersymmetry.

2.2.1 Motivation of Supersymmetry

Since the topic of this thesis is about probing physics at the LHC, we will focus only on the motivation most directly related to physics at the TeV scale, *i.e.* the gauge hierarchy problem.

In Section 1.2, we postulated a potential for the Higgs field as

$$V(\Phi) = \mu^2 |\Phi|^2 + \lambda |\Phi|^4,$$

with $\mu < 0$ for generating electroweak symmetry breaking to induce the masses for various gauge bosons and fermions. From experiments, we know that $\langle \Phi \rangle = \sqrt{-\mu^2/2\lambda}$ is roughly 174 GeV, which is equivalent to say that $\mu^2 \sim -(100\text{GeV})^2$. However, μ is a renormalizable coupling constant of the theory, which cannot be computed from the first principles, and will receive large radiative correction from loop diagrams.

For example, the two diagrams shown in Fig. 2 are the one-loop corrections to the Higgs squared mass μ^2 . If the Yukawa coupling between the Higgs and fermion f with mass m_f is of the form $-\lambda_f \Phi \bar{f} f$, the contribution from Fig. 2(a) is

$$\Delta\mu^2 = \frac{\lambda_f}{16\pi^2} [-2\Lambda^2 + \dots] . \quad (2.1)$$

If there is a complex scalar particle S with mass m_S coupling to the Higgs as $-\lambda_S |\Phi|^2 |S|^2$, then the contribution from Fig. 2(b) is

$$\Delta\mu^2 = \frac{\lambda_S}{16\pi^2} [\Lambda^2 + \dots] . \quad (2.2)$$

If we treat the Standard Model as an effective theory, Λ should be the cutoff energy where the theory is still valid. Changing Λ within a large range of validity, one can easily change the sign of μ^2 and find $-\mu^2 \gg (100 \text{ GeV})^2$ if the theory is valid up to Planck scale $\Lambda \sim 10^{19} \text{ GeV}$. Obviously, we need a fine tuning between two contributions even at one-loop level to achieve observed Higgs bare mass. This is the "gauge hierarchy problem".

There are two approaches to solve the problem. Firstly, one tries to replace the elementary Higgs fields with some dynamical symmetry breaking mechanism based on a new strong dynamics [18]. Higgs proposed his original idea about the Higgs field as a phenomenological description of a fermion pair condensation, which is the reason



Figure 2: One loop diagrams contributing to the Higgs squared mass μ^2 , from (a) a Dirac fermion f loop, and (b) a scalar S loop. Adapted from [20]

why sometimes and originally the electroweak symmetry breaking is also called electroweak superconductivity [9]. In technicolor [19], the spontaneous symmetry breaking is associated with the expectation of a fermion bilinear, analogous to QCD.

The alternative is to postulate that the electroweak symmetry breaking is generated by a weakly coupled Higgs field, with the Higgs mass term μ^2 generated by well-defined physics within the model. This idea requires that the quadratically divergences from the fermion and boson loops cancel. Supersymmetry falls into this category. As seen in Eqn.(2.1)(2.2), if one could pair each fermion with two complex scalars with $\lambda_S = \lambda_f^2$, then the contributions would be naturally cancelled, leaving the finite contributions to μ^2 of the order of the supersymmetry breaking scale.

2.2.2 Formalism of Supersymmetry

The metric we use throughout the section is of the form $g^{\mu\nu} = \mathbf{diag}(-1, +1, +1, +1)$. For most of the conventions, we follow what are adapted in [20] and [21].

For convenience, we employ two-component Weyl spinor rather than four-component Dirac or Majorana spinors for the expression of fermion fields. Consider the theory of a

free Dirac 4-fermion Ψ_D with mass M

$$\mathcal{L}_{\text{Dirac}} = i\bar{\Psi}_D \gamma^\mu \partial_\mu \Psi_D - M\bar{\Psi}_D \Psi_D, \quad (2.3)$$

where the 4×4 gamma matrices take the forms of

$$\gamma^\mu = \begin{pmatrix} 0 & \sigma^\mu \\ \bar{\sigma}^\mu & 0 \end{pmatrix}, \quad \gamma_5 = \begin{pmatrix} -1 & 0 \\ 0 & 1 \end{pmatrix}, \quad (2.4)$$

and Pauli matrices are

$$\begin{aligned} \sigma^0 = \bar{\sigma}^0 &= \begin{pmatrix} 1 & 0 \\ 0 & 1 \end{pmatrix}, & \sigma^1 = -\bar{\sigma}^1 &= \begin{pmatrix} 0 & 1 \\ 1 & 0 \end{pmatrix}, \\ \sigma^2 = -\bar{\sigma}^2 &= \begin{pmatrix} 0 & -i \\ i & 0 \end{pmatrix}, & \sigma^3 = -\bar{\sigma}^3 &= \begin{pmatrix} 1 & 0 \\ 0 & -1 \end{pmatrix}. \end{aligned} \quad (2.5)$$

A Dirac 4-spinor could be written in terms of two Weyl 2-spinors, which are complex and anti-commuting objects

$$\Psi_D = \begin{pmatrix} \xi_\alpha \\ \chi^{\dagger\dot{\alpha}} \end{pmatrix}. \quad (2.6)$$

The field ξ_α is a left-handed Weyl spinor, and $\chi^{\dagger\dot{\alpha}}$ is a right-handed Weyl spinor, with two distinct types of spinor indices $\alpha = 1, 2$ and $\dot{\alpha} = 1, 2$. The Hermitian conjugate operation connects the two kinds of spinors by

$$\xi_\alpha^\dagger \equiv (\xi_\alpha)^\dagger = (\xi^\dagger)_{\dot{\alpha}}, \quad (\xi^{\dagger\dot{\alpha}})^\dagger = \xi^\alpha. \quad (2.7)$$

The heights of the spinor indices are important, and the right-handed spinor is always with dotted indices and daggered. It is convenient to raise and lower the spinor indices

by the anti-symmetric tensor $\epsilon^{\alpha\beta}$ and $\epsilon_{\alpha\beta}$ with the convention $\epsilon^{12} = \epsilon_{21} = 1$. The Pauli matrices carry spinor indices as $(\sigma^\mu)_{\alpha\dot{\alpha}}$ and $(\bar{\sigma}^\mu)^{\dot{\alpha}\alpha}$.

One can construct the Lorentz scalar from fermion bilinears of the form

$$\xi\chi = \chi\xi = \epsilon_{\alpha\beta}\xi^\alpha\chi^\beta, \quad \xi^\dagger\chi^\dagger = \chi^\dagger\xi^\dagger = (\xi\chi)^*, \quad (2.8)$$

and left- and right-handed spinor can be combined into a Lorentz vector as

$$\xi_\alpha^\dagger(\bar{\sigma}^\mu)^{\dot{\alpha}\alpha}\chi_\alpha \equiv \xi^\dagger\bar{\sigma}^\mu\chi = -\chi\sigma^\mu\xi^\dagger = (\chi^\dagger\bar{\sigma}^\mu\xi)^* = -(\xi\sigma^\mu\chi^\dagger)^*. \quad (2.9)$$

With these conventions, after dropping off the total derivative term, the Dirac Lagrangian can be rewritten as:

$$\mathcal{L}_{\text{Dirac}} = i\xi^\dagger\bar{\sigma}^\mu\partial_\mu\xi + i\chi^\dagger\bar{\sigma}^\mu\partial_\mu\chi - M(\xi\chi + \xi^\dagger\chi^\dagger). \quad (2.10)$$

For a Majorana spinor

$$\Psi_M = \begin{pmatrix} \xi_\alpha \\ \xi^{\dagger\dot{\alpha}} \end{pmatrix}, \quad (2.11)$$

the free fermion Lagrangian could be expressed as:

$$\begin{aligned} \mathcal{L}_M &= \frac{i}{2}\bar{\Psi}_M\gamma^\mu\partial_\mu\Psi_M - \frac{1}{2}M\bar{\Psi}_M\Psi_M \\ &= i\xi^\dagger\bar{\sigma}^\mu\partial_\mu\xi - \frac{1}{2}M(\xi\xi + \xi^\dagger\xi^\dagger). \end{aligned} \quad (2.12)$$

For the theory multiple fermion fields $\Psi_i^T = (\xi_i \chi_i^\dagger)$, one could easily translate the Lagrangian with 4-spinor into Weyl 2-spinor version using the following dictionary:

$$\begin{aligned} \bar{\Psi}_i P_L \Psi_j &= \chi_i \xi_j, & \bar{\Psi}_i P_R \Psi_j &= \xi_i^\dagger \chi_j^\dagger, \\ \bar{\Psi}_i \gamma^\mu P_L \Psi_j &= \xi_i^\dagger \bar{\sigma}^\mu \xi_j, & \bar{\Psi}_i \gamma^\mu P_R \Psi_j &= \chi_i \sigma^\mu \chi_j^\dagger. \end{aligned} \quad (2.13)$$

To construct a quantum field theory with the symmetry relating fermions and bosons, a.k.a., supersymmetry, one needs to introduce a generator for the symmetry

$$Q|\text{fermion}\rangle = |\text{boson}\rangle, \quad Q|\text{boson}\rangle = |\text{fermion}\rangle. \quad (2.14)$$

Therefore, Q must be fermionic and anti-commuting. Analogous to Weyl fields ξ and χ^\dagger , we will introduce fermionic charge Q_α , $\alpha = 1, 2$, and their conjugates Q_α^\dagger , $\alpha = 1, 2$.

By Coleman-Mandula Theorem [22] and Haag-Lopuszanski-Sobniewski Theorem [23], under reasonable assumptions, there exist a unique non-trivial extension of the Poincare symmetry by including fermionic generators, which forms a graded Lie algebra [24] defined as

$$\begin{aligned} \{Q_\alpha, Q_\beta^\dagger\} &= 2\sigma_{\alpha\beta}^\mu P_\mu, \\ \{Q_\alpha, Q_\beta\} &= \{Q_\alpha^\dagger, Q_\beta^\dagger\} = 0, \\ [Q_\alpha, P_\mu] &= [Q_\alpha^\dagger, P_\mu] = 0, \\ [Q_\alpha, T^a] &= [Q_\alpha^\dagger, T^a] = 0, \end{aligned} \quad (2.15)$$

where P^μ is the momentum generator of spacetime translations, and T^a are gauge symmetry generators. The first equation of (2.15) implies

$$\langle 0|H|0\rangle = \frac{1}{4}\langle 0|Q_1Q_1^\dagger + Q_1^\dagger Q_1 + Q_2Q_2^\dagger + Q_2^\dagger Q_2|0\rangle \geq 0. \quad (2.16)$$

So the ground state of a supersymmetric field theory would have non-negative energy. If the supersymmetry is unbroken, *i.e.*, $Q|0\rangle = Q^\dagger|0\rangle = 0$, the vacuum energy must be zero, $\langle 0|H|0\rangle = 0$. Otherwise the supersymmetry is broken, the vacuum energy is positive, which is likely to be the case for us, since we haven't seen any super-partner of the Standard Model particles.

Due to limitation of the space, for the detail formalism of *superspace*, *superfield* and *superpotential*, and their transformation properties under $\mathcal{N} = 1$ supersymmetry,

we will blindly adapt all the conventions and notations introduced in Section 3 of *A Supersymmetry Primer* [20].

2.2.3 The Minimal Supersymmetric Standard Model

From Eqn. (2.14), we see that single particle states fall into supermultiplets, each of which consists of same numbers of fermionic n_f and bosonic n_b degree of freedom, *i.e.*, $n_f = n_b$. Bosons and fermions within a supermultiplet are superpartners of each other. If $|\Omega\rangle$ and $|\Omega'\rangle$ are superpartners, then they would transform into each other under the operation of supercharge $|\Omega'\rangle = f(Q, Q^\dagger)|\Omega\rangle$. Awaiting $[Q, P^2] = 0$ and $[Q, T^a] = 0$, superpartners must have the same (mass)² and the same gauge charges.

In supersymmetric field theory there are three kinds of supermultiplets. The combination of a two-component Weyl fermion and a complex scalar is called *chiral* supermultiplet. For the massless fermion, there are two helicity states providing $n_f = 2$, while for a complex scalar (or two real scalar) $n_b = 2$. The Standard Model quarks, leptons, and Higgs fit into chiral supermultiplets.

The combination of a spin-1/2 gaugino and a spin-1 gauge boson is called *gauge* or *vector* supermultiplet. A *gaugino*, which is a Weyl fermion, and a massless gauge boson, are both having two helicity states. The gaugino transforms as the adjoint representation of a gauge group, since it's superpartner, gauge boson, does so. The adjoint representation is its own conjugate, so the left- and right-handed component of gaugino has the same transformation properties. For the Standard Model particles, photon, W bosons, Z boson, and gluons fall into this category.

For models including gravity, we have the spin-2 graviton and its superpartner, a

Names		spin 0	spin 1/2	$SU(3)_C, SU(2)_L, U(1)_Y$
squarks, quarks ($\times 3$ families)	Q	$(\tilde{u}_L \ \tilde{d}_L)$	$(u_L \ d_L)$	$(\mathbf{3}, \mathbf{2}, \frac{1}{6})$
	\bar{u}	\tilde{u}_R^*	u_R^\dagger	$(\bar{\mathbf{3}}, \mathbf{1}, -\frac{2}{3})$
	\bar{d}	\tilde{d}_R^*	d_R^\dagger	$(\bar{\mathbf{3}}, \mathbf{1}, \frac{1}{3})$
sleptons, leptons ($\times 3$ families)	L	$(\tilde{\nu} \ \tilde{e}_L)$	$(\nu \ e_L)$	$(\mathbf{1}, \mathbf{2}, -\frac{1}{2})$
	\bar{e}	\tilde{e}_R^*	e_R^\dagger	$(\mathbf{1}, \mathbf{1}, 1)$
Higgs, higgsinos	H_u	$(H_u^+ \ H_u^0)$	$(\tilde{H}_u^+ \ \tilde{H}_u^0)$	$(\mathbf{1}, \mathbf{2}, +\frac{1}{2})$
	H_d	$(H_d^0 \ H_d^-)$	$(\tilde{H}_d^0 \ \tilde{H}_d^-)$	$(\mathbf{1}, \mathbf{2}, -\frac{1}{2})$

Table 2: Chiral supermultiplets of the Minimal Supersymmetric Standard Model.

massless spin-3/2 particle, *gravitino* forming a supermultiplet with $n_f = n_b = 2$.

Particle Contents of the MSSM

Each Standard Model quark, lepton is a Dirac fermion, *i.e.*, two Weyl fermions. Let's take electron field ψ_e as an example, $\psi_e^T = (e_L \ e_R)$, where e_L and e_R are two-component left-handed and right-handed Weyl fermions, respectively, Each one of which has an independent spin-0 superpartner. \tilde{e}_L is the left-handed selectron, which means the superpartner of e_L , being a complex scalar, while \tilde{e}_R is the right-handed selectron.

Table 2 summarizes all the chiral supermultiplets of the MSSM, and it is arranged according to the Standard Model gauge group charges. Scalar partners of quarks and leptons are called *squarks* and *sleptons*, respectively, and fermionic partner of Higgs is called *higgsinos*.

In the Standard Model, there is only one $SU(2)_L$ Higgs field with $I = 1/2$. Depending on which field we taking to be the primary field, we can take the hypercharge of Higgs field to be either $Y = +1/2$, or its conjugate $-1/2$, which is not a problem in

$$\text{SU}(2) \text{ wavy} \text{ } \triangle \text{ wavy } \text{U}(1) \quad \psi(Y=\frac{1}{2}) \quad + \quad \text{SU}(2) \text{ wavy} \text{ } \triangle \text{ wavy } \text{U}(1) \quad \psi(Y=-\frac{1}{2}) \quad = 0$$

Figure 3: Cancellation of anomaly by two higgsinos in the Minimal Supersymmetric Standard Model

the Standard Model. However, in supersymmetric field theory, the superpotential is an analytical function of superfields, which means it can only contain the field but not its conjugate. Then two different choices of Higgs hypercharge will give different couplings.

As in Table 2, we include both of the possibilities, H_u with $Y = +1/2$ and H_d with $Y = -1/2$. There are two reasons that it is necessary to include two Higgs supermultiplets. The first reason is to cancel the gauge anomalies to maintain the gauge invariance of the model,

$$\text{Tr}[T_3^2 Y] = \text{Tr}[T_3^2 Y] = 0, \quad (2.17)$$

where T_3 is the third component of weak isospin. In the Standard Model, the anomaly cancels non-trivially by the quarks and leptons. In the supersymmetric field theory, each higgsino will make a non-zero contribution to the traces and spoil the cancellation. However, this could be avoid if we include a pair of higgsinos with opposite hypercharges, as shown in Fig. 3.

Secondly, it is necessary to include both Higgs fields to provide all the needed couplings in the superpotential. More explicitly, only a $Y = +1/2$ Higgs chiral supermultiplet can generate the masses to up-type quarks, and only a $Y = -1/2$ Higgs chiral supermultiplet can generate the masses to down-type quarks and to the leptons.

Names	spin 1/2	spin 1	$SU(3)_C, SU(2)_L, U(1)_Y$
gluino, gluon	\tilde{g}	g	$(\mathbf{8}, \mathbf{1}, 0)$
wino, W boson	$\tilde{W}^\pm \ \tilde{W}^0$	$W^\pm \ W^0$	$(\mathbf{1}, \mathbf{3}, 0)$
bino, B boson	\tilde{B}^0	B^0	$(\mathbf{1}, \mathbf{1}, 0)$

Table 3: Vector supermultiplets of the Minimal Supersymmetric Standard Model.

The vector gauge bosons and their superpartners, which are called gauginos collectively, reside in the gauge supermultiplets, as shown in Table 3. So far, all the gauge bosons and gauginos are massless. Electroweak symmetry breaking will mix the W^3 and B to give the mass eigenstates of Z and γ . And winos and bino will mix with higgsinos to form charginos and neutralinos as we discuss later in the section.

Table 2 and Table 3 together make up the particle content of the Minimal Supersymmetric Standard Model. By now, none of the superpartners of the Standard Model particles is found in the collider experiment, so the supersymmetry must be broken, (for a review TASI Lecture by Luty, M. A. [25]).

The supersymmetry could be broken explicitly or spontaneously. There are several reasons why it should be spontaneous broken, *e.g.* , a milder supersymmetry breaking scale comparing to Planck scale, limited numbers of parameters, suppression on flavor changing neutral current, connection to string theory and portable connection with supergravity, *etc* . However, a effective theory relevant at the low energy regime may introduce the breaking terms explicitly as we do in the MSSM. The breaking must be *soft* to prevent reintroducing of the Higgs hierarchy problems, and by "soft" we mean only mass terms and cubic scalar interactions, *i.e.* , couplings with positive mass dimensions. The Lagrangian need to be amended by the SUSY breaking mass term $\mathcal{L}_{\text{soft}}$ term with

the mass scale m_{soft} ,

$$\mathcal{L} = \mathcal{L}_{\text{SUSY}} + \mathcal{L}_{\text{soft}}. \quad (2.18)$$

Then, the correction to the Higgs mass is of the form:

$$\Delta m_H^2 = m_{\text{soft}}^2 \left[\frac{\lambda}{16\pi^2} \ln \left(\frac{\Lambda}{m_{\text{soft}}} \right) + \dots \right]. \quad (2.19)$$

So we expect $m_{\text{soft}} \leq 1 \text{ TeV}$ for the Higgs to be within the reach of the LHC.

Building the Supersymmetric Lagrangian

To build the supersymmetric Lagrangian for chiral supermultiplets, let's start with the simplest massless non-interacting action with a single chiral supermultiplet, a.k.a., Wess-Zumino Model [26]:

$$\begin{aligned} S_{\text{WZ}} &= \int d^4x \left(\mathcal{L}_{\text{scalar}} + \mathcal{L}_{\text{fermion}} \right), \\ \mathcal{L}_{\text{scalar}} &= -\partial^\mu \phi^* \partial_\mu \phi, \quad \mathcal{L}_{\text{fermion}} = i\psi^\dagger \bar{\sigma}^\mu \partial_\mu \psi. \end{aligned} \quad (2.20)$$

The simplest possible SUSY transformation turning a scalar field into a fermion fields is:

$$\delta\phi = \epsilon\psi, \quad \delta\phi^* = \epsilon^\dagger\psi^\dagger, \quad (2.21)$$

where ϵ is an anti-commuting, infinitesimal, constant Weyl fermion as the parameter for the SUSY transformation. Then under this operation, the scalar Lagrangian is transformed as:

$$\delta\mathcal{L}_{\text{scalar}} = -\epsilon\partial^\mu\psi\partial_\mu\phi^* - \epsilon^\dagger\partial^\mu\psi^\dagger\partial_\mu\phi + (\text{total derivatives}). \quad (2.22)$$

To make the theory invariant under SUSY transformation, one needs to cancel $\delta\mathcal{L}_{\text{scalar}}$ by $\delta\mathcal{L}_{\text{fermion}}$ up to some total derivative terms. In other words, $\delta\psi$ must be linear in ϵ^\dagger

and ϕ , and containing one partial derivative. The only option here is:

$$\delta\psi_\alpha = -i(\sigma^\mu\epsilon^\dagger)_\alpha\partial_\mu\phi, \quad \delta\psi^\dagger_{\dot{\alpha}} = +i(\epsilon\sigma^\mu)_{\dot{\alpha}}\partial_\mu\phi^*. \quad (2.23)$$

This leaves $\delta\mathcal{L}_{\text{fermion}} = -\delta\mathcal{L}_{\text{scalar}} + \partial_\mu(\dots)$ and $\delta S = 0$. To make a consistent theory, we still need to check whether the above infinitesimal transformations are closed under SUSY algebra (2.15). Using (2.21) and (2.23), one finds the commutators of two infinitesimal transformations have the forms:

$$\begin{aligned} \delta_{\epsilon_2}(\delta_{\epsilon_1}\phi) - \delta_{\epsilon_1}(\delta_{\epsilon_2}\phi) &= i(\epsilon_2\sigma^\mu\epsilon_1^\dagger - \epsilon_1\sigma^\mu\epsilon_2^\dagger)\partial_\mu\phi, \\ \delta_{\epsilon_2}(\delta_{\epsilon_1}\psi_\alpha) - \delta_{\epsilon_1}(\delta_{\epsilon_2}\psi_\alpha) &= i(\epsilon_2\sigma^\mu\epsilon_1^\dagger - \epsilon_1\sigma^\mu\epsilon_2^\dagger)\partial_\mu\psi_\alpha \\ &\quad + i\epsilon_{1\alpha}\epsilon_2^\dagger\bar{\sigma}^\mu\partial_\mu\psi - i\epsilon_{2\alpha}\epsilon_1^\dagger\bar{\sigma}^\mu\partial_\mu\psi, \end{aligned} \quad (2.24)$$

where ∂_μ corresponds to the generator of spacetime translation operator P_μ . The scalar part of Eqn. (2.24) complies with the form of (2.15) directly, but the fermion part only satisfies (2.15) on-shell, due to the fermion equation of motion $\bar{\sigma}^\mu\partial_\mu\psi = 0$. To fix this, one has to introduce an auxiliary complex scalar field F , with the Lagrangian

$$\mathcal{L}_{\text{aux}} = F^*F. \quad (2.25)$$

Therefore, the auxiliary field has the dimension (mass)² with equation of motion $F^* = F = 0$, and transforms non-trivially as:

$$\begin{aligned} \delta\phi &= \epsilon\psi, \\ \delta\psi_\alpha &= -i(\sigma^\mu\epsilon^\dagger)_\alpha\partial_\mu\phi + \epsilon_\alpha F, \\ \delta F &= -i\epsilon^\dagger\bar{\sigma}^\mu\partial_\mu\psi. \end{aligned} \quad (2.26)$$

One could check the SUSY Lagrangian for chiral supermultiplets $\mathcal{L} = \mathcal{L}_{\text{scalar}} + \mathcal{L}_{\text{fermion}} + \mathcal{L}_{\text{aux}}$ is invariant under (2.26).

A free theory without any interaction certainly is not a promising candidate for the underlining theory of the Standard Model. In a renormalizable supersymmetric field theory, the interactions and masses are uniquely determined by their gauge transformation properties and by the superpotential W , which, by construction, has to be a holomorphic function of the complex scalar fields ϕ_i [20]. In the language of superfield, W is said to be an analytical function of chiral superfields. A superfield is an analogous of a weak isospin doublet, being a single object that contains as components all of the bosonic, fermionic, and auxiliary fields within the corresponding supermultiplet, for example $\Phi_i \supset (\phi_i, \psi_i, F_i)$. The gauge quantum numbers and the mass dimension of a chiral superfield are the same as that of its scalar component. In the superfield formulation, one writes the superpotential as

$$W = L^i \Phi_i + \frac{1}{2} M^{ij} \Phi_i \Phi_j + \frac{1}{6} y^{ijk} \Phi_i \Phi_j \Phi_k, \quad (2.27)$$

where the parametr L^i is only allowed if Φ_i is a gauge singlet, where there is no such chiral supermultiplet in the MSSM, so $L^i = 0$. Let

$$W^i = \frac{\partial W}{\partial \Phi_i}, \quad W^{ij} = \frac{\partial^2 W}{\partial \Phi_i \partial \Phi_j}, \quad (2.28)$$

one find the invariant Lagrangian under the supersymmetric transformation would be of the form:

$$\begin{aligned} \mathcal{L} &= \mathcal{L}_{\text{free}} + \mathcal{L}_{\text{int}}, \text{ with} \\ \mathcal{L}_{\text{free}} &= -\partial^\mu \phi^{*i} \partial_\mu \phi_i + i \psi^{\dagger i} \bar{\sigma}^\mu \partial_\mu \psi_i + F^{*i} F_i, \\ \mathcal{L}_{\text{int}} &= \left(-\frac{1}{2} W^{ij} \psi_i \psi_j + W^i F_i \right) + c.c.. \end{aligned} \quad (2.29)$$

After integrating out the auxiliary fields F_i , F^{*i} , one finds

- the scalar squared masses are $(m_\phi^2)_j^i = M^{ik} M_{kj}^*$;

- the fermion mass terms are M^{ij} and its conjugate M_{ij}^* ;
- the scalar-fermion-fermion Yukawa interactions have the vertex couplings $-iy^{ijk}$ and its conjugate $-iy_{ijk}^*$;
- (scalar)³ vertices are of the form $M_{il}^* y^{jkl}$ and the conjugate $M^{il} y_{jkl}^*$.

All masses and non-gauge couplings of the chiral supermultiplets are fixed by superpotential W .

For the vector supermultiplets, one could built up the SUSY gauge theory Lagrangian following the same idea. There are three fields residing in the gauge supermultiplets, vector bosons A_μ^a , gauginos λ_α^a , and the real scalar auxiliary field D^a , where $a = 1, \dots, 8$ for $SU(3)_C$, $a = 1, 2, 3$ for $SU(2)_L$ and $a = 1$ for $U(1)_Y$. The SUSY gauge Lagrangian could be written as:

$$\mathcal{L}_{\text{gauge}} = -\frac{1}{4}F^{a\mu\nu}F_{\mu\nu}^a + i\lambda^{a\dagger}\bar{\sigma}^\mu D_\mu\lambda^a + \frac{1}{2}D^a D^a, \quad (2.30)$$

where $F_{\mu\nu}^a = \partial_\mu A_\nu^a - \partial_\nu A_\mu^a + gf^{abc}A_\mu^b A_\nu^c$ is the field strength tensor, and the covariant derivative of the gaugino field is $D_\mu\lambda^a = \partial_\mu\lambda^a + gf^{abc}A_\mu^b\lambda^c$. In the *Wess-Zumino gauge* [26], the supersymmetric transformation of the gauge supermultiplets are:

$$\begin{aligned} \delta A_\mu^a &= -\frac{1}{\sqrt{2}}(\epsilon^\dagger\bar{\sigma}_\mu\lambda^a + \lambda^{\dagger a}\bar{\sigma}_\mu\epsilon), \\ \delta\lambda_\alpha^a &= \frac{i}{2\sqrt{2}}(\sigma^\mu\bar{\sigma}^\nu\epsilon)_\alpha F_{\mu\nu}^a + \frac{1}{\sqrt{2}}\epsilon_\alpha D^a, \\ \delta D^a &= \frac{i}{\sqrt{2}}(-\epsilon^\dagger\bar{\sigma}^\mu D_\mu\lambda^a + D_\mu\lambda^{\dagger a}\bar{\sigma}^\mu\epsilon). \end{aligned} \quad (2.31)$$

Suppose that the chiral supermultiplets transform under the gauge group in a representation T^a satisfying $[T^a, T^b] = if^{abc}T^c$. Then the last two transformation rules of

Eqn. (2.26) should be implemented as

$$\begin{aligned}\delta\psi_{i\alpha} &= -i(\sigma^\mu\epsilon^\dagger)_\alpha D_\mu\phi_i + \epsilon_\alpha F_i, \\ \delta F_i &= -i\epsilon^\dagger\bar{\sigma}^\mu D_\mu\psi_i + \sqrt{2}g(T^a\phi)_i\epsilon^\dagger\lambda^{\dagger a}.\end{aligned}\tag{2.32}$$

The general Lagrangian density for a renormalizable supersymmetric field theory is:

$$\mathcal{L} = \mathcal{L}_{\text{chiral}} + \mathcal{L}_{\text{gauge}} - \sqrt{2}g(\phi^*T^a\psi)\lambda^a - \sqrt{2}g\lambda^{\dagger a}(\psi^\dagger T^a\phi) + g(\phi^*T^a\phi)D^a. \tag{2.33}$$

One could integrate out the D term by its equation of motion $D^a = -g\phi^*T^a\phi$.

The last ingredient for a recipe for constructing the supersymmetric interaction at TeV scale is the soft SUSY breaking terms, which is required since the SUSY is broken at the current collider scale as discussed in previous section. The possible soft SUSY breaking terms in the Lagrangian of a theory free of quadratic divergence [27] are:

$$\mathcal{L}_{\text{soft}} = -\left(t^i\phi_i + \frac{1}{2}M_a(\lambda^a)^2 + \frac{1}{2}b^{ij}\phi_i\phi_j + \frac{1}{6}a^{ijk}\phi_i\phi_j\phi_k + c.c.\right) - (m^2)_j^i\phi^{*j}\phi_i, \tag{2.34}$$

where the tadpole coupling only shows up when ϕ_i is a gauge singlet which is absent from the MSSM. The gaugino masses, M_a , scalar squared mass terms, $(m^2)_j^i$ and b^{ij} , and the (scalar)³ coupling, a^{ijk} , are to be explained by deeper underlining models, and all mass terms have mass scale $m_{\text{soft}} \leq 1$ TeV to be observed at the LHC.

Based on the recipe above, we will build the Minimal Supersymmetric Standard Model in the following section.

The Lagrangian of the Minimal Supersymmetric Standard Model

The kinetic terms and gauge couplings of the MSSM Lagrangian are completely determined by supersymmetry, the choice of the gauge group $\text{SU}(3)_C \times \text{SU}(2)_L \times \text{U}(1)_L$, and

the choice of the quantum numbers of the matter fields. The Lagrangian must be of the form (2.34). The only input parameters are the gauge couplings g_1 , g_2 , and g_3 .

As discussed in the previous section, the superpotential induces nonlinear fermion-scalar interaction, so the Higgs Yukawa coupling should be generated by terms included in the superpotential. For the MSSM, the superpotential generating Yukawa coupling is:

$$W_{\text{Yuk}} = \bar{u}^{ia}(\mathbf{y}_{\mathbf{u}})^{ij} Q_{\alpha a}^j (H_u)_\beta \epsilon^{\alpha\beta} - \bar{d}^{ia}(\mathbf{y}_{\mathbf{d}})^{ij} Q_{\alpha a}^j (H_d)_\beta \epsilon^{\alpha\beta} - \bar{e}^i(\mathbf{y}_{\mathbf{e}})^{ij} L_\alpha^j (H_d)_\beta \epsilon^{\alpha\beta}. \quad (2.35)$$

The notations for chiral superfields follow what are introduced in Table 2. The indices $i, j = 1, 2, 3$ are family indices running over the three generations. The indices $\alpha, \beta = 1, 2$ and $a = 1, 2, 3$ are SU(2) isospin indices and SU(3) color index. Notice that the first term requires a $Y = +1/2$ Higgs field H_u , while the latter two require a $Y = -1/2$ Higgs field H_d . The dimensionless Yukawa coupling parameters $\mathbf{y}_{\mathbf{u}}, \mathbf{y}_{\mathbf{d}}, \mathbf{y}_{\mathbf{e}}$ are 3×3 complex matrices, each of which could be diagonalized by two unitary transformation, *e.g.*, $\mathbf{y}_{\mathbf{d}} = \mathbf{U}_{\mathbf{d}} \mathbf{Y}_{\mathbf{d}} \mathbf{V}_{\mathbf{d}}^\dagger$, with $\mathbf{U}_{\mathbf{d}}$ and $\mathbf{V}_{\mathbf{d}}$ being unitary matrices for field redefinitions and leaving $\mathbf{Y}_{\mathbf{d}}$ a positive real diagonal matrix. The unitary transformation cancels out in the kinetic and gauge coupling terms the Lagrangian, but for the weak coupling, it introduces the Cabibbo-Kobayashi-Maskawa matrix $\mathbf{V}_{CKM} = \mathbf{V}_{\mathbf{d}}^\dagger \mathbf{V}_{\mathbf{u}}$ as in the case of the Standard Model.

To generating the Higgs masses, we need to introduce μ term

$$W_\mu = \mu H_{u\alpha} H_{d\beta} \epsilon^{\alpha\beta}. \quad (2.36)$$

Because this term is in the superpotential, it does not receive additive radiative corrections. The scalar potential of the MSSM depends on two types of dimensionful

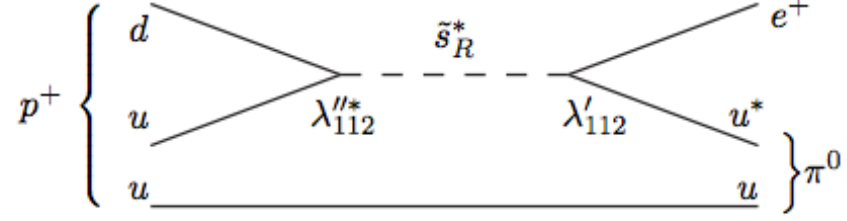


Figure 4: Proton decay $p \rightarrow e^+ \pi^0$ mediated by a sstrange or a sbottom. Adapted from [20]

parameters, the SUSY preserving mass μ and the SUSY breaking soft mass m_{soft} . The observed the electroweak symmetry breaking suggested that both masses should be of the order of 100 GeV. This is "the μ problem".

Other than μ , there is another new parameter beyond those in the Standard Model, the ratio of the vacuum expectation values of two Higgs doublets:

$$\tan \beta \equiv \langle H_u \rangle / \langle H_d \rangle. \quad (2.37)$$

Actually, one could also add some more terms into the superpotential, like:

$$\begin{aligned} W_{\Delta L=1} &= \frac{1}{2} \lambda^{ijk} L_i L_j \bar{e}_k + \lambda'^{ijk} L_i Q_j \bar{d}_k + \mu^i L_i H_u, \\ W_{\Delta B=1} &= \frac{1}{2} \lambda^{ijk} \bar{u}_i \bar{d}_j \bar{d}_k. \end{aligned} \quad (2.38)$$

If both terms are present, one could expect rapid proton decay, as in Fig. 4. Then the life-time of proton would be

$$\Gamma_p \sim \frac{m_p^5}{m_{\tilde{q}}^4} |\lambda'' \lambda'|. \quad (2.39)$$

If the coupling strengths are of order $\lambda'', \lambda' \sim 1$, and squark masses are of the order 1

TeV, the life-time is far less than 1 second. This contradicts the observed limit of proton life-time, which is in excess of 10^{32} years.

In constructing a SUSY model, it is necessary to forbid these terms either by imposing discrete symmetry or arranging the couplings to be extremely small by hand [28]. In the MSSM, a discrete symmetry, called *R-parity*, is introduced to conserve the baryon number B and the lepton number L ,

$$R = (-1)^{3B+L+2J}, \quad (2.40)$$

where J is the spin of the particle. By construction, the particles of the Standard Model have $R = +1$, and their superpartners have $R = -1$.

If the R-parity is conserved, the lightest supersymmetric particle (LSP) is absolutely stable, and all other sparticles will eventually decay to LSP. Therefore, the LSP will be a good candidate [29] for dark matter. Also, superpartners of the Standard Model particles must be produced in pairs.

The last piece of the MSSM Lagrangian is the soft SUSY breaking terms:

$$\begin{aligned} \mathcal{L}_{\text{soft}}^{\text{MSSM}} = & -\frac{1}{2} \left(M_3 \tilde{g} \tilde{g} + M_2 \tilde{W} \tilde{W} + M_1 \tilde{B} \tilde{B} + c.c. \right) \\ & - \tilde{Q}^\dagger \mathbf{m}_{\tilde{\mathbf{Q}}}^2 \tilde{Q} - \tilde{L}^\dagger \mathbf{m}_{\tilde{\mathbf{L}}}^2 \tilde{L} - \tilde{u} \mathbf{m}_{\tilde{\mathbf{u}}}^2 \tilde{u}^\dagger - \tilde{d} \mathbf{m}_{\tilde{\mathbf{d}}}^2 \tilde{d}^\dagger - \tilde{e} \mathbf{m}_{\tilde{\mathbf{e}}}^2 \tilde{e}^\dagger \\ & - m_{H_u}^2 H_u^* H_u - m_{H_d}^2 H_d^* H_d - (b H_u H_d + c.c.) \\ & - \left(\tilde{u} \mathbf{a}_{\tilde{\mathbf{u}}} \tilde{Q} H_u - \tilde{d} \mathbf{a}_{\tilde{\mathbf{d}}} \tilde{Q} H_d - \tilde{e} \mathbf{a}_{\tilde{\mathbf{e}}} \tilde{L} H_d + c.c. \right). \end{aligned} \quad (2.41)$$

In the first line of Eqn. (2.41), M_3 , M_2 and M_1 are the gluino, wino and bino masses. The terms in the second line is the 3×3 squarks and slepton squared mass matrices, which are complex and hermitian so that make the Lagrangian to be real. The last two lines are the SUSY breaking contribution to the Higgs potential and (scalar)³ couplings.

After a careful counting and proper redefinition, there are 105 new parameters [30] that were not present in the Standard Model.

Mass Spectrum of the MSSM

There are two Higgs doublets $H_u = (H_u^+, H_u^0)$ and $H_d = (H_d^0, H_d^-)$ in the MSSM. The scalar potential consists of three kind of terms: F-term, D-term and soft contribution,

$$\begin{aligned}
V &= V_F + V_D + V_{\text{soft}}, \\
V_F &= |\mu|^2 (|H_u^0|^2 + |H_u^+|^2) + |\mu|^2 (|H_d^0|^2 + |H_d^-|^2), \\
V_D &= \frac{1}{8}(g^2 + g'^2) (|H_u^0|^2 + |H_u^+|^2 - |H_d^0|^2 - |H_d^-|^2)^2 \\
&\quad + \frac{1}{2}g^2 |H_u^+ H_d^{0*} + H_u^0 H_d^{-*}|^2, \\
V_{\text{soft}} &= m_{H_u}^2 (|H_u^0|^2 + |H_u^+|^2) + m_{H_d}^2 (|H_d^0|^2 + |H_d^-|^2) \\
&\quad + [b (H_u^+ H_d^- - H_u^0 H_d^0) + c.c.].
\end{aligned} \tag{2.42}$$

We can set b to be real and positive by a field redefinition, and set $\langle H_u^+ \rangle = 0$ and $\langle H_u^0 \rangle$ real and positive by an $SU(2)_L \times U(1)_Y$ gauge transformation. V_D is minimized with $\langle H_d^- \rangle = 0$, and b term is minimized with $\langle H_d^0 \rangle$ being real positive. Collectively, the VEV of the two Higgs fields are

$$v_u \equiv \langle H_u \rangle = \begin{pmatrix} 0 \\ \frac{1}{\sqrt{2}}v \sin \beta \end{pmatrix}, \quad v_d \equiv \langle H_d \rangle = \begin{pmatrix} \frac{1}{\sqrt{2}}v \cos \beta \\ 0 \end{pmatrix}, \tag{2.43}$$

CP cannot be spontaneously broken by the Higgs scalar potential, since the VEVs and b terms can be simultaneously chosen real. Therefore, the Higgs mass eigenstates can

be assigned well-defined eigenvalues of CP. The scalar potential is simplified as

$$\begin{aligned}
 V &= m_u^2 v_u^2 + m_d^2 v_d^2 - 2b v_u v_d + \frac{1}{8}(g^2 + g'^2)(v_u^2 - v_d^2)^2 \\
 &= (v_u \ v_d) M^2 \begin{pmatrix} v_u \\ v_d \end{pmatrix} + \frac{1}{8}(g^2 + g'^2)(v_u^2 - v_d^2)^2,
 \end{aligned} \tag{2.44}$$

where

$$m_u^2 \equiv (|\mu|^2 + m_{H_u}^2) \quad m_d^2 \equiv (|\mu|^2 + m_{H_d}^2) \quad M^2 \equiv \begin{pmatrix} m_u^2 & -b \\ -b & m_d^2 \end{pmatrix}.$$

We know at the minimum $v_u^2 + v_d^2 \sim (174 \text{ GeV})^2$, so that $m_W = gv/2$. In the situation of $v_u = v_d$, the quartic interaction is identically zero. To have the scalar potential bounded below, *i.e.* the vacuum stability requires

$$m_u^2 + m_d^2 > 2b. \tag{2.45}$$

The electroweak symmetry breaking requires that $v_u = v_d = 0$ is not a stable minimum, in other word, one of the eigenvalues of M^2 has to be negative, $\det M^2 < 0$. We get another constraint:

$$m_u^2 m_d^2 < b^2. \tag{2.46}$$

In the situation of both (2.45) and (2.46) satisfied, one can minimize V to find

$$\begin{aligned}
 \sin(2\beta) &= \frac{2b}{m_u^2 + m_d^2}, \\
 m_Z^2 &= \frac{|m_{H_d}^2 - m_{H_u}^2|^2}{\sqrt{1 - \sin^2(2\beta)}} - m_{H_d}^2 - m_{H_u}^2 - 2|\mu|^2.
 \end{aligned} \tag{2.47}$$

From the second equation, one finds that without unnatural cancellations, all of the input parameters should be of the same order with $m_Z = \frac{1}{2}(g^2 + g'^2)(v_u^2 + v_d^2)$, which demonstrates "the μ problem" in the MSSM.

There are two complex isospin doublets for the MSSM Higgs fields, equivalently, there are eight real degrees of freedom. After electroweak symmetry breaking, three of them would be Nambu-Goldstone bosons, denoted as G^0 and G^\pm , which will be eaten by massive Z^0 and W^\pm to be longitudinal modes. The remaining five would become: two neutral scalars h^0 and H^0 , one neutral pseudoscalar A^0 , and two charged scalar H^\pm .

The gauge eigenstate fields could be express in terms of mass eigenstate fields as

$$\begin{aligned} \begin{pmatrix} H_u^0 \\ H_d^0 \end{pmatrix} &= \begin{pmatrix} v_u \\ v_d \end{pmatrix} + \frac{1}{\sqrt{2}} \begin{pmatrix} \cos \alpha & \sin \alpha \\ -\sin \alpha & \cos \alpha \end{pmatrix} \begin{pmatrix} h^0 \\ H^0 \end{pmatrix} \\ &+ \frac{i}{\sqrt{2}} \begin{pmatrix} \sin \beta & \cos \beta \\ -\cos \beta & \sin \beta \end{pmatrix} \begin{pmatrix} G^0 \\ A^0 \end{pmatrix}, \\ \begin{pmatrix} H_u^+ \\ H_d^{-*} \end{pmatrix} &= \begin{pmatrix} \sin \beta & \cos \beta \\ -\cos \beta & \sin \beta \end{pmatrix} \begin{pmatrix} G^+ \\ H^+ \end{pmatrix}. \end{aligned} \quad (2.48)$$

The mass of mass eigenstate fields are

$$\begin{aligned} m_{G^0}^2 &= m_{G^\pm}^2 = 0, \\ m_{A^0}^2 &= 2b/\sin(2\beta) = m_u^2 + m_d^2, \\ m_{h^0, H^0}^2 &= \frac{1}{2} (m_{A^0}^2 + m_Z^2 \mp \sqrt{(m_{A^0}^2 + m_Z^2)^2 - 4m_{A^0}^2 m_Z^2 \cos^2(2\beta)}) , \\ m_{H^\pm}^2 &= m_{A^0}^2 + m_W^2. \end{aligned} \quad (2.49)$$

At tree-level, one finds another constraint from manipulating the third equation above,

$$m_{h^0}^2 \leq m_Z^2 \cos^2(2\beta) \leq m_Z^2, \quad (2.50)$$

where the equalities hold when $m_{A^0} \gg m_Z$, which is called "decoupling limit". At that limit, We see that, in contrast to the Standard Model, there is an upper limit

for the Higgs mass, and the h^0 is the lightest Higgs boson in the MSSM, which is the Standard Model liked Higgs. At loop level, large stop masses make important radiative contributions to the upper limit [31], and the upper limit is replaced by

$$m_{h^0}^2 < m_Z^2 + \frac{3g^2 m_t^4}{8\pi^2 m_W^2} \left[\ln \left(\frac{m_{\tilde{t}_1}^2 + m_{\tilde{t}_2}^2}{2m_t^2} \right) + \frac{2X_t^2}{m_{\tilde{t}_1}^2 + m_{\tilde{t}_2}^2} \left(1 - \frac{X_t^2}{6(m_{\tilde{t}_1}^2 + m_{\tilde{t}_2}^2)} \right) \right], \quad (2.51)$$

where $m_{\tilde{t}_{1,2}}$ are the stop mass in the mass eigenstate after mixing between $m_{\tilde{t}_L}$ and $m_{\tilde{t}_R}$, and X_t is a stop mixing parameter will be defined later in this section. Under reasonable assumptions, like maximal stop mixing $X_t^2 = 3(m_{\tilde{t}_1}^2 + m_{\tilde{t}_2}^2)$, the upper bound could be weakened to $m_{h^0} \lesssim 130$ GeV [32], or in case of the MSSM being perturbative up to the Planck or GUTs scale $m_{h^0} \lesssim 150$ GeV [33].

For the sfermion sector, in principle, any scalars with the same quantum numbers can mix up with each other. Henceforth, with completely general soft SUSY breaking terms (2.41), the mass eigenstates of sfermions should be from diagonalizing three 6×6 (mass)² matrices for $(\tilde{u}_L, \tilde{c}_L, \tilde{t}_L, \tilde{u}_R, \tilde{c}_R, \tilde{t}_R)$, $(\tilde{d}_L, \tilde{s}_L, \tilde{b}_L, \tilde{d}_R, \tilde{s}_R, \tilde{b}_R)$, and $(\tilde{e}_L, \tilde{\mu}_L, \tilde{\tau}_L, \tilde{e}_R, \tilde{\mu}_R, \tilde{\tau}_R)$, and one 3×3 (mass)² matrix for sneutrinos $(\tilde{\nu}_e, \tilde{\nu}_\mu, \tilde{\nu}_\tau)$. Fortunately, some experiments show that some organizing principle must underline the soft SUSY breaking terms, since most of parameters in (2.41) would induce flavor mixing or CP violation at the level severely restricted by experiments.

For example, if $\mathbf{m}_{\tilde{\mathbf{e}}}^2$ is not diagonalized, we would expect there is mixing between smuon and selectron, as shown in Fig. 5. One finds that life time [34] of $\mu \rightarrow e\gamma$ decay channel is:

$$\Gamma(\mu \rightarrow e\gamma) = 5 \times 10^{-15} \text{ eV} \left(\frac{m_{\tilde{\mu}_R^* \tilde{e}_R}^2}{m_{\tilde{l}_R}^2} \right)^2 \left(\frac{100 \text{ GeV}}{m_{\tilde{l}_R}} \right)^4, \quad (2.52)$$

where $m_{\tilde{\mu}_R^* \tilde{e}_R}^2 \equiv (\mathbf{m}_{\tilde{\mathbf{e}}}^2)_{12} = (\mathbf{m}_{\tilde{\mathbf{e}}}^2)_{21}^*$, with $m_{\tilde{l}_R}^2$ being almost degenerate slepton masses.

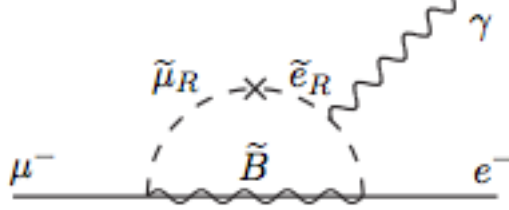


Figure 5: $\mu \rightarrow e\gamma$ with contribution from soft supersymmetric breaking terms. Adapted from [20]

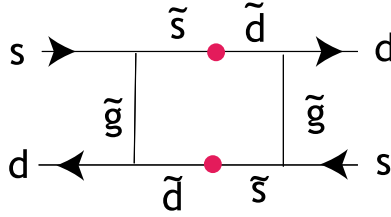


Figure 6: $K - \bar{K}$ mixing with contribution from soft supersymmetric breaking terms.

The current experiment limit [35] is $\Gamma(\mu \rightarrow e\gamma) < 3.6 \times 10^{-21}$ eV, so one would expect

$$\left(\frac{m_{\tilde{\mu}_R^* \tilde{e}_R}^2}{m_{\tilde{l}_R}^2} \right) < 0.02 \left(\frac{m_{\tilde{l}_R}}{500 \text{ GeV}} \right)^2. \quad (2.53)$$

The off diagonal terms $m_{\tilde{s}_R^* \tilde{d}_R}^2$ could also induce undesired meson mixing, as shown in Fig. 6. Weaker constraints also come from $D^0 - \bar{D}^0$ mixing, $B_d^0 - \bar{B}_d^0$ mixing and $B_s^0 - \bar{B}_s^0$ mixing. This is called "the flavor problem" of the MSSM. Theories generating the soft SUSY breaking terms should address this problem. Like in the models of gauge-mediated [36] and anomaly-mediated [37] SUSY breaking, the soft terms only depend on the $SU(2)_L \times U(1)_Y$ quantum numbers, hence automatically diagonal in flavor. If we assume the soft SUSY breaking terms in Eqn. (2.41) is diagonal in flavor, we reduce the

number of overall new parameters from 105 to 22.

There are two sources of the sfermion masses. One is from the soft term Eqn. (2.41). Without flavor mixing, this is

$$\mathcal{L}_{\text{soft}} = -M_f^2 |\tilde{f}|^2. \quad (2.54)$$

The other one comes from the D -term potential, which is the last term in Eqn. (2.30), with $D^a = -g(\phi^* T^a \phi)$. The potential contains the cross terms between the Higgs field and sfermion field as

$$\begin{aligned} V_D &= g^2 (H_d^\dagger \frac{\sigma^3}{2} H_d + H_u^\dagger \frac{\sigma^3}{2} H_u) (\tilde{f}^* T_3 \tilde{f}) \\ &\quad + g'^2 (-\frac{1}{2} H_d^\dagger H_d + \frac{1}{2} H_u^\dagger H_u) (\tilde{f}^* Y \tilde{f}). \end{aligned} \quad (2.55)$$

Inserting the VEVs of Higgs doublets, one can rewrite the potential as

$$\begin{aligned} V_D &= \tilde{f}^* \left[\frac{v^2}{4} (\cos^2 \beta - \sin^2 \beta) (g^2 T_3 - g'^2 Y) \right] \tilde{f} \\ &= \tilde{f}^* \left[\frac{(g^2 + g'^2) v^2}{4} \cos 2\beta (T_3 - \sin^2 \theta_W (T_3 + Y)) \right] \tilde{f} \\ &= \tilde{f}^* [m_Z^2 \cos 2\beta (T_3 - \sin^2 \theta_W Q)] \tilde{f}. \end{aligned} \quad (2.56)$$

For convenience, we define

$$\Delta_f = m_Z^2 \cos 2\beta (T_3 - \sin^2 \theta_W Q). \quad (2.57)$$

The mass of the first and second generation sfermions takes the form

$$m_f^2 = M_f^2 + \Delta f, \quad (2.58)$$

where the mass proportional to fermion masses could be neglected since they are far below electroweak scale. For the third generation sfermions, the contribution from Yukawa

coupling and A terms in (2.41) could be significant. Carefully putting everything together, we have a squared-mass matrix for the stops in gauge eigenstate

$$\mathcal{L}_{\text{stop}} = -(\tilde{t}_L^* \tilde{t}_R^*) \mathbf{m}_{\tilde{t}}^2 \begin{pmatrix} \tilde{t}_L \\ \tilde{t}_R \end{pmatrix}, \quad (2.59)$$

where

$$\mathbf{m}_{\tilde{t}}^2 = \begin{pmatrix} M_t^2 + \Delta_t + m_t^2 & m_t X_t \\ m_x X_t & M_{\tilde{t}}^2 + \Delta_{\tilde{t}} + m_{\tilde{t}}^2 \end{pmatrix}, \quad (2.60)$$

with the stop mixing parameter $X_t = A_t - \mu \cot \beta$. Similarly, we can find the mass matrices for $\tilde{\tau}$, $\tilde{\bar{\tau}}$ and \tilde{b} , $\tilde{\bar{b}}$ of the same structure with $\cot \beta$ replaced by $\tan \beta$. Because of mixing, in the third generation, one sfermion in mass eigenstate is pushed down in mass, which is often the lightest squark or even the LSP of the models.

In a word, for the sfermion sector, the first and second generation sfermions come in 7 nearly degenerate unmixed pairs, $(\tilde{e}_R, \tilde{\mu}_R)$, $(\tilde{e}_L, \tilde{\mu}_L)$, $(\tilde{\nu}_e, \tilde{\nu}_\mu)$, $(\tilde{u}_L, \tilde{c}_L)$, $(\tilde{u}_R, \tilde{c}_R)$, $(\tilde{d}_L, \tilde{s}_L)$, $(\tilde{d}_R, \tilde{s}_R)$. The third generation sfermions are different, because of large renormalization group effects [20] from Yukawa and (scalar)³ couplings.

Finally, let's scrutinize the gaugino and Higgsino masses. Since, gauginos and Higgsinos have the same quantum numbers after electroweak symmetry breaking, they will mix with each other. The neutral Higgsinos \tilde{H}_u^0 and \tilde{H}_d^0 will mix with the neutral gauginos \tilde{B} and \tilde{W}^0 to form 4 mass eigenstates called *neutralinos*, denoted as $\tilde{N}_i (i = 1, 2, 3, 4)$. The charged Higgsinos \tilde{H}_u^+ and \tilde{H}_d^- will mix with two charged winos \tilde{W}^\pm to form 2 mass eigenstates called *charginos*, denoted as $\tilde{C}_i^\pm (i = 1, 2)$, where $\tilde{W}^\pm = (\tilde{W}^1 \mp i \tilde{W}^2)/\sqrt{2}$.

From the fermion-gaugino-scalar coupling in (2.33), one finds the neutralino mass term:

$$\mathcal{L}_{\tilde{N}} = -\frac{1}{2} \begin{pmatrix} \tilde{B} & \tilde{W}^0 & \tilde{H}_d^0 & \tilde{H}_u^0 \end{pmatrix} \mathbf{M}_{\tilde{N}} \begin{pmatrix} \tilde{B} \\ \tilde{W}^0 \\ \tilde{H}_d^0 \\ \tilde{H}_u^0 \end{pmatrix} + c.c., \quad (2.61)$$

with mass matrix being

$$\mathbf{M}_{\tilde{N}} = \begin{pmatrix} M_1 & 0 & -g'v_d/\sqrt{2} & g'v_u/\sqrt{2} \\ 0 & M_2 & gv_d/\sqrt{2} & -gv_u/\sqrt{2} \\ -g'v_d/\sqrt{2} & gv_d/\sqrt{2} & 0 & -\mu \\ g'v_u/\sqrt{2} & -gv_u/\sqrt{2} & -\mu & 0 \end{pmatrix}. \quad (2.62)$$

The matrix is complex and symmetric, so can be diagonalized by a unitary matrix \mathbf{N} to obtain the mass eigenstates,

$$\mathbf{M}_{\tilde{N}} = \mathbf{N}^* \mathbf{diag}(m_{\tilde{N}_1}, m_{\tilde{N}_2}, m_{\tilde{N}_3}, m_{\tilde{N}_4}) \mathbf{N}^\dagger, \quad \tilde{N}_i = \mathbf{N}_{ij} \begin{pmatrix} \tilde{B} & \tilde{W}^0 & \tilde{H}_d^0 & \tilde{H}_u^0 \end{pmatrix}^T. \quad (2.63)$$

Similarly, one finds the chargino mass matrix

$$\mathcal{L}_{\tilde{C}} = -(\tilde{W}^+ \tilde{H}_u^+) \begin{pmatrix} M_2 & gv_u \\ gv_d & \mu \end{pmatrix} \begin{pmatrix} \tilde{W}^- \\ \tilde{H}_d^- \end{pmatrix}. \quad (2.64)$$

After diagonalizing, one get the double degenerate mass eigenvalue

$$m_{\tilde{C}_{1,2}}^2 = \frac{1}{2} [|M_2|^2 + |\mu|^2 + 2m_W^2] \mp \sqrt{(|M_2|^2 + |\mu|^2 + 2m_W^2)^2 - 4|\mu M_2 - m_W^2 \sin 2\beta|^2}. \quad (2.65)$$

One should notice that μ must be non-zero, otherwise, $\det(\mathbf{M}_{\tilde{\mathbf{N}}}) = 0$, and the lightest neutralino will be massless, the lightest chargino will have mass below 100 GeV. If $m_Z \ll |\mu \pm M_{1,2}|$, and $M_1, M_2 \ll \mu$, typical mass spectrum would be the lightest neutralino \tilde{N}_1 is the LSP and "bino-like", with the mass roughly M_1 ; the neutralino \tilde{N}_2 and the charginos \tilde{C}_1^\pm are "wino-like", with the mass roughly M_2 ; the neutralinos $\tilde{N}_{3,4}$ and the charginos \tilde{C}_2^\pm are "higgsino-like", with the mass roughly μ .

For the gluinos, they are color octet fermions, which cannot mix with anything else. A popular assumption is $M_1 = M_2 = M_3$ at the grand unification scale, then with the RG runs down to the TeV scale, the gluino mass parameter is related with bino, wino masses by

$$M_3 : M_2 : M_1 \approx 6 : 3 : 1. \quad (2.66)$$

So far, we briefly introduce the minimal supersymmetric standard model. For more detail, one could see any up-to-date textbooks [38] or lecture notes [39].

2.3 Minimal SU(5) Grand Unification

The Standard Model quarks and leptons of each generation could fill in a multiplet of gauge group SU(5). This suggests that one could fit the Standard Model gauge group $SU(3) \times SU(2) \times U(1)$ into larger single gauge group, SU(5), SO(10) or E_6 , which describes fundamental gauge symmetry. The Standard Model would be a lower energy version of the unified theory after spontaneously breaking the unified group into the Standard Model gauge group.

The generators of SU(5) can be represented as 5×5 Hermitian matrices which acts on a vector in the fundamental representation. The Standard Model gauge group could

be embedded in block diagonal forms. The generators correspond to the Standard Model are identified as

$$SU(3) : \begin{pmatrix} T^a & \\ & 0 \end{pmatrix}, \quad SU(2) : \begin{pmatrix} 0 & \\ & \tau^a \end{pmatrix}, \quad U(1) : \sqrt{\frac{3}{5}} \begin{pmatrix} -\frac{1}{3}\mathbf{1} & \\ & \frac{1}{2}\mathbf{1} \end{pmatrix}, \quad (2.67)$$

where T^a is a 3×3 $SU(3)$ generator, τ^a is a 2×2 Pauli matrix, and they are both normalized as $\text{tr}[T^A, T^B] = \frac{1}{2}\delta^{AB}$. The $U(1)$ matrix tells the hypercharges by $\sqrt{3/5}Y$.

The vacuum expectation value of a Higgs field in the adjoint representation of $SU(5)$ can cause the symmetry-breaking. The VEV

$$\langle \Phi \rangle = v \begin{pmatrix} -\frac{1}{3}\mathbf{1} & \\ & \frac{1}{2}\mathbf{1} \end{pmatrix}, \quad (2.68)$$

commutes with the Standard Model generators in (2.67), but not commutes with other off-diagonal generators of $SU(5)$ gauge group. Therefore the VEV gives mass to off-diagonal generators and break the gauge group $SU(5)$ to $SU(3) \times SU(2) \times U(1)$.

The matter field of the model could be organized as left-handed Weyl fermions in the conjugate of fundamental representation $\bar{\mathbf{5}}$ of $SU(5)$, or in the representation $\mathbf{10}$ of $SU(5)$, which is the anti-symmetric matrix:

$$\bar{\mathbf{5}} : \begin{pmatrix} \bar{d} \\ \bar{d} \\ \bar{d} \\ e \\ \nu \end{pmatrix}, \quad \mathbf{10} : \begin{pmatrix} 0 & \bar{u} & \bar{u} & u & d \\ -\bar{u} & 0 & \bar{u} & u & d \\ -\bar{u} & -\bar{u} & 0 & u & d \\ -u & -u & -u & 0 & \bar{e} \\ -d & -d & -d & -\bar{e} & 0 \end{pmatrix}. \quad (2.69)$$

By letting the generators in (2.67) acting on the fields, one could check that the quantum numbers are the same with those of the Standard Model. $\bar{\mathbf{5}}$ and $\mathbf{10}$ could be decompose into the Standard Model gauge group as

$$\begin{aligned}\bar{\mathbf{5}} &= (\bar{\mathbf{3}}, \mathbf{1}, +2/3) \oplus (\mathbf{1}, \mathbf{2}, -1), \\ \mathbf{10} &= (\mathbf{1}, \mathbf{1}, +2) \oplus (\bar{\mathbf{3}}, \mathbf{1}, -4/3) \oplus (\mathbf{3}, \mathbf{2}, +1/3).\end{aligned}\tag{2.70}$$

The covariant derivative of SU(5) model is of the form

$$D_\mu = \partial_\mu - ig_U A_\mu^a T_U^a, \tag{2.71}$$

where g_U is the unique SU(5) gauge coupling constant, and T_U^a are the full set of SU(5) generators. Since there is only one gauge group, it must have an unique coupling constant, which requires all the Standard Model couplings related by

$$g_1 = g_2 = g_3 = g_U, \quad \text{where } g_1 = \sqrt{\frac{5}{3}}g', \quad g_2 = g, \quad g_3 = g_s. \tag{2.72}$$

This is certainly not the case at current collider energy scale, or electroweak scale, so we require they are unified when run to the so called *grand unification scale*, which is also the way to define the GUTs scale.

At one-loop level, the renormalization group equations evolve as

$$\frac{d\alpha_i}{d \log Q} = -\frac{b_i}{2\pi} \alpha_i^2, \quad \text{where } \alpha_i \equiv \frac{g_i^2}{4\pi}. \tag{2.73}$$

For the U(1) part of the Standard Model gauge group, the RG coefficient

$$b_1 = -\frac{2}{3} \sum_f \frac{3}{5} Y_f^2 - \frac{1}{3} \sum_b \frac{3}{5} Y_b^2, \tag{2.74}$$

which sum over all left-handed fermions and complex bosons, with the coefficient $\frac{3}{5}$ following the definition in (2.67). For the non-Abelian parts of the gauge group, the RG

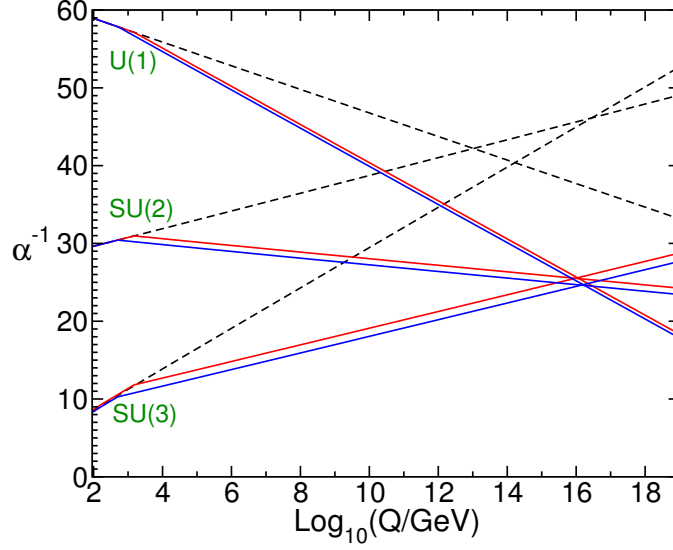


Figure 7: Renormalization group evolution of $\alpha_i^{-1}(Q)$, with dashed lines for the Standard Model and solid lines for the MSSM

coefficient

$$b = -\frac{11}{3}C_2(G) - \frac{2}{3}\sum_f C(r_f) - \frac{1}{3}\sum_b C(r_b), \quad (2.75)$$

where $C_2(G)$ is the quadratic Casimir of the group G , and $C(r)$ is the Casimir invariant defined as $\text{Tr}[T_r^a, T_r^b] = C(r)\delta^{ab}$ with generators T_r in the representation r .

The solution to the RGE (2.73) is

$$\alpha_i(Q) = \frac{\alpha_i(\Lambda_U)}{1 - \frac{b_i}{2\pi} \log \frac{Q}{\Lambda} \alpha_i(\Lambda_U)}, \quad (2.76)$$

where Λ_U is the grand unification mass scale, at which three gauge couplings g_i become equal, which is also the $SU(5)$ symmetry breaking scale.

For the Standard Model gauge group, one finds

$$\begin{aligned}
b_1 &= -\frac{4}{3}n_f - \frac{1}{10}n_H, \\
b_2 &= \frac{22}{3} - \frac{4}{3}n_f - \frac{1}{6}n_H, \\
b_3 &= 11 - \frac{4}{3}n_f,
\end{aligned} \tag{2.77}$$

where n_f is the number of generations, which equals to 3 for the case of the Standard Model, and n_H is the number of Higgs doublets, which is 1. For a supersymmetric model, one finds

$$\begin{aligned}
b_1 &= -2n_f - \frac{3}{10}n_H, \\
b_2 &= 6 - 2n_f - \frac{1}{2}n_H, \\
b_3 &= 9 - 2n_f,
\end{aligned} \tag{2.78}$$

where in the MSSM, $n_f = 3$ and $n_H = 2$. Fig. 7 compares the renormalization group evolutions of $\alpha_i^{-1}(Q)$ for the Standard Model (dashed lines) and the MSSM (solid lines), where the sparticle mass thresholds are varied between 250 GeV and 1 TeV with $\alpha_3(m_Z)$ between 0.113 and 0.123. Unlike the Standard Model, the MSSM ensures that the gauge couplings can unify at a scale $\Lambda_U \sim 10^{16}$ GeV, which is an important phenomenon in favor of the grand unification theory. For a more detailed analysis, see [40].

We give a fairly brief introduction about the idea of SU(5) GUT in this section, and for a detail of grand unification theories, one could check the standard text books [41].

2.4 Top Quarks as a Window to High Scale Physics

The top quark plays a special role in the Standard Model and the searching for new physics beyond the Standard Model. There are several considerations make it interested

by high energy physicists [42]:

- Top quark has a mass at the electroweak scale $m \sim v/\sqrt{2}$, and largest Yukawa coupling among the Standard Model fermions.
- Top quark loop makes the largest contribution to the quadratic divergence of the Standard Model Higgs mass, which makes the top quark mass a crucial parameter for precision electroweak test.
- Heavy mass of top quark make the decay to heavy final states a larger phase space.
- It decays before getting hadronized, which save the opportunity for us to explore properties of a "bare quark", especially making the study of the spin correlation possible.

There are two directions to study high scale physics via top quarks, *i.e.*, decay and production.

We are expecting 80 million $t\bar{t}$ events plus 34 million single-top events with the designed luminosity at the LHC. This high production rate for the top quarks make us a great chance to search for top quark rare decay with a branching fraction as small as 10^{-6} . Those rare decays might be a torch for new physics searching.

For the study of resonant production of top quarks via a heavy intermediate state, such as a string resonance, with semi-leptonic decaying top pairs, it is possible to fully reconstruct the resonance kinematics. This opens up a way to fully exploring of the properties of the resonant state at the center-of-mass frame.

In the following sections, we will study the string resonances and baryon number violation processes involving top quarks along these two directions.

Chapter 3

String Resonance in $t\bar{t}$ Channel at the LHC

¹With the turn-on of the CERN Large Hadron Collider (LHC), a new era of discovery has just begun. This is an opportune time to explore and anticipate various exotic signatures of physics beyond the Standard Model (BSM) that could potentially be revealed at the LHC. Arguably, a major driving force behind the consideration of BSM physics is the hierarchy problem, *i.e.*, the puzzle of why there is such a huge disparity between the electroweak scale and the apparent scale of quantum gravity. Thus, it is of interest to identify what kind of novel signatures can plausibly arise in theories with the capacity to describe physics over this enormous range of scales. String theory being our most developed theory of quantum gravity provides a perfect arena for such investigations.

Despite this promise, attempts to extract collider signatures of string theory have been plagued with difficulties. First of all, the energy scale associated with string theory, known as the string scale $M_s \sim 1/\sqrt{\alpha'}$, is often assumed to be close to the Planck scale or the Grand Unification (GUT) scale [44], making *direct* signals difficult to access. Secondly, most if not all string constructions come equipped with additional light fields even in the point particle (*i.e.*, $\alpha' \rightarrow 0$) limit. These light BSM particles may include new

¹This section is based on the paper by Z.D., *et. al.* [43].

gauge bosons, an extended Higgs sector, or matter with non-Standard Model charges. Their quantum numbers and couplings vary from model to model, and thus their presence makes it difficult to separate the “forest” (genuine stringy effects) from the “trees” (peculiarities of specific models). Without reference to specific models, most studies resort to finding “footprints” of string theory on low energy observables and the relations among them, e.g., the pattern of the resulting soft supersymmetry Lagrangian [45–47].

In recent years, however, it has become evident that the energy scale associated with string effects can be significantly lower than the Planck or GUT scale. With the advent of branes and fluxes (field strengths of generalized gauge fields), it is possible for the extra dimensions in string theory to be large [48, 49] (realizing concretely earlier suggestions [50, 51]) or warped [52–57] while maintaining the observed gauge and gravitational couplings. In the presence of large extra dimensions, the fundamental string scale is lowered by the dilution of gravity. For warped extra dimensions, the fundamental string scale remains high but there can be strongly warped regions in the internal space where the *local* string scale is warped down. In either case, the energy scale associated with string effects is greatly reduced and can in principle be within the reach of the current and upcoming collider experiments. Indeed, preliminary studies have demonstrated that if the string scale (fundamental or local) is sufficiently low, such string states can induce observable effects at the LHC [58–70].

Another development which motivates our current studies is the interesting observation that for a large class of string models where the Standard Model is realized on the worldvolume of D-branes², the leading contributions to certain processes at hadron colliders are *universal* [62]. This is because the string amplitudes which describe $2 \rightarrow 2$

²For some recent reviews on D-brane model building, see, e.g., [71–74].

parton scattering subprocesses involving four gluons as well as two gluons plus two quarks are, to leading order in string coupling (but all orders in α'), independent of the details of the compactification. More specifically, the string corrections to such parton subprocesses are the same regardless of the configuration of branes, the geometry of the extra dimensions, and whether supersymmetry is broken or not. This model-independence makes it possible to compute the leading string corrections to dijet signals at the LHC [63]. Naively, the four fermion subprocesses like quark-antiquark scattering, include (even in leading order of the string coupling) also the exchanges of heavy Kaluza-Klein (KK) and winding states and hence they are model specific. However, their contribution to the dijet production computed in [63] is color and parton distribution function (PDF) suppressed. Moreover, the s -channel excitation of string resonances is absent in these four fermion amplitudes. Therefore, not only do these four fermion subprocesses not affect the universality of the cross section around string resonances, the effective four-fermion contact terms generated by the KK recurrences can be used as discriminators of different string compactifications [64]. Furthermore, due to the structure of the Veneziano amplitude, the effective four-fermion interactions resulting from integrating out the heavy string modes come as dimension-8 rather than the usual dimension-6 operators (and thus further suppressed by s/M_s^2), leading to a much weaker constraint on M_s from precision electroweak tests [75]. Thus, within this general framework of D-brane models, one can cleanly extract the leading model-independent genuine stringy effects, while precision experiments may allow us to constrain the subleading model-dependent corrections and hence the underlying string compactification.

In this section, we revisit the prospects of detecting string resonances at the LHC in light of the above developments. By considering various possible decay products of

the string resonances, we identify a unique detection channel as $t\bar{t}$ production. Besides the enhancement of quark production in comparison to the electroweak processes like diphoton or ZZ by the group (so called Chan-Paton) factors, the Standard Model background for $t\bar{t}$ production is about 10^{-2} of a generic jet and thus provides a good signal to background ratio for detection of new physics (see e.g. [42])). In contrast to other quarks, top quarks promptly decay via weak interaction before QCD sets in for hadronization [76]. Rather than complicated bound states, the properties of “bare” top quarks may be accessible for scrutiny, e.g., through their semi-leptonic decay [42], or the more recently discussed methods to identify highly boosted tops. Among the most distinctive features of string theory is the existence of a tower of excited states with increasing mass and spin, the so called Regge behavior. The exchanges of such higher spin states lead to unusual angular distributions of various cross sections, which can be used to distinguish these string resonances from other new BSM massive particles such as Z' . We investigate the discovery potential of string resonances at the LHC, with particular emphasis on $t\bar{t}$ production and their angular distributions.

This section is organized as follows. In Section 3.1, we discuss string theory amplitudes relevant for $t\bar{t}$ production at the LHC. We decompose the cross sections in terms of the Wigner d-functions to facilitate the analysis of their angular distributions. We also derive the decay widths of the first and second excited string resonances into Standard Model particles. In Section 3.2, we present the results of our detailed phenomenological study for the signal final state of $t\bar{t}$ at the LHC. We further extend the signal study to include the $t\bar{t}g$ channel in Section 3.3, which leads to the possibility to discover both $n = 1$ and 2 string states in the same event sample. We comment on the signal treatment for a significantly heavier string state in Section 3.4. We conclude in Section 3.5.

3.1 $t\bar{t}$ Production via a String Resonance

Let us start with the string amplitudes relevant to $t\bar{t}$ production. At the parton level, the main contribution comes from the $gg \rightarrow t\bar{t}$ subprocess since, as explained in [63], the $q\bar{q} \rightarrow t\bar{t}$ amplitude is suppressed compared to gluon fusion by both color group factors and parton luminosity. We can adopt the gluon fusion amplitude computed in [63] as it does not distinguish, for the purpose of our discussions³, different types of quarks:

$$|\mathcal{M}(gg \rightarrow t\bar{t})|^2 = \frac{g^4}{6} \frac{t^2 + u^2}{s^2} \left[\frac{1}{ut} (tV_t + uV_u)^2 - \frac{9}{4} V_t V_u \right], \quad (3.1)$$

$$V_t \equiv V(s, t, u) \equiv \Gamma(1 - \frac{s}{M_s^2}) \Gamma(1 - \frac{u}{M_s^2}) / \Gamma(1 + \frac{t}{M_s^2}), \quad V_u \equiv V(s, u, t), \quad (3.2)$$

and for completeness $V_s \equiv V(t, s, u)$. The Veneziano amplitude V may develop simple poles near the Regge resonances. In the following, we analyze this amplitude around the $n = 1, 2$ resonances.

3.1.1 $n = 1$ Resonances

There are no massless particles propagating in the s -channel in the energy regime far below the string scale. We will focus on the first Regge string resonance when $s \rightarrow M_s^2$. Expanding the expression around $s = M_s^2$, we have for $n = 1$

$$|\mathcal{M}(gg \rightarrow t\bar{t})|^2 = \frac{7}{24} \frac{g^4}{M_s^4} \left[0.24 \frac{ut(u^2 + t^2)}{(s - M_s^2)^2 + (\Gamma_{g^*}^{J=2} M_s)^2} + 0.76 \frac{ut(u^2 + t^2)}{(s - M_s^2)^2 + (\Gamma_{C^*}^{J=2} M_s)^2} \right] \quad (3.3)$$

where g^* and C^* label the string resonances of $SU(3)$ gluon and $U(1)$ gauge boson on the $U(3)$ QCD bane stack. We have included their decay widths to regularize the resonances.

³As we will discuss in Section 3.5, model-dependent processes such as four-fermion amplitudes can distinguish different quarks as well as their chiralities.

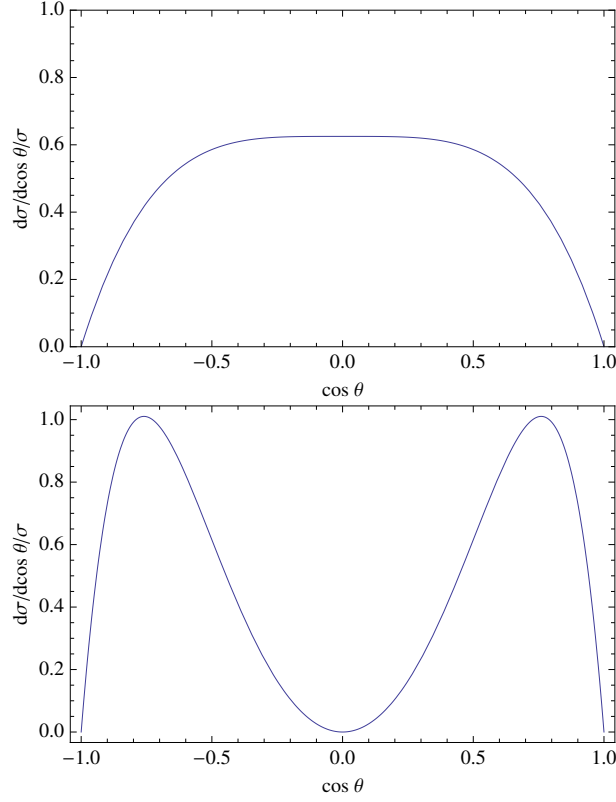


Figure 8: The normalized angular distribution of $gg \rightarrow t\bar{t}$ via the exchange of a string resonance for (a) $n = 1$ (top), and (b) $n = 2$ (bottom).

The decay rates are given by [68]

$$\Gamma_{g^*}^{J=2} = 45 \left(\frac{M_s}{1 \text{ TeV}} \right) \text{ GeV}, \quad \text{and} \quad \Gamma_{C^*}^{J=2} = 75 \left(\frac{M_s}{1 \text{ TeV}} \right) \text{ GeV}. \quad (3.4)$$

Let the angle between the outgoing t quark and the scattering axis (\hat{z}) be θ , the Mandelstam variables t and u can be written as

$$t = -\frac{s}{2}(1 + \cos \theta), \quad u = -\frac{s}{2}(1 - \cos \theta). \quad (3.5)$$

It is intuitive to see the feature of the amplitudes in terms of the contributions from

states with a fixed angular momentum. The amplitudes can be decomposed as follows

$$\mathcal{M}(s, t, u) = 16\pi \sum_{j, m, m'} (2j+1) a_{j, m, m'}(s) d_{m, m'}^j(\theta), \quad (3.6)$$

where the Wigner d -function $d_{m, m'}^j(\theta)$ signifies a state of total angular momentum j , with m (m') the helicity difference of the initial (final) state particles. We thus find

$$|\mathcal{M}(gg \rightarrow t\bar{t})|^2 = \frac{7}{96} g^4 M_s^4 \left[0.24 \frac{|d_{2,1}^2(\theta)|^2 + |d_{2,-1}^2(\theta)|^2}{(s - M_s^2)^2 + (\Gamma_{g^*=2} M_s)^2} + 0.76 \frac{|d_{2,1}^2(\theta)|^2 + |d_{2,-1}^2(\theta)|^2}{(s - M_s^2)^2 + (\Gamma_{C^*=2} M_s)^2} \right]. \quad (3.7)$$

It yields a spin $J = 2$ resonance, with a dominant P-wave behavior. The angular distribution of the $gg \rightarrow t\bar{t}$ amplitude for $n = 1$ is depicted in Fig. 8(a).

The integrated cross section is, for $m_t \ll M_s$,

$$\begin{aligned} \sigma(gg \rightarrow t\bar{t})_{n=1} &= \int_{-1}^1 \frac{d \cos \theta}{32\pi s} |\mathcal{M}(gg \rightarrow t\bar{t})|^2 \\ &= \frac{7}{240} \frac{g^4 M_s^2}{32\pi} \left[\frac{0.24}{(s - M_s^2)^2 + (\Gamma_{g^*=2} M_s)^2} + \frac{0.76}{(s - M_s^2)^2 + (\Gamma_{C^*=2} M_s)^2} \right] \end{aligned} \quad (3.8)$$

3.1.2 $n = 2$ Resonances

Amplitudes

The Veneziano amplitude near the second Regge resonance is approximated by expanding around $s = 2M_s^2$ as

$$V(s, t, u) = \frac{\Gamma(1 - \frac{u}{M_s^2}) \Gamma(1 - \frac{s}{M_s^2})}{\Gamma(1 + \frac{t}{M_s^2})} \approx \frac{u(u + M_s^2)}{M_s^2(s - 2M_s^2)}. \quad (3.9)$$

Therefore, we find

$$|\mathcal{M}(gg \rightarrow t\bar{t})|^2 = \frac{3}{8} g^4 M_s^4 \frac{(1 - \cos \theta)^2 + (1 + \cos \theta)^2}{(s - 2M_s^2)^2} \left(\frac{\sin \theta \cos \theta}{2} \right)^2. \quad (3.10)$$

The angular distribution can be expressed again in terms of the Wigner d -functions as follows

$$\begin{aligned}\frac{1 - \cos(\theta)}{2} \frac{\sin(\theta) \cos(\theta)}{2} &= \frac{1}{3} \sqrt{\frac{2}{5}} d_{2,1}^3(\theta) + \frac{1}{6} d_{2,1}^2(\theta), \\ \frac{1 + \cos(\theta)}{2} \frac{\sin(\theta) \cos(\theta)}{2} &= \frac{1}{3} \sqrt{\frac{2}{5}} d_{2,-1}^3(\theta) - \frac{1}{6} d_{2,-1}^2(\theta).\end{aligned}\quad (3.11)$$

Rewriting (3.10) in Breit-Wigner form,

$$\begin{aligned}|\mathcal{M}(gg \rightarrow t\bar{t})|^2 &= g^4 M_s^4 \left[\frac{1}{15} \frac{|d_{2,1}^3(\theta)|^2 + |d_{2,-1}^3(\theta)|^2}{(s - 2M_s^2)^2 + 2(\Gamma_{g^{**}}^{J=3} M_s)^2} \right. \\ &\quad \left. + \frac{1}{24} \frac{|d_{2,1}^2(\theta)|^2 + |d_{2,-1}^2(\theta)|^2}{(s - 2M_s^2)^2 + 2(\Gamma_{g^{**}}^{J=2} M_s)^2} + \frac{1}{6} \sqrt{\frac{2}{5}} \frac{d_{2,1}^3(\theta) d_{2,1}^2(\theta) - d_{2,-1}^3(\theta) d_{2,-1}^2(\theta)}{(s - 2M_s^2)^2 + \Gamma_{g^{**}}^{J=3} \Gamma_{g^{**}}^{J=2} (2M_s^2)} \right] \quad (3.12)\end{aligned}$$

There are two string resonances of spin $J = 2, 3$ propagating in the s -channel. The third term on the right-hand side is an interference term between $J = 2$ and $J = 3$ resonances. In Fig. 8(b) we plot the angular distribution. It is a superposition of P- and D-waves. The interference vanishes upon integration and the cross section in the center of mass frame is

$$\sigma(gg \rightarrow t\bar{t})_{n=2} = \frac{g^4 M_s^2}{32\pi} \left[\frac{1}{60} \frac{1}{(s - 2M_s^2)^2 + 2(\Gamma_{g^{**}}^{J=2} M_s)^2} + \frac{2}{105} \frac{1}{(s - 2M_s^2)^2 + 2(\Gamma_{g^{**}}^{J=3} M_s)^2} \right],$$

where $\Gamma_{g^{**}}^{J=2}$ and $\Gamma_{g^{**}}^{J=3}$ are the decay widths of the $n = 2$ string resonances with spin $J = 2$ and $J = 3$. The decay rates to Standard Model particles are calculated in the following subsection, and can be found in Table 4. The total decay rate should also include the decay channel to an $n = 1$ string resonance plus Standard Model particles. Though we have not calculated this later decay rate in detail here, we argue below that it should be comparable to the decay rates to a pair of Standard Model particles.

The decay rate of an $n = 2$ string resonance into Standard Model particles

We calculate some decay rates of an $n = 2$ string resonance into Standard Model particles such as gluons and quarks, following the approach in [68]. The Veneziano amplitude can be expanded around the second pole as in Eq. (3.9).

We first look at the 4-gluon amplitudes. Using the approach in [68], the decay width of g^{**} resonance with spin J and color index a into two gluons with helicities and color indices $\lambda_1, \lambda_2, a_1, a_2$ can be written as

$$\Gamma_{\lambda_1 \lambda_2; a_1 a_2}^{aJ} = \frac{1}{16(2J+1)\sqrt{2}\pi M_s} |F_{\lambda_1 \lambda_2; a_1 a_2}^{aJ}|^2 \quad (3.13)$$

Here $F_{\lambda_1 \lambda_2; a_1 a_2}^{aJ}$ is the matrix element for the decay of a resonance g^{**} with $J_z = \lambda_1 - \lambda_2$ into the two gluons, and can be extracted from the 4-gluon amplitude as

$$\begin{aligned} \langle 34; \theta | \mathcal{M} | 12; 0 \rangle &= \sum_{a, J} \langle 34; \theta | \mathcal{M}^{aJ} | 12; 0 \rangle \\ &= (s - 2M_s^2)^{-1} F_{\lambda_3 \lambda_4; a_3 a_4}^{aJ} F_{\lambda_1 \lambda_2; a_1 a_2}^{aJ} d_{\lambda_1 - \lambda_2; \lambda_3 - \lambda_4}^J(\theta) \end{aligned} \quad (3.14)$$

where d^J is the Wigner d -function as before.

We expand the 4-gluon amplitude around $s = 2M_s^2$

$$\begin{aligned} \mathcal{M}(g_1^-, g_2^-, g_3^+, g_4^+) &= 4g^2 \left[\frac{s}{u} V_t \text{Tr}(T^{a_1} T^{a_2} T^{a_3} T^{a_4} + T^{a_2} T^{a_1} T^{a_4} T^{a_3}) \right. \\ &\quad + \frac{s}{t} V_u \text{Tr}(T^{a_2} T^{a_1} T^{a_3} T^{a_4} + T^{a_1} T^{a_2} T^{a_4} T^{a_3}) \\ &\quad \left. + \frac{s^2}{tu} V_s \text{Tr}(T^{a_1} T^{a_3} T^{a_2} T^{a_4} + T^{a_3} T^{a_1} T^{a_4} T^{a_2}) \right] \\ &= \frac{8g^2 M_s^2 \cos(\theta)}{s - 2M_s^2} \text{Tr}([T^{a_1}, T^{a_2}][T^{a_3}, T^{a_4}]) \\ &= -\frac{8g^2 M_s^2}{s - 2M_s^2} d_{0,0}^1(\theta) f^{a_1 a_2 a} f^{a_3 a_4 a} \end{aligned} \quad (3.15)$$

Here $f^{a_1 a_2 a}$ is the antisymmetric $SU(N)$ structure constant. The color index $a = 0$ corresponds to the $U(1)$ gauge boson C in the $U(N)$, and since $f^{a_1 a_2 0} = 0$ we see that

the $n = 2$ resonance C^{**} is not produced in gluon scattering and has no decay channel into two gluons. This feature of $n = 2$ string resonances is different from that of the lowest $n = 1$ resonances studied in [68].

From the above equation we see the string resonance has spin $J = 1$ and up to a phase factor, the matrix element is

$$F_{++a_1a_2}^{a,J=1} = F_{--a_1a_2}^{a,J=1} = 2\sqrt{2}gM_sf^{a_1a_2a} \quad (3.16)$$

After taking into account a factor of $\frac{1}{2}$ from the double counting of identical particles, and also the fact that in this case these are two degenerate resonances with distinct chiral properties, one of which decays into $(++)$ and the other one into $(--)$, we derive the decay width of the $J = 1$ resonance into two gluons

$$\Gamma_{g^{**} \rightarrow gg}^{J=1} = \frac{1}{2} \frac{1}{16\sqrt{2}(2J+1)\pi M_s} \sum_{a_1, a_2} |F_{++a_1a_2}^{a,J=1}|^2 = \frac{g^2 M_s}{12\sqrt{2}\pi} N \quad (3.17)$$

Here the color index $a \neq 0$, and we have used the $SU(N)$ Casimir invariant $C_2(N) = N$.

The other partial amplitudes can be obtained using cross symmetry. For example, the partial amplitude $\mathcal{M}(g_1^-, g_2^+, g_3^-, g_4^+)$ is obtained from the $\mathcal{M}(g_1^-, g_2^-, g_3^+, g_4^+)$ above by exchanging s and t variables, a_2 and a_3 indices. We again expand around the second pole $s = 2M_s^2$,

$$\begin{aligned} \mathcal{M}(g_1^-, g_2^+, g_3^-, g_4^+) &= -\frac{8g^2}{s - 2M_s^2} \left(\frac{1 + \cos \theta}{2} \right)^2 \cos \theta f^{a_1a_2a} f^{a_3a_4a} \\ &= -\frac{8g^2}{s - 2M_s^2} \left(\frac{1}{3} d_{2,2}^3(\theta) + \frac{2}{3} d_{2,2}^2(\theta) \right) f^{a_1a_2a} f^{a_3a_4a} \end{aligned} \quad (3.18)$$

We see there are spin $J = 2$ and $J = 3$ resonances propagating in the s-channel. The

channel	$\Gamma_{g^{**}}^{J=1}$	$\Gamma_{g^{**}}^{J=2}$	$\Gamma_{g^{**}}^{J=3}$
gg	$\frac{N}{3\sqrt{2}}$	$\frac{4N}{15\sqrt{2}}$	$\frac{2N}{21\sqrt{2}}$
$q\bar{q}$	0	$\frac{N_f}{240\sqrt{2}}$	$\frac{N_f}{105\sqrt{2}}$

Table 4: The decay widths of $n = 2$ string resonances. All quantities are to be multiplied by the factor $\frac{g^2}{4\pi}M_s$. For the Standard Model, $N = 3$, $N_f = 6$.

matrix elements and decay widths are

$$F_{\pm\mp a_1 a_2}^{a, J=2} = \frac{4}{\sqrt{3}} g M_s f^{a_1 a_2 a}, \quad F_{\pm\mp a_1 a_2}^{a, J=3} = \frac{2\sqrt{2}}{\sqrt{3}} g M_s f^{a_1 a_2 a} \quad (3.19)$$

$$\Gamma_{g^{**} \rightarrow gg}^{J=2} = \frac{g^2 M_s}{15\sqrt{2}\pi} N, \quad \Gamma_{g^{**} \rightarrow gg}^{J=3} = \frac{g^2 M_s}{42\sqrt{2}\pi} N \quad (3.20)$$

We then consider the decay channel to quarks

$$\mathcal{M}(q_1^-, \bar{q}_2^+, g_3^-, g_4^+) = 4g^2 M_s^2 \left(\frac{1}{3} \sqrt{\frac{2}{5}} d_{2,-1}^3(\theta) - \frac{1}{6} d_{2,-1}^2(\theta) \right) [T^{a_3}, T^{a_4}]_{\alpha_1 \alpha_2}, \quad (3.21)$$

where α_1, α_2 are indices for quarks. We find the matrix elements and decay widths

$$F_{\pm\frac{1}{2}\mp\frac{1}{2}\alpha_1\alpha_2}^{a, J=2} = \frac{\sqrt{3}}{6} g M_s T_{\alpha_1\alpha_2}^a, \quad F_{\pm\frac{1}{2}\mp\frac{1}{2}\alpha_1\alpha_2}^{a, J=3} = \frac{2}{\sqrt{15}} g M_s T_{\alpha_1\alpha_2}^a \quad (3.22)$$

$$\Gamma_{g^{**} \rightarrow q\bar{q}}^{J=2} = \frac{g^2 M_s}{960\sqrt{2}\pi} N_f, \quad \Gamma_{g^{**} \rightarrow q\bar{q}}^{J=3} = \frac{g^2 M_s}{420\sqrt{2}\pi} N_f \quad (3.23)$$

We list the decay widths of various channels in Table 4. We see the decay width to quarks are much smaller than the decay width to gluons. In our analysis of the $t\bar{t}$ channel for the $n = 2$ string resonances, we will encounter the spin $J = 2$ and $J = 3$ resonances, but not the $J = 1$ resonance.

Estimation of the total decay width of $n = 2$ string resonance

It is well known that the highest spin of string excitations at level n is $J = n + 1$. Therefore, for an $n = 2$ string resonance, there are three possible spins associating with

it, listed in Table 4, and the states of different J should correspond to different particles, as in the case of the Standard Model. Thus we could estimate the decay widths for the different J states separately.

In section 3.1.2, we derived the decay widths for the various channels of an $n = 2$ string resonance decaying into two Standard Model particles (both identified as $n = 0$ ground states). Other than these channels, the $n = 2$ string resonance (SR_2) could also decay into an $n = 1$ string resonance (SR_1) and an $n = 0$ Standard Model particle (SM). The decay width of these later processes is what we would like to estimate here. We will leave an explicit calculation of such decay width for future work, as it is sufficient for our purpose to estimate and compare it with the decay width of $\text{SR}_2 \rightarrow \text{SM} + \text{SM}$. We will assume that the decay matrix elements for $\text{SR}_2 \rightarrow \text{SR}_1 + \text{SM}$ to be comparable with $\text{SR}_2 \rightarrow \text{SM} + \text{SM}$. We then count the multiplicity N of the possible decay channels and multiply N by the typical $\text{SR}_2 \rightarrow \text{SM} + \text{SM}$ widths to get an estimate of these partial widths (and thus eventually the total width).

Although there are many excited string states, most of them are not charged under the Standard Model and their presence does not concern us since they will not be produced on resonance. Meanwhile, we can make a physically justified assumption that the $n = 0$ states do not contain non-Standard Model fields charged under the Standard Model gauge group⁴ (implicitly assumed in [59, 77, 78]) or else these new particles would have been observed in experiments. In principle, the SR_1 states can decay to SMs with internal indices (e.g. a gluon in higher dimensions appear to be a scalar in 4-D) but such states are absent by assumption, so we only need to consider SR_1 states with 4-D

⁴This means we assume that there are no chiral exotics charged under the Standard Model, and any vector-like states are made massive by whatever mechanism that stabilizes the moduli.

indices.

Take $n = 2$ $J = 3$ string resonance ($\text{SR}_2^{J=3}$) as an example. It could decay to either a pair of fermionic states or a pair of bosonic states. For the bosonic pair (i.e. a SR_1 with integer spin ($J = 1, 2, 3$) + a gluon), at $n = 1$ level, we know there are 5 string resonances of gluons (see Appendix A), and each one corresponds to a particle, i.e. consisting of a spin 2 particle, two spin 1 particles and two spin 0 particles. Since there are 5 $n = 1$ particles, in the worst scenario, the multiplicity is 5. However this is very unlikely, since the two $\text{SR}_1^{J=1}$ have different chiralities, so a SR_2 usually decays to only one of them. The same argument applies to two $\text{SR}_1^{J=0}$. So the multiplicity is at most 3. Based on this argument and Table 4, the decay width of $\text{SR}_2^{J=3} \rightarrow \text{integer spin SR}_1 + \text{gluon}$ should be roughly $60 \text{ GeV}(M_S/1 \text{ TeV})$.

For the fermionic pair (i.e. a SR_1 with half-integer spin ($J = 3/2, 1/2$) and a fermion), there are at most 4 $J = 3/2$ resonances, and 2 $J = 1/2$ resonances. So the number of decay channels is at most 6 times bigger than that of $\text{SR}_2 \rightarrow q\bar{q}$. Then the decay width of these channels should be no more than $25 \text{ GeV}(M_S/1 \text{ TeV})$.

Collectively, the total decay width of $\text{SR}_2^{J=3}$ is roughly $100 \text{ GeV}(M_S/1 \text{ TeV})$. On account of the same assumptions and method, the decay widths of $\text{SR}_2^{J=2}$ and $\text{SR}_2^{J=1}$ are roughly $250 \text{ GeV}(M_S/1 \text{ TeV})$ and $300 \text{ GeV}(M_S/1 \text{ TeV})$, respectively. Since $J = 3$ resonance has the narrowest width, it will be the dominant SR_2 signal.

3.2 $t\bar{t}$ Final State And String Resonances at the LHC

As a top factory, the LHC will produce more than 80 million pairs of top quarks annually at the designed high luminosity [42], largely due to the high gluon luminosity at the

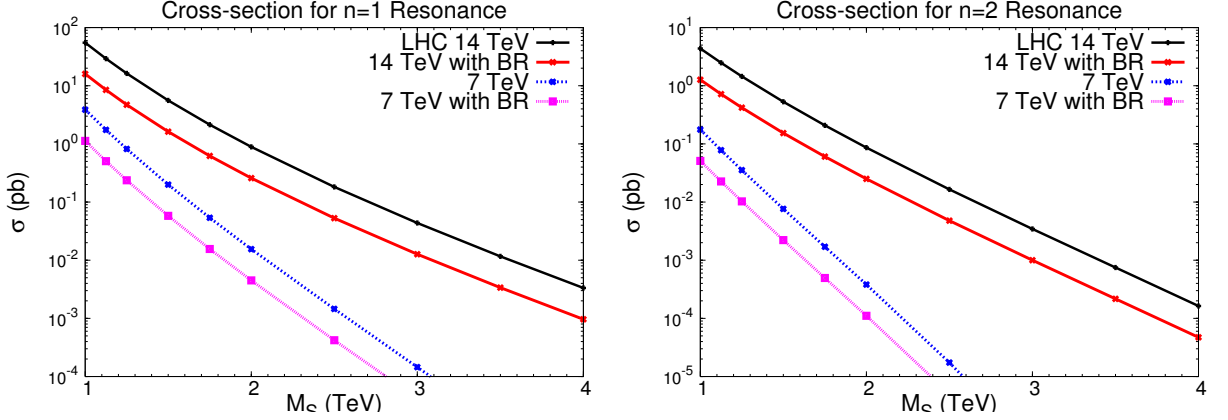


Figure 9: Total cross section for a string resonance production at the LHC versus it mass scale M_s for (a) $n = 1$ and (b) $n = 2$ (mass $1.4M_s$). Solid curves represent $gg \rightarrow t\bar{t}$. Dashed curves include the top quark decay branching fractions for the semi-leptonic mode $t\bar{t} \rightarrow b\bar{\ell}\nu, b\bar{j}j'$.

initial state. It is therefore of great potential to observe string resonances in the $t\bar{t}$ channel if they couple to the gluons strongly. The Chan-Paton coefficient is unsuppressed (compared to say ZZ production), and the Standard Model background is several orders of magnitude lower than that of the di-jet signal. Furthermore, the top quark is the only SM quark that the fundamental properties such as the spin and charge may be carried through with the final state construction, and thus may provide additional information on the intermediate resonances. The total production cross sections for a $t\bar{t}$ final state via a string resonance are shown in Fig. 9 by the solid curves at the LHC for 7 and 14 TeV, respectively. The dashed curves include the semi-leptonic branching fraction. The signal rates are calculated near the resonance peak with $\pm 10\%M_s$. We see that the rate can be quite high. With 100 fb^{-1} integrated luminosity at 14 TeV, there will be about 100 $t\bar{t} \rightarrow b\bar{\ell}\nu, b\bar{j}j'$ events for an $n = 1$ string resonance of 4 TeV mass, and a handful events for $n = 2$ of 5.7 TeV mass.

Table 5: Basic acceptance cuts for $t\bar{t}$ events at the LHC.

	p_T (GeV)	η rapidity
ℓ	20	3
j	30	3
\cancel{E}_T	30	N/A
ΔR^{cut}	0.4	0.4

3.2.1 Invariant Mass Distribution of $t\bar{t}$ Events

With the semi-leptonic decay of $t\bar{t}$ one can effectively suppress the other SM backgrounds [79] Furthermore, the $t\bar{t}$ events may be fully reconstructable with the kinematical constraints [80]. Thus, we consider here the semi-leptonic final state

$$t\bar{t} \rightarrow b\bar{\ell}\nu, \bar{b}jj, \quad (3.24)$$

with a combined branching fraction about 30%, including $\ell = e, \mu$. The total signal production rates including this semi-leptonic branching fraction are plotted in Fig. 9 by the dashed curves.

To simulate the detector effects, we impose some basic acceptance cuts on the momentum and rapidity of the final state leptons, jets and missing energy. We also demand the separation ΔR among the leptons and jets. The cuts are summarized in Table 5. Figure 10 shows that both $n = 1$ (peak position at $M_S=1$ TeV) and $n = 2$ (peak position at $M_S=1.41$ TeV) string resonances are evident at LHC with the c.m. energy at 14 TeV and 7 TeV.

Though the Standard Model background is large as seen in the figure for the continuum spectrum, we still get abundant resonant events in the peak region. Assuming the annual luminosity at the LHC to be $10^{34} \text{ cm}^{-2}\text{s}^{-1} \sim 100 \text{ fb}^{-1}$ per year with the c.m. energy 14 TeV, one would expect to have about a million $n = 1$ string resonance events

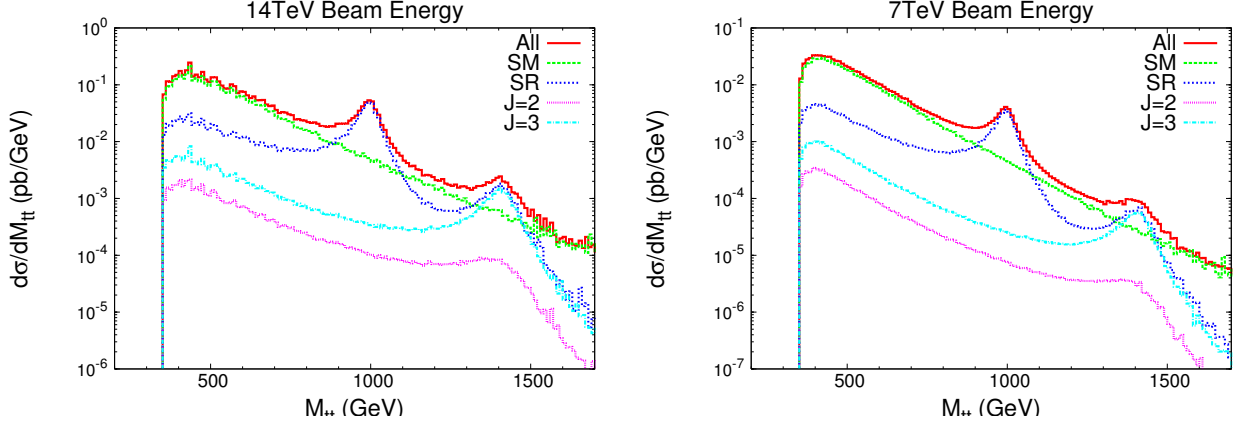


Figure 10: Invariant mass distribution of $t\bar{t}$ at the LHC (a) with the c.m. energy 14 TeV, (b) with the c.m. energy 7 TeV. Decay branching fractions with one hadronically and the other leptonically have been included. All channels (All), in the figure, include both string resonance signal (SR) and Standard Model background (SM). The distributions of $J = 2$ and $J = 3$ states are shown for $n = 2$ resonance, respectively.

in the peak region 900-1100 TeV, for $M_s=1$ TeV (with decay width calculated by [68]). Similarly, one may expect about a thousand events around $m_{t\bar{t}} \approx 1.4$ TeV. At the lower energy of 7 TeV with an integrated luminosity 1 fb^{-1} as the current planing for the initial LHC running, we would expect to have about 500 events near $m_{t\bar{t}} = 1$ TeV, and about one event at 1.4 TeV.

A distinctive feature of string resonances is their mass ratio. Suppose the masses of the first and the second excited string states are $M_{t\bar{t}1}$, and $M_{t\bar{t}2}$ respectively, then $M_{t\bar{t}2}/M_{t\bar{t}1} = \sqrt{2} \approx 1.4$ (as in Figure 10), which can potentially distinguish them from other kinds of resonances. It is important to note that, at leading order of the gauge coupling, this mass ratio is *model independent* and does not depend on the geometry of compactification, the configuration of branes, and the number of supersymmetries. Higher order corrections to this ratio depend on model specific details, and if measurable,

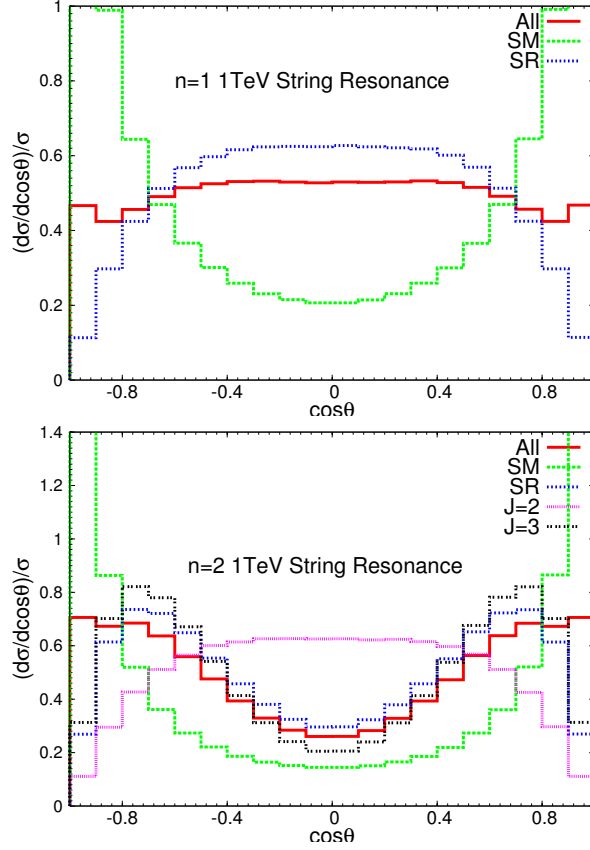


Figure 11: Normalized angular distribution of $t\bar{t}$ at the LHC via the string resonance exchange in the peak region $900 - 1100$ GeV for $n = 1$, and in the region $1350 - 1450$ GeV for $n = 2$.

can serve as a discriminator of different string theory compactifications.

3.2.2 Angular Distribution of $t\bar{t}$ Events

Other than the distinctive invariant mass distribution, the normalized angular distribution can provide a great discriminator between string resonances and the Standard Model background. The shape of the angular distribution for a string resonance is

mainly a result of the Regge behavior of the string amplitudes. Figure 11 shows the normalized angular distributions according to the cross section of all channels (including string resonance and Standard Model $t\bar{t}$ background) in the 900 – 1100 GeV peak region for $n = 1$, and in the 1350 – 1450 GeV region for $n = 2$. The angle is defined for the outgoing top quark with respect to the incoming beam direction in the $t\bar{t}$ c.m. frame, which can be reconstructed for the semi-leptonic channel on an event-by-event basis. We observe the qualitative difference between the string resonance signal and the SM background: The signal is protrudent at the large scattering angular region $\cos\theta \rightarrow 0$, where the Standard Model background is collimated with the beam direction, due to the dominant behavior of the t - or u -channel, scaling as $(1 \pm \cos\theta)^{-1}$. As shown earlier, there is even a clear difference in shape between the $n = 1$ and $n = 2$ states, as indicated by the solid curves (All). It is interesting to note that for an $n = 2$ resonance, the shape difference between $J = 2$ and $J = 3$ states is also evident. However, since they are all degenerate in mass, one would have to use more sophisticated fits to their angular distributions to disentangle them.

The major advantages for considering the semi-leptonic decay of the $t\bar{t}$ are that (1) we will be able to tag the top versus anti-top, and (2) the angular distribution of the charged lepton in the reconstructed c.m. frame can carry information about the top-quark spin correlation [81], and thus provides an effective test for the nature of the top-quark coupling. Since the resonance couplings under our consideration are all vector-like, we will not pursue further detail studies of these variables.

3.3 $t\bar{t}g$ Final State And String Resonances at the LHC

For an $n = 2$ string resonance, it could decay not only directly to two $n = 0$ Standard Model particles as discussed above, but also to an $n = 1$ string resonance and an $n = 0$ Standard Model particle. Thus, there is an additional decay chain

$$(n = 2) \rightarrow (n = 1) + g \rightarrow t\bar{t} + g, \quad (3.25)$$

following an $n = 2$ resonance production. The kinematics of this channel may lead to further distinctive signatures. First of all, the additional gluonic jet is highly energetic, with an energy of the order $M_s/\sqrt{2}$, quite distinctive from QCD jets. Secondly, there are two resonances with $n = 1$ and 2 respectively, both appearing in the same event sample. One would thus expect to establish a convincing signal observation with the mass peaks at $M_{t\bar{t}} \sim M_s$ and $M_{t\bar{t}j} \sim 1.4M_s$. Figure 12 shows the invariant mass distributions for $t\bar{t}g$ production from an $M_s = 1$ TeV string resonance and the Standard Model background. The upper panels present the $M_{t\bar{t}}$ distribution where an $n = 1$ resonance peak is apparent. The lower panels are for the $M_{t\bar{t}j}$ distribution which shows the expected $n = 2$ resonance peak. The two linear plots on the right column are the blow-up view near the resonances in units of number of events per bin (10 GeV) with an integrated luminosity of 10 fb^{-1} . The different angular momentum states $J = 1, 2, 3$ are also separately plotted. Since they are all degenerate in mass, one would have to use more sophisticated fits to their angular distributions to disentangle them, as discussed in the previous sections.

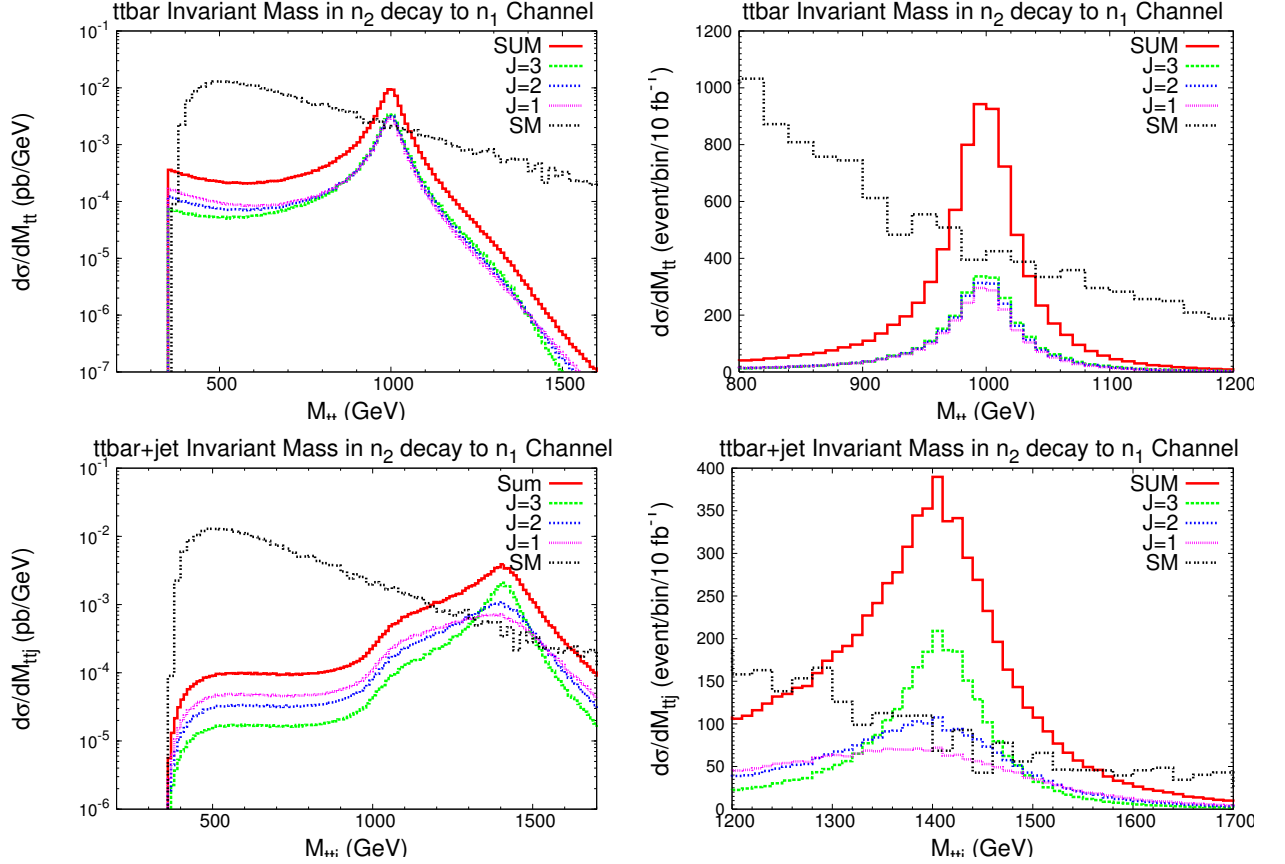


Figure 12: Invariant mass distributions in the $g + g \rightarrow n = 2$ resonance $\rightarrow n = 1$ resonance $+ g \rightarrow t\bar{t} + g$ channel. Upper two graphs: $t\bar{t}$ invariant mass signal and the Standard Model background. Lower two graphs: $t\bar{t} + g$ invariant mass signal and the Standard Model background. The summed signal, in the figure, includes the contributions from both $J = 2$ and $J = 3$ resonances.

3.4 Higher String Scale signal

As seen from Fig. 9, a string resonance of mass about 4 TeV for both $n = 1$ and 2 may be copiously produced at the LHC with the designed luminosity of 100 fb^{-1} . However, as the mass of the string resonance increases, the decay products become more and more collimated, and the fast moving top quark is a “top jet”. Figure 13 reveals the dependance of the cross section on the minimum separation between any two jets from top decay in the peak region ($\pm 100 \text{ GeV}$ around the peak). Based on the figures, one notices that, for an 1 – 1.5 TeV string resonance, $\Delta R^{\text{cut}} = 0.3$ is efficient in defining an isolated lepton or jet. For a higher string mass, the top quarks are highly boosted and too collimated to be identified as multiple jets. One may use various methods [82,83] to identify the highly boosted top produced by string resonances as a single “fat top jet”. Non-isolated muons from the top decay may still help in top-quark identification.

Furthermore, the granularity of the hadronic calorimeter is roughly $\Delta\eta \times \Delta\phi \sim 0.1 \times 0.1$ [79]. To identify individual decay products, one needs the separation ΔR between any two decay products to be at least 0.1 – 0.2. From Figure 13, we see that we could identify the boosted tops if the string scale is below 4 TeV. For a string scale above 4 TeV, we could not tell the difference between top quarks and other QCD jets from light quarks or gluons. Then, our background will be from QCD dijet, and there would be no advantage in considering $t\bar{t}$ final state. The situation is similar to the study in [63] for light quark final states.

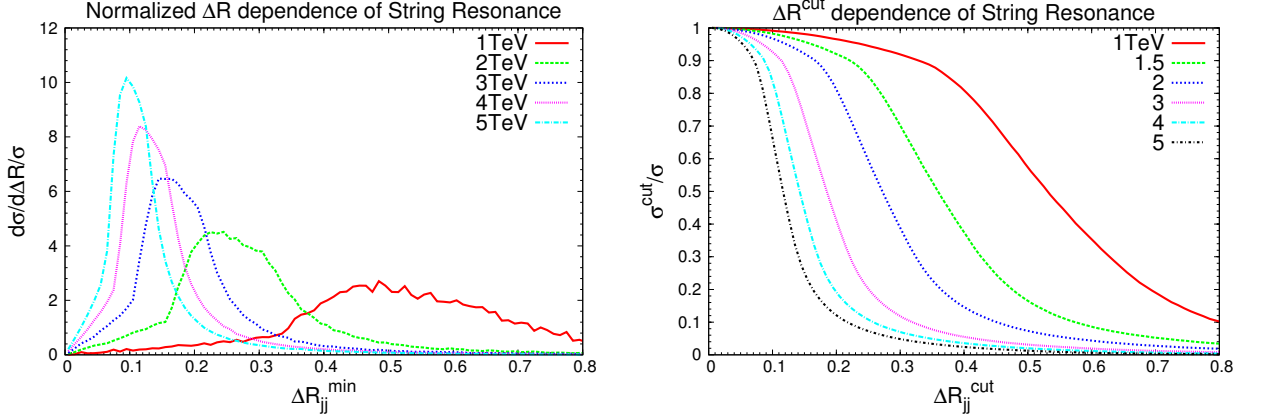


Figure 13: (a) The distribution of the minimum separation between any two jets from $t(\bar{t})$ decay ΔR_{jj} . (b) $\Delta R_{jj}^{\text{cut}}$ Efficiency: Peak region cross section percentage versus $\Delta R_{jj}^{\text{cut}}$ of $t\bar{t}$ semi-leptonic decay at the LHC. The energy labels in the legends stand for the resonance masses.

3.5 Discussions and Conclusion

In this section, we have studied the discovery potential of string resonances at the LHC via the $t\bar{t}$ final state. In a large class of string models where the Standard Model fields are localized on the worldvolume of D-branes, the string theory amplitudes of certain processes at hadron colliders are *universal* to leading order in the gauge couplings. This universality makes it possible to compute these *genuine* string effects which are independent of the geometry of the extra dimensions, the configuration of branes, and whether supersymmetry is broken or not. Among the various processes, we found the production of $t\bar{t}$ pairs at the LHC to be advantageous to uncover the properties of excited string states which appear as resonances in these amplitudes. The top quark events are distinctive in event construction and have less severe QCD backgrounds than other light jet signals from string resonance decays. The swift decay of top quarks via

weak interaction before hadronization sets in makes it possible to reconstruct the full decay kinematics and to take advantage of its spin information. We investigated the invariant mass distributions and the angular distributions of $t\bar{t}$ production which may signify the exchange of string resonances.

Our detailed phenomenological studies suggest that string resonances can be observed in the $t\bar{t}$ channel for a string scale up to 4 TeV by analyzing both the invariant mass distributions and the angular distributions. For a string scale less than 1.5 TeV, we proposed to use semi-leptonic decay to reconstruct the $t\bar{t}$ c.m. frame and obtain the angular distributions to disentangle string resonances with different angular momenta. For a string scale between 1.5 TeV and 4 TeV, we need to identify the boosted tops as a single top jet and directly observe the angular distribution. If the string scale is higher than 4 TeV, we cannot observe the substructure of quark jets and so the signal will be submerged by the QCD dijet background. The potential benefits for using the $t\bar{t}$ final state in the semi-leptonic mode is that one would be able to tag t from \bar{t} , so that the coupling properties of the string resonance, such as parity, CP, and chirality, could be studied via the angular distributions of the top, especially the distributions of the charged lepton with the help of the spin-correlation.

The current work focuses on string amplitudes which give the leading order (in string coupling) contribution to $q\bar{q}$ production at the LHC. These amplitudes are model-independent as they do not involve exchange of KK modes. As a result, such amplitudes do not distinguish between different quarks (their flavors or chiralities) even though they may have different wavefunctions (classical profiles) in the internal space. This is however not the case for the subleading contributions to $q\bar{q}$ production as one finds KK modes propagating as intermediate states in these processes (e.g. in 4 fermion amplitudes). The

overlap of the KK mode wavefunctions with that of the quarks determines the coupling strength of these processes. For example, in warped extra dimensional scenarios, the KK modes are localized in the highly warped (or the so called infrared) region so are the heavy quarks. In these scenarios, the production of $t\bar{t}$ is dominant among such 4-fermion amplitudes. Given that phenomenological constraints imply that string states are generically at most a factor of a few heavier than the lightest KK modes [70, 84, 85] in Randall-Sundrum like scenarios, it is worthwhile to explore warped extra dimensional models in the context of string theory⁵. For example, the open string wavefunctions obtained in [88] and the effective action describing closed string fluctuations (massless and KK modes) in warped compactifications [89, 90]⁶ may be useful in determining the aforementioned amplitudes. Furthermore, quarks with different chiralities can attribute differently to these amplitudes, as they have a different origin in D-brane constructions. The left-handed quarks are doublets under the weak interaction and so the corresponding open strings end on the weak $SU(2)$ branes whereas those associated with the right-handed quarks do not. Thus, e.g., in the Drell-Yan process $q\bar{q} \rightarrow \ell\bar{\ell}$, certain parts of the amplitudes are only attributed to the left-handed quarks [62]. Similar features are expected for processes involving quark final states such as $q\bar{q} \rightarrow t\bar{t}$. It would be interesting to study whether measurements of these chiral couplings can be used to distinguish between different string theory models.

⁵Even within an effective field theory context, the kinds of warped geometries arising in string theory have motivated new model building possibilities, see, e.g., [86, 87].

⁶For some earlier work discussing issues in the effective theory of warped string compactifications, see e.g., [91–93].

Chapter 4

Baryon Number Violating Processes with Top Quarks

¹In the Standard Model (SM) for fundamental interactions, baryon (B) and lepton (L) numbers, associated with accidental global symmetries, are classically conserved quantities; a (tiny) violation is, however, induced by non-perturbative effects [95]. Baryon number violation (BNV) also naturally occurs in Supersymmetry [96], in Grand Unified Theories [97], where BNV is notably mediated by new gauge bosons, and in black hole physics [98]. The cosmological production of matter from a matter–anti-matter symmetric initial condition moreover requires B to have been violated in the early Universe [99].

On the other hand, experimental constraints on several BNV processes have reached impressive heights. Nucleon decay channels provide the best examples, though baryon-number-violating decays of the τ lepton or, much more recently, of heavy mesons have also been investigated [100]. These latter measurements opened the way for direct experimental tests of the baryon number conservation law within the second and third generations of quarks and leptons but have not really extended the range of energy scales. The only direct experimental constraints on BNV beyond the GeV scale are bounds on the $Z \rightarrow p e^-$, $p \mu^-$ branching ratios obtained at LEP [100]. The LHC comes

¹This section is based on the paper by Z.D., *et. al.* [94].

as a natural step forward in probing the baryon number conservation law beyond the TeV scale and the first generation. In particular, with a very large production rate and unique experimental signatures, top quarks are an interesting option: the top flavor can be clearly identified, the t and \bar{t} are distinguishable via the charged lepton in their decay, and the hadronization effects unimportant. Consequently, BNV could be probed at the quark level.

We choose to consider interactions involving one single top quark and a charged lepton. The presence of a single final state lepton produced from the proton-proton initial state implies a total change in lepton number $\Delta L = \pm 1$, and, by conservation of angular momentum $\Delta(L + 3B) \in 2\mathbb{Z}$, requires a simultaneous violation of B . Thus a single charged lepton without missing energy points toward BNV. In the presence of neutrinos in the production process, though, the lepton number is intractable. Consequently, baryon-number-violating processes would be more difficult to identify unambiguously, and could, for instance, be confused with flavor-changing neutral currents [101, 102].

4.1 Effective operators

The effective BNV Lagrangian can easily be built out of five lowest dimensional effective operators [103–105] that preserve Lorentz invariance and $SU(3)_C \otimes SU(2)_L \otimes U(1)_Y$ gauge symmetries, along with an accidental global $B - L$ symmetry. Following the notation of Ref. [103], we write

$$\mathcal{L}_{\text{BNV}}^{\text{dim}=6} = \frac{1}{\Lambda^2} \sum_{i=1}^5 c_i O^{(i)}, \quad (4.1)$$

where c_i are the effective (dimensionless) coefficients of the corresponding operators $O^{(i)}$ and Λ is the mass scale associated with physics responsible for BNV beyond the Standard

Model.

Expanding $SU(2)_L$ indices in operators $O^{(1-5)}$ and identifying one up-type quark as the top, the effective terms that do not contain neutrinos can be parametrized as linear combinations of only two operators (and their Hermitian conjugates),

$$\begin{aligned} O^{(s)} &\equiv \epsilon^{\alpha\beta\gamma} [\bar{t}_\alpha^c (aP_L + bP_R) D_\gamma] [\bar{U}_\beta^c (cP_L + dP_R) E], \\ O^{(t)} &\equiv \epsilon^{\alpha\beta\gamma} [\bar{t}_\alpha^c (a'P_L + b'P_R) E] [\bar{U}_\beta^c (c'P_L + d'P_R) D_\gamma], \end{aligned} \quad (4.2)$$

where D, U, E respectively denote generic down-, up-type quarks and charged leptons. We emphasize that fermions in Eq. (4.2) are taken as mass eigenstates. Charge conjugated fields are defined as $\psi^c \equiv C\bar{\psi}^T$ with C , the charge conjugation matrix; $2P_{L/R} \equiv 1 \mp \gamma^5$; colors are labeled by Greek indices; a, a', \dots are fermion-flavor-dependent effective parameters.

Three comments are in order. First, the $(s), (t)$ labeling in Eq. (4.2) reminds that the scale Λ in Eq. (4.1) may be linked to the mass of a heavy mediator (with electric charge 1/3) exchanged in s or t channels, respectively. If so identified, then the coupling parameters a, a', \dots could be naturally of the order of unity. We stress that the operator $O^{(u)} \equiv \epsilon^{\alpha\beta\gamma} [\bar{t}_\alpha^c P_L U_\beta] [\bar{D}_\gamma^c P_L E]$ arising from $O^{(4)}$ and possibly associated with a mediator of electric charge 4/3 exchanged in the u channel does not need to be introduced at the effective level. The reason is that the Schouten identity,

$$[CP_L]_{ij}[CP_L]_{kl} - [CP_L]_{ik}[CP_L]_{jl} + [CP_L]_{il}[CP_L]_{jk} = 0,$$

can be used to express $O^{(u)}$ in terms of $O^{(s)}$ and $O^{(t)}$, *i.e.*, $O^{(u)} = -O^{(s)}(a = c = 1, b = d = 0) - O^{(t)}(a' = c' = 1, b' = d' = 0)$. Second, heavy gauge mediators (vectors) give rise to $O^{(1,2)}$ only [103, 106], which in our basis, Eq. (4.2), entails $a = 0 = d$ or $b = 0 = c$ (or primed analogs). Third, operators involving two top quarks can also be obtained

from Eq. (4.2) by substituting t for U . Note, however, that in this case $O^{(s)}$ and $O^{(t)}$ are no longer independent and considering only one of the two is then sufficient. Such operators could, for example, mediate processes like $e^-d \rightarrow \bar{t}\bar{t}$ in future e^-p colliders, or $gd \rightarrow \bar{t}\bar{t}e^+$ at the LHC.

4.2 Processes

At the LHC, possibly relevant BNV processes involving a top quark are

$$\begin{aligned} t &\xrightarrow{\text{BNV}} \bar{U} \bar{D} E^+ \quad (\text{decay}) \\ U D &\xrightarrow{\text{BNV}} \bar{t} E^+ \quad (\text{production}) \end{aligned} \tag{4.3}$$

(and their charge conjugate analogs) where, in the first case, top quarks are produced through SM processes. Since, as mentioned above, a single charged lepton without any missing transverse energy (\cancel{E}_T) in the final state is a clear signal for BNV, it is simpler to avoid signatures that lead to neutrinos in the final state. Fully reconstructed top leptonic decays could be considered in more refined analyses. We also note that the flavor assignments can be very relevant from the phenomenological point of view. In decay, heavy flavors such as charm and bottom could be tagged in jets. In production, the relevance of initial quark flavors is determined also by proton parton distribution functions (PDFs).

Neglecting all fermion masses but the top one, m_t , and using the algebraic rules introduced in Ref. [107], the squared amplitude for the processes in Eq. (4.3) induced

by the operators of Eq. (4.2) reads

$$\begin{aligned} \sum_{\text{spin,color}} |\mathcal{M}|^2 = \frac{24}{\Lambda^4} & \left[(p_t \cdot p_D) (p_U \cdot p_E) (A + C) \right. \\ & - (p_t \cdot p_U) (p_D \cdot p_E) C \\ & \left. + (p_t \cdot p_E) (p_D \cdot p_U) (B + C) \right] \end{aligned} \quad (4.4)$$

where

$$\begin{aligned} A &\equiv (|a|^2 + |b|^2) (|c|^2 + |d|^2), \\ B &\equiv (|a'|^2 + |b'|^2) (|c'|^2 + |d'|^2), \\ C &\equiv \Re\{a^* c^* a' c' + b^* d^* b' d'\}, \end{aligned} \quad (4.5)$$

arise respectively from the square of $O^{(s)}$, of $O^{(t)}$ and from the interference between these two operators.

For a BNV decay, we obtain the following partial width:

$$\begin{aligned} \Gamma_t^{\text{BNV}} &= \int_0^{m_t/2} dE_E \frac{m_t^2 E_E^2}{32\pi^3 \Lambda^4} \left[\left(\frac{A}{3} + B + C \right) \left(1 - \frac{2E_E}{m_t} \right) + \frac{A}{6} \right] \\ &= \frac{m_t^5}{192\pi^3} \frac{1}{16\Lambda^4} [A + B + C], \end{aligned}$$

where E_E is the lepton energy in the top rest frame. In Fig. 14, we compare the charged lepton energy spectrum in a SM decay to that in a BNV decay for three different representative choices of A, B and C . Inputting the SM width for the top quark (1.4 GeV), the BNV branching ratio can be conveniently written as

$$\text{Br}_t^{\text{BNV}} = 1.2 \times 10^{-6} \left(\frac{m_t}{173 \text{ GeV}} \right)^5 \left(\frac{1 \text{ TeV}}{\Lambda} \right)^4 [A + B + C].$$

Taking the $t\bar{t}$ production cross section at the 7 (14) TeV LHC to be 150 (950) pb, we can expect 0.35 (2.2)/fb⁻¹ BNV top decays if $A + B + C = 1$, for each allowed flavor combination.

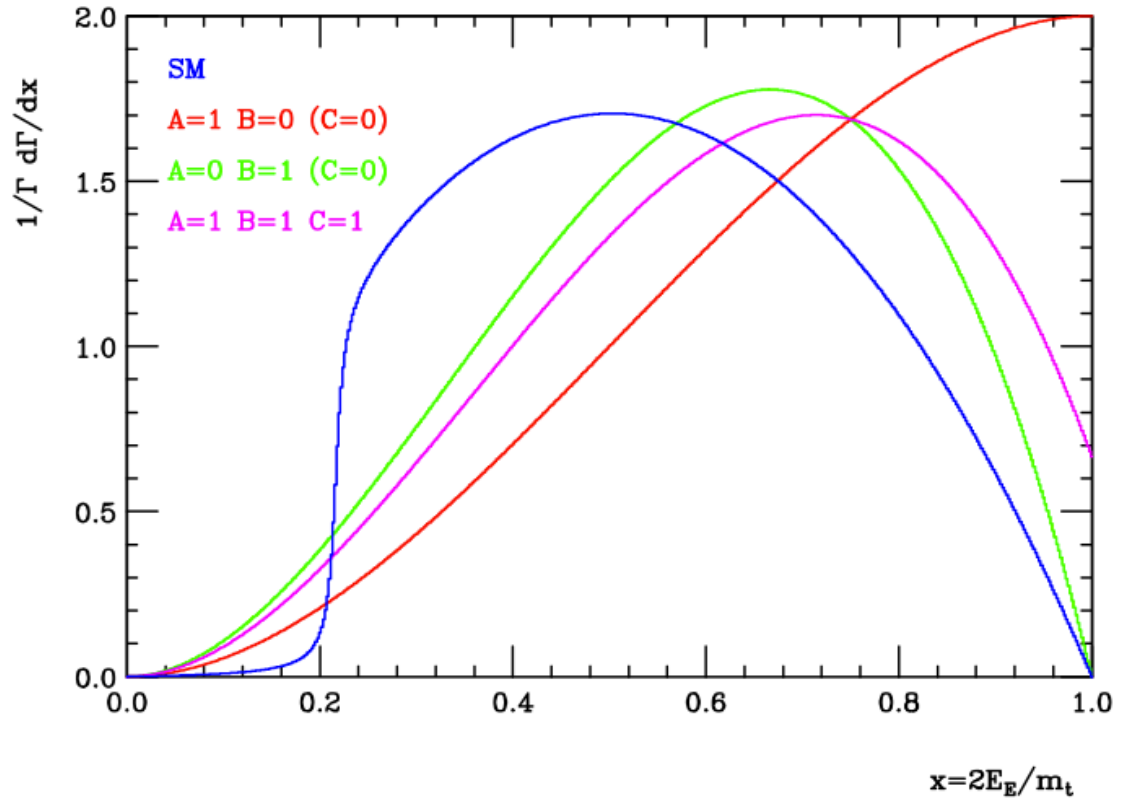


Figure 14: Energy spectrum of the charged lepton in the SM $t \rightarrow bE^+\nu_E$ (blue curve) and in BNV $t \rightarrow \bar{U}\bar{D}E^+$ top decays.

For BNV production, the partonic cross section reads

$$\begin{aligned}\hat{\sigma}_t^{\text{BNV}} &= \frac{1}{96\pi\Lambda^4} \int_{m_t^2-\hat{s}}^0 d\hat{t} \left[A \frac{\hat{t}(\hat{t}-m_t^2)}{\hat{s}^2} + B \frac{(\hat{s}-m_t^2)}{\hat{s}} + 2C \frac{\hat{t}}{\hat{s}} \right] \\ &= \frac{\hat{s}}{96\pi\Lambda^4} \left(1 - \frac{m_t^2}{\hat{s}} \right)^2 \left[\left(\frac{A}{3} + B + C \right) + \frac{m_t^2}{\hat{s}} \frac{A}{6} \right],\end{aligned}\quad (4.6)$$

with the Mandelstam variables $\hat{s} \equiv (p_U + p_D)^2$ and $\hat{t} \equiv (p_U - p_E)^2$. As expected from dimensional arguments the cross section induced by the operators in Eq. (4.2) grows as \hat{s}/Λ^4 . However, in setting lower bounds on the scale of new physics, it is important to always keep in mind that the validity (and unitarity) of the effective field theory itself assumes $\hat{s} \ll \Lambda^2$.

Out of the six possible initial quark flavor assignments, (namely, ud , us , ub , cd , cs and cb), we consider

$$\begin{aligned}u d \rightarrow \bar{t} E^+ &\quad - \quad \text{the most PDF - favored,} \\ u b \rightarrow \bar{t} e^+ &\quad - \quad \text{possibly flavor - unsuppressed,} \\ c b \rightarrow \bar{t} \mu^+ &\quad - \quad \text{the most PDF - suppressed,} \\ &\quad - \quad \text{possibly flavor - unsuppressed,}\end{aligned}$$

as well as their charge conjugate analogs. Operators with two pairs of fermions in the same generation could be favored by the flavor structure of the underlying theory. In Table 6, we collect the cross sections for the different processes at the LHC with $\sqrt{s} = 7$ (14) TeV. To enforce unitarity and not to artificially overestimate cross sections, we impose $\sqrt{\hat{s}} < \Lambda$. This cut has an important effect on valence quark initiated processes but a very mild one on processes initiated by sea quarks.

$\sigma[\text{fb}]$	$ud \rightarrow \bar{t}E^+$	$ub \rightarrow \bar{t}e^+$	$cb \rightarrow \bar{t}\mu^+$
$A \ B \ C$	$\bar{u}\bar{d} \rightarrow tE^-$	$\bar{u}\bar{b} \rightarrow te^-$	$\bar{c}\bar{b} \rightarrow t\mu^-$
1 0 0	250 (690)	30 (150)	1.2 (10)
	14 (74)	3.1 (21)	1.2 (10)
0 1 0	910 (1 900)	110 (440)	3.7 (28)
	45 (220)	9.1 (60)	3.7 (28)
1 1 1	2 100 (4 600)	240 (980)	9.1 (66)
	110 (500)	22 (140)	9.1 (66)

Table 6: Cross sections (fb) for representative BNV production processes at the LHC, with three different choices of A, B and C , $\sqrt{s} < \Lambda = 1 \text{ TeV}$, $\sqrt{s} = 7 \text{ TeV}$ (14 TeV in parentheses) and CTEQ6L1 PDF [108] (renormalization and factorization scales set at $m_t = 173 \text{ GeV}$).

4.3 LHC searches

We now briefly discuss BNV signatures at the LHC. For the sake of illustration we make a definite choice for the fermion flavors in Eq. (4.3) and consider

1. BNV decay: $pp \xrightarrow{\text{SM}} t\bar{t}$ with the top decaying via a BNV interaction $t \xrightarrow{\text{BNV}} \bar{b}\bar{c}\mu^+$ and the anti-top decaying fully hadronically, which leads to the $\mu^+ + 5\text{-jet}$ final state;
2. BNV production: $pp \xrightarrow{\text{BNV}} \bar{t}\mu^+$ with u, d flavors in the initial state, the anti-top decaying fully hadronically, leading to $\mu^+ + 3 \text{ jets}$.

The first interesting observation is that there are no irreducible backgrounds to such signatures as both of them have no \cancel{E}_T . On the other hand, processes resulting from a leptonically decaying W with a small reconstructed \cancel{E}_T could mimic the signal. A proper investigation of such backgrounds requires not only parton showering, hadronization

and realistic detector simulation but also data driven methods. However, a few relevant observations can already be made with a simple parton-level simulation. To this aim, we have implemented BNV interactions in MADGRAPH 5 [109] via FEYNRULES [110] and generated events for both signal and representative backgrounds in the same simulation framework.

The search for BNV decays proceeds through the selection of $\mu^+ + 5$ jets with an upper cut on the \cancel{E}_T . The presence of two tops, one hadronically decaying W and possibly two b -tagged jets can be efficiently used to better reconstruct the event kinematics. In addition, note that the BNV decay of a top quark gives $\mu^+ \bar{b}$ at variance with the SM semi-leptonic decay which gives $\mu^+ b$. Determining the bottom quark charge (*e.g.*, via a lepton tag) in the BNV decay could therefore offer crucial discrimination power. The main SM backgrounds to this signature come from $t \bar{t} + 1$ jet and $W^+ + 5$ jets, the former being dominant after b tagging.

The search for BNV production proceeds through the selection of $\mu^+ + 3$ jets with an upper cut on the \cancel{E}_T . The reconstruction is simpler than in the BNV decay search, as there is no combinatorial background and the top and W mass constraints can be used to improve the resolution on the signal kinematics. In Fig. 15, we compare the p_T of the charged lepton in the signal to that of the $W^+ + 3$ -jet and $\bar{t} W^+$ (with $W^+ \rightarrow \mu^+ \nu_\mu$) backgrounds. We require three central jets ($p_T > 40$ GeV, $|\eta| < 2.5$, $\Delta R_{jj} > 0.5$), a central isolated lepton ($|\eta| < 2.5$, $\Delta R_{j\mu} > 0.5$) and $\cancel{E}_T < 30$ GeV. In the $W^+ + 3$ -jet background we also demand $|m_{jjj} - m_t| < 40$ GeV and a b tag. As expected from the \hat{s} enhancement in the cross section, eventually tamed by requiring $\sqrt{\hat{s}} < \Lambda = 1$ TeV, the p_T distribution of the lepton in the signal is much harder than in the backgrounds.

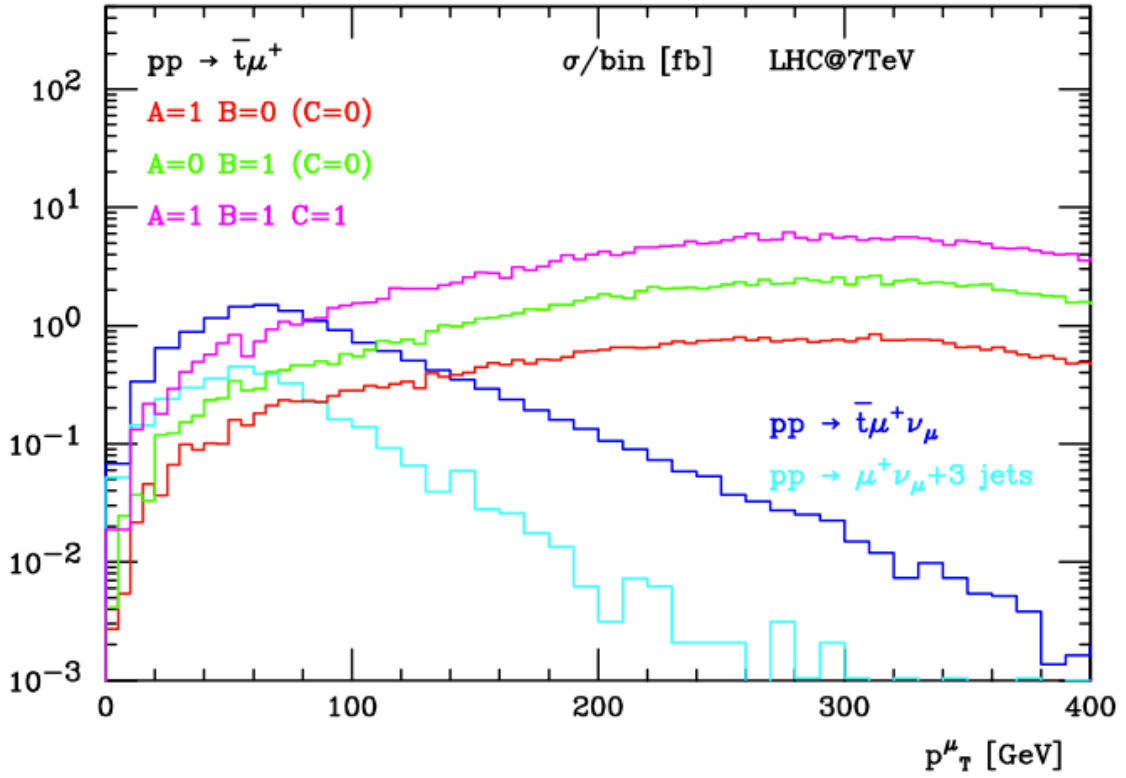


Figure 15: Transverse momentum for the charged lepton in the BNV production signal $\bar{t}\mu^+$ (from ud initial state) and in the $W^++3\text{-jet}$ and $\bar{t}W^+$ backgrounds. Top quarks are decayed hadronically. Selection cuts on the three jets and the muon are given in the text.

The LHC reach for the processes in Table 6 can be expressed in terms of the minimal value for the parameters defined in Eq. (4.5) leading to a sensitivity $S/\sqrt{S+B} \geq 5$. For the sake of illustration we consider 30 (100) fb⁻¹ of collected luminosity at the LHC for $\sqrt{s} = 7$ (14) TeV, the event selection described in the above paragraph with the additional requirement $p_T > 150$ GeV for the charged lepton (one flavor), both t and \bar{t} production, only the tW background, and $A = B = C$. In so doing, we find

$$u d \rightarrow t E : \quad A, B, C \geq 0.0076 \quad (0.0046)$$

$$u b \rightarrow t e : \quad A, B, C \geq 0.084 \quad (0.026)$$

$$c b \rightarrow t \mu : \quad A, B, C \geq 1.6 \quad (0.21)$$

which point to a sensitivity at the $10^{-1} - 10^{-2}$ level for the effective coefficients c_i of Eq. (4.1) at the TeV scale.

Finally, we stress that, for both BNV production and decay signatures, selecting high- p_T tops could be advantageous. In this limit, the BNV production signal is enhanced with respect to the backgrounds, while for the BNV decay search, top decay products might cluster into one jet, curbing, for instance, the combinatorial problems in the $\mu^+ + 5$ -jet signature and also controlling better \cancel{E}_T uncertainties. To this aim, efficient boosted reconstruction techniques for the top quark should be employed [111].

4.4 Indirect constraints

In principle, the operators considered in Eq. (4.2) also contribute indirectly to nucleon decays [112] through tree and/or loop diagrams. Tree-level diagrams with one W -emission, such as that in Fig. 16a provide formidable high lower bounds on Λ (or equivalently upper bounds on the effective parameters) if the lepton is not a τ . In fact, two W -emissions

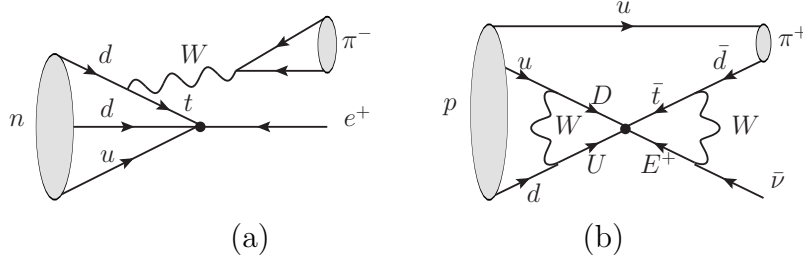


Figure 16: Representative (a) tree-level and (b) two-loop-level diagrams involving the BNV operators given in Eq. (4.2) and leading, in principle, to nucleon decay.

are needed for a $udt\tau$ -operator to be relevant in nucleon decays and the constraints become weaker. Moreover, if the dominant BNV dimension-six operators only involve the third and second generations of quarks and leptons, three W -emissions are required, and the rate is suppressed to a level consistent with the data. In BNV production, these theoretical considerations tend to favor the PDF-suppressed processes of Table 6. By considering a single operator contribution at a time, with fixed flavors in the two-loop diagram of Fig. 16b, extremely small upper bounds on the effective parameters can also be obtained [112]. Yet, strong cancellations may occur when summing over all possible $UDUE$ virtual contributions and allow effective parameters to be large (say, of order one). Mechanisms that could lead to such *GIM-like* cancellations at one- and two-loop level remain to be examined within a complete theory for flavor, starting from dimension-six BNV operators expressed in terms of weak eigenstates.

Chapter 5

Summary

Although the Standard Model has been quite successful in explaining high energy particle physics phenomena up to the energy scale reached by the current collider experiments, people believe there is deeper underlining theory governing the desert between the electroweak scale and the Planck scale and giving rise to the electroweak symmetry breaking and Higgs mass, which is the last missing piece of the Standard Model measurements.

We study the discovery potential of high scale physics via top quarks at the Large Hadron Collider.

For the study of string resonance decaying to $t\bar{t}$ final state, we point out that top quark pair production is a promising and an advantageous channel for studying such resonances, due to their low Standard Model background and unique kinematics. We find that string resonances for a string scale below 4 TeV can be detected via the $t\bar{t}$ channel at the LHC, either from reconstructing the $t\bar{t}$ semi-leptonic decay or recent techniques in identifying highly boosted tops.

For the study of baryon number violation processes involving top quark, we find that subject to strong experimental constraints at low energies, baryon number violation is nonetheless well motivated from a theoretical point of view. We adopt a model independent effective approach and focus on operators with minimal mass-dimension.

Corresponding effective coefficients could be directly probed at the Large Hadron Collider (LHC) already with an integrated luminosity of 1 inverse femtobarn at 7 TeV, and further constrained with 30 (100) inverse femtobarns at 7 (14) TeV.

To conclude the discussion in this thesis, high scale physics is under the spotlight with the LHC reaching the TeV scale, and being a golden key for new physics searches, the study of top quark physics at high scale will keep in great demand with remarkable pace.

Appendix A

Physical Degrees of Freedom

Counting for $n = 1$ Resonance

Here we focus on gluons and their excited string modes. In D-brane model building, the gluons are realized as open strings attached to a stack of 3 D-branes, forming adjoint representation of a $U(3)$ gauge group. The gluons are represented by a vertex operator:

$$T^a e_\mu \psi_{-\frac{1}{2}}^\mu |0; k\rangle \quad (\text{A.1})$$

where T^a is the Chan-Paton matrix, e_μ is the polarization vector of the gluon, $\psi_{-\frac{1}{2}}$ is a world-sheet fermion creation operator, and $|0; k\rangle$ is the open string vacuum state in the NS sector. Here we consider string states in 4 dimension, so the index μ goes over 0, 1, 2, 3 and the momentum k is a 4-dimensional momentum. We will use the $(-, +, +, +)$ signature. The gluons are massless, and are the lowest string states because the NS vacuum is projected out by the GSO projection. The physical state conditions constrain the momentum $k^2 = 0$ so this is a massless vector particle. The polarization vector also satisfies the physical state condition $e \cdot k = 0$ with the equivalence condition $e \cong e + k$.

We can write the vertex operator of gluons using the state-operator correspondence.

For open strings, we replace the bosonic and fermionic creation operators with world-sheet bosons and fermions as follows:

$$\begin{aligned}\alpha_{-m}^\mu &\rightarrow i\left(\frac{1}{2\alpha'}\right)^{\frac{1}{2}}\frac{1}{(m-1)!}\partial^m X, \\ \psi_{-r}^\mu &\rightarrow \frac{1}{(r-\frac{1}{2})!}\partial^{r-\frac{1}{2}}\psi^\mu\end{aligned}\tag{A.2}$$

The vertex operators for gluons in the -1 and 0 pictures are the following:

$$\begin{aligned}\mathcal{O}(z)_{-1} &= T^a e_\mu e^{-\phi} \psi^\mu(z) e^{ik \cdot X(z)}, \\ \mathcal{O}(z)_0 &= T^a e_\mu [i\partial X^\mu + (2\alpha')(k \cdot \psi)\psi^\mu] e^{ik \cdot X(z)}\end{aligned}\tag{A.3}$$

Now we consider the next level of string states. Because of the GSO projection, the next level number is $\frac{3}{2}$. They will be referred to as the first excited string modes (or $n = 1$ string modes), and we refer to the gluons as $n = 0$ string modes. Using the bosonic and fermionic creation operators, a general $n = 1$ open string state can be written as

$$|\chi\rangle = [(\xi_1)_\mu \psi_{-\frac{3}{2}}^\mu + (\xi_2)_{\mu\nu} \psi_{-\frac{1}{2}}^\mu \alpha_{-1}^\nu + (\xi_3)_{\mu\nu\rho} \psi_{-\frac{1}{2}}^\mu \psi_{-\frac{1}{2}}^\nu \psi_{-\frac{1}{2}}^\rho] |0; k\rangle\tag{A.4}$$

where $(\xi_3)_{\mu\nu\rho}$ is antisymmetric since the fermionic operators $\psi_{-\frac{1}{2}}$ anti-commute.

We will use the OCQ (old covariant quantization) method for quantizing string theory, as we only need to deal with the matter sector in this formulation. The physical state conditions for $|\chi\rangle$ are as follows:

$$(L_0 - \frac{1}{2})|\chi\rangle = 0, \quad L_1|\chi\rangle = 0, \quad G_{\frac{1}{2}}|\chi\rangle = 0, \quad G_{\frac{3}{2}}|\chi\rangle = 0\tag{A.5}$$

Here the L_m and G_r are superconformal Virasoro generators for the matter sector on the world-sheet, and the constant $-\frac{1}{2}$ in the first equation takes into account the contributions from the ghost sector in the NS vacuum. The superconformal Virasoro generators

are:

$$\begin{aligned}
L_m &= \frac{1}{2} \sum_{n \in \mathcal{Z}} : \alpha_{m-n}^\mu \alpha_{\mu n} : + \frac{1}{4} \sum_{r \in \mathcal{Z} + \frac{1}{2}} (2r - m) : \psi_{m-r}^\mu \psi_{\mu r} : + a \delta_{m0}, \\
G_r &= \sum_{n \in \mathcal{Z}} \alpha_n^\mu (\psi_\mu)_{r-n}
\end{aligned} \tag{A.6}$$

Here the constant $a = 0$ in the NS sector, and the zero mode bosonic generator is related to the momentum $\alpha_0^\mu = (2\alpha')^{\frac{1}{2}} k^\mu$ for the open string sector we consider. The $::$ denotes normal ordering of creation operators with negative indices and annihilation operators with positive indices.

The zero mode of the Virasoro generator is $L_0 = \alpha' k^2 + N$ where $N = \frac{3}{2}$ is the level number for the string state $|\chi\rangle$ in (A.4), so the the first physical state condition in (A.5) gives $k^2 = -\frac{1}{\alpha'}$. The mass of the $n = 1$ string mode $|\chi\rangle$ is

$$m = \frac{1}{\sqrt{\alpha'}} \equiv M_s \tag{A.7}$$

Using the commutation relation of the bosonic and fermionic operators $\{\psi_r^\mu, \psi_s^\nu\} = \eta^{\mu\nu} \delta_{r,-s}$, $[\alpha_m^\mu, \alpha_n^\nu] = m \eta^{\mu\nu} \delta_{m,-n}$, we find that the rest of the physical state conditions in (A.5) are given by:

$$\begin{aligned}
(2\alpha')^{\frac{1}{2}} (\xi_1) \cdot k + (\xi_2)_{\mu\nu} \eta^{\mu\nu} &= 0 \\
(\xi_1)_\nu + (2\alpha')^{\frac{1}{2}} k^\mu (\xi_2)_{\mu\nu} &= 0 \\
(\xi_2)_{\mu\nu} - (\xi_2)_{\nu\mu} + 6(2\alpha')^{\frac{1}{2}} k^\rho (\xi_3)_{\mu\nu\rho} &= 0
\end{aligned} \tag{A.8}$$

We also need to consider possible “null states” which are states that can be written as $L_n|\phi\rangle$ or $G_r|\phi\rangle$ with $n, r > 0$ for any state $|\phi\rangle$. It turns out that at this level $\frac{3}{2}$, all physical states satisfying the constraints (A.8) are not null. An intuitive understanding is that because the $n = 1$ states are massive, all physical polarizations are non-trivial,

as opposed to the case of massless vector particle where one does not have longitudinal polarization.

Let us count the physical degrees of freedom in 4 dimensions. Since the polarization tensor ξ_3 is antisymmetric, the total number of polarization before taking into account the physical state condition is $4 + 4 \times 4 + 4 = 24$. The physical state condition (A.8) imposes 11 conditions, so we have $24 - 11 = 13$ physical degree of freedom. In 4 dimension, a massive spin J particle has $2J + 1$ physical degrees of freedom. From the calculations in a previous work [68], we know the $n = 1$ string modes include two $J = 0$ particles, one of which decays exclusively to two gluons with $(++)$ helicity and the other to two gluons with $(--)$ helicity. Therefore, the 13 degrees of freedom correspond naturally to that of one $J = 2$, two $J = 1$, and two $J = 0$ string resonance modes.

Using the state-operator correspondence (A.2), we can easily write the vertex operator for the $n = 1$ string mode (A.4) in the (-1) picture as follows:

$$\mathcal{O}(z) = [(\xi_1)_\mu \partial \psi^\mu + \frac{i}{(2\alpha')^{\frac{1}{2}}} (\xi_2)_{\mu\nu} \partial X^\mu \psi^\nu + (\xi_3)_{\mu\nu\rho} \psi^\mu \psi^\nu \psi^\rho] T^a e^{-\phi(z)} e^{ik \cdot X(z)} \quad (\text{A.9})$$

Appendix B

Complete set of independent operators

We discuss here the independent operators respecting $SU(3)_C \otimes SU(2)_L \otimes U(1)_{Y/2}$ and Lorentz symmetries while violating baryon (and lepton) number(s) (with $B - L$ conserved).

Let us first remind a few equalities concerning Lorentz scalar and vector bi- or quadri-linears made of chiral fields. They are extensively used to manipulate operators and obtain the results presented below. We have:

$$[CP_{R,L}]_{pq} = -[CP_{R,L}]_{qp} \quad \text{and} \quad [C\gamma^\mu P_{R,L}]_{pq} = [C\gamma^\mu P_{L,R}]_{qp}, \quad (\text{B.1})$$

$$[CP_{R,L}]_{pq}[CP_{R,L}]_{rs} - [CP_{R,L}]_{pr}[CP_{R,L}]_{qs} + [CP_{R,L}]_{ps}[CP_{R,L}]_{qr} = 0, \quad (\text{B.2})$$

$$[C\gamma^\mu P_{R,L}]_{pq}[C\gamma_\mu P_{R,L}]_{rs} = -[C\gamma^\mu P_{R,L}]_{ps}[C\gamma_\mu P_{R,L}]_{qr}, \quad (\text{B.3})$$

$$[C\gamma^\mu P_{R,L}]_{pq}[C\gamma_\mu P_{L,R}]_{rs} = +2[CP_{L,R}]_{ps}[CP_{R,L}]_{qr}. \quad (\text{B.4})$$

We start from the operators' classification of [103–105]:

$$\begin{aligned}
O_{abcd}^{(1)} &\equiv (\bar{d}^c)_a^\alpha (u)_b^\beta (\bar{q}^c)_c^{i\gamma} (l)_d^j \quad \epsilon_{\alpha\beta\gamma} \quad \epsilon_{ij}, \\
O_{abcd}^{(2)} &\equiv (\bar{q}^c)_a^{i\alpha} (q)_b^{j\beta} (\bar{u}^c)_c^\gamma (e)_d \quad \epsilon_{\alpha\beta\gamma} \quad \epsilon_{ij}, \\
O_{abcd}^{(3)} &\equiv (\bar{q}^c)_a^{i\alpha} (q)_b^{j\beta} (\bar{q}^c)_c^{k\gamma} (l)_d^l \quad \epsilon_{\alpha\beta\gamma} \quad \epsilon_{ij} \epsilon_{kl}, \\
O_{abcd}^{(4)} &\equiv (\bar{q}^c)_a^{i\alpha} (q)_b^{j\beta} (\bar{q}^c)_c^{k\gamma} (l)_d^l \quad \epsilon_{\alpha\beta\gamma} \quad [\epsilon\boldsymbol{\tau}]_{ij} \cdot [\epsilon\boldsymbol{\tau}]_{kl}, \\
O_{abcd}^{(5)} &\equiv (\bar{d}^c)_a^\alpha (u)_b^\beta (\bar{u}^c)_c^\gamma (e)_d \quad \epsilon_{\alpha\beta\gamma},
\end{aligned}$$

with the $\psi^c = C\bar{\psi}^T$ and therefore $\bar{\psi}^c = \psi^T C$ and $\boldsymbol{\tau}_j^i$ the Pauli matrices. This is a complete and independent set (basis) of B -violating operators constructed with the fields and preserving the symmetries of the Standard Model. Note the sixth operator of [103] can be re-expressed in terms of $O^{(5)}$ and $O^{(3,4)}$ alternatively rewritten as combinations of a new $\tilde{O}^{(4)}$ [105, Eq. (1.6) – (1.9)].

These five operators can be interpreted as originating from the exchange of heavy bosons. The exhaustive list of their possible transformation properties under $SU(3)_C \otimes SU(2)_L \otimes U(1)_{Y/2}$ is the following [103]:

- $(\mathbf{3}, \mathbf{1}, -1/3)$ scalar for $O^{(1,2,3,5)}$ or tensor for $O^{(3,5)}$,
- $(\mathbf{3}, \mathbf{3}, -1/3)$ scalar or tensor for $O^{(4)}$,
- $(\mathbf{3}, \mathbf{1}, -4/3)$ scalar for $O^{(5)}$,
- $(\mathbf{3}, \mathbf{2}, -5/6)$ vector for $O^{(1,2)}$ and,
- $(\mathbf{3}, \mathbf{2}, 1/6)$ vector for $O^{(1)}$.

Instead of $O^{(1,2)}$, we can indeed choose equivalent vector operators, for instance:

$$\begin{aligned}
O_{abcd}^{(1)V} &\equiv (\bar{d}^c)_a^\alpha \gamma^\mu (q)_b^{i\beta} (\bar{u}^c)_c^\gamma \gamma_\mu (l)_d^j \quad \epsilon_{ij} \quad \epsilon_{\alpha\beta\gamma} = -2O_{acbd}^{(1)}, \\
O_{abcd}^{(2)V} &\equiv (\bar{q}^c)_a^{i\alpha} \gamma^\mu (u)_b^\beta (\bar{q}^c)_c^{j\gamma} \gamma_\mu (e)_d \quad \epsilon_{ij} \quad \epsilon_{\alpha\beta\gamma} = -2O_{acbd}^{(2)}.
\end{aligned}$$

We can form an equivalent basis with $SU(2)_L$ indices expanded. Given the notation convention $\overline{\psi_{L,R}^c} \equiv (\overline{\psi_{L,R}})^c$, we have the following complete set of independent operators:

$$\begin{aligned}
O_{abcd}^{(a)} &\equiv (\overline{u_R^c})_a^\alpha (d_R)_b^\beta (\overline{u_L^c})_c^\gamma (e_L)_d \epsilon_{\alpha\beta\gamma}, & O_{abcd}^{(a,\nu)} &\equiv (\overline{d_R^c})_a^\alpha (u_R)_b^\beta (\overline{d_L^c})_c^\gamma (\nu_L)_d \epsilon_{\alpha\beta\gamma}, \\
O_{abcd}^{(b)} &\equiv (\overline{u_L^c})_a^\alpha (d_L)_b^\beta (\overline{u_R^c})_c^\gamma (e_R)_d \epsilon_{\alpha\beta\gamma}, \\
O_{abcd}^{(c)} &\equiv (\overline{u_L^c})_a^\alpha (d_L)_b^\beta (\overline{u_L^c})_c^\gamma (e_L)_d \epsilon_{\alpha\beta\gamma}, & O_{abcd}^{(c,\nu)} &\equiv (\overline{d_L^c})_a^\alpha (u_L)_b^\beta (\overline{d_L^c})_c^\gamma (\nu_L)_d \epsilon_{\alpha\beta\gamma}, \\
O_{abcd}^{(d)} &\equiv (\overline{u_R^c})_a^\alpha (d_R)_b^\beta (\overline{u_R^c})_c^\gamma (e_R)_d \epsilon_{\alpha\beta\gamma}.
\end{aligned}$$

The alternative vector operators for $O^{(a,b)}$,

$$\begin{aligned}
O_{abcd}^{(a)V} &\equiv (\overline{u_L^c})_a^\alpha \gamma^\mu (d_R)_b^\beta (\overline{u_R^c})_c^\gamma \gamma_\mu (e_L)_d \epsilon_{\alpha\beta\gamma}, & O_{abcd}^{(a,\nu)V} &\equiv (\overline{d_L^c})_a^\alpha \gamma^\mu (u_R)_b^\beta (\overline{d_R^c})_c^\gamma \gamma_\mu (\nu_L)_d \epsilon_{\alpha\beta\gamma}, \\
O_{abcd}^{(b)V} &\equiv (\overline{u_R^c})_a^\alpha \gamma^\mu (d_L)_b^\beta (\overline{u_L^c})_c^\gamma \gamma_\mu (e_R)_d \epsilon_{\alpha\beta\gamma},
\end{aligned}$$

satisfy $O_{abcd}^{(\cdot)V} = 2O_{cbad}^{(\cdot)}$. The explicit correspondence with the $O^{(1,2,3,4,5)}$ basis is established by the following equalities:

$$O_{abcd}^{(1)} = -O_{bacd}^{(a)} - O_{abcd}^{(a,\nu)}, \quad (\text{B.5})$$

$$O_{abcd}^{(2)} = O_{abcd}^{(b)} + O_{bacd}^{(b)}, \quad (\text{B.6})$$

$$\begin{aligned}
O_{abcd}^{(3)} &= O_{abcd}^{(c)} + O_{bacd}^{(c)} \\
&\quad + O_{abcd}^{(c,\nu)} + O_{bacd}^{(c,\nu)}, \quad (\text{B.7})
\end{aligned}$$

$$\begin{aligned}
O_{abcd}^{(4)} &= O_{abcd}^{(c)} - O_{bacd}^{(c)} + 2O_{bcad}^{(c)} \\
&\quad + O_{abcd}^{(c,\nu)} - O_{bacd}^{(c,\nu)} - 2O_{bcad}^{(c,\nu)}, \quad (\text{B.8})
\end{aligned}$$

$$O_{abcd}^{(5)} = -O_{bacd}^{(d)}. \quad (\text{B.9})$$

Let us now focus on operators involving one top quark and no neutrino. Choosing to work in the scalar operators basis, we have four operators that do not involve neutrino,

$O^{(a,b,c,d)}$, with for each of them two possible assignments for the top flavor: $a \rightarrow t$ or $c \rightarrow t$. The eight operators obtained in this way can then be gathered in the following compact form:

$$\begin{aligned}
O_{abc}^{(s)} &\equiv (\bar{t}^c)^\alpha (a + b\gamma^5)(d)_c^\gamma (\bar{u}^c)_b^\beta (c + d\gamma^5)(e)_a \quad \epsilon_{\alpha\beta\gamma}, \\
O_{abc}^{(t)} &\equiv (\bar{t}^c)^\alpha (a' + b'\gamma^5)(e)_a (\bar{u}^c)_b^\beta (c' + d'\gamma^5)(d)_c^\gamma \quad \epsilon_{\alpha\beta\gamma}.
\end{aligned} \tag{B.10}$$

Bibliography

- [1] G. Arnison *et al.* [UA1 Collaboration], Phys. Lett. B **166**, 484 (1986).
- [2] R. Ansari *et al.* [UA2 Collaboration], Phys. Lett. B **186**, 440 (1987).
- [3] F. Abe *et al.* [CDF Collaboration], Phys. Rev. Lett. **74**, 2626 (1995) [hep-ex/9503002].
- [4] S. Abachi *et al.* [D0 Collaboration], Phys. Rev. Lett. **74**, 2422 (1995) [hep-ex/9411001].
- [5] K. Kodama *et al.* [DONUT Collaboration], Phys. Lett. B **504**, 218 (2001) [hep-ex/0012035].
- [6] S. Weinberg, Phys. Rev. Lett. **19**, 1264 (1967); Phys. Rev. **D5**, 1412 (1972); A. Salam, in *Elementary Particle Theory: Relativistic Groups and Analyticity (Nobel Symposium No. 8*, ed. N. Svartholm (Almqvist and Wiksell, Stockholm, 1968); S. Glashow, Nucl. Phys. **22**, 579 (1961).
- [7] L. Alvarez-Gaume and E. Witten, Nucl. Phys. B **234**, 269 (1984).
- [8] G. 't Hooft, Nucl. Phys. B **35**, 167 (1971); G. 't Hooft and M. J. G. Veltman, Nucl. Phys. B **44**, 189 (1972); B. W. Lee and J. Zinn-Justin, Phys. Rev. D **5**, 3121 (1972).
- [9] F. Englert and R. Brout, Phys. Rev. Lett. **13**, 321 (1964); P. W. Higgs, Phys. Lett. **12**, 132 (1964); P. W. Higgs, Phys. Rev. **145**, 1156 (1966); G. S. Guralnik,

- C. R. Hagen and T. W. B. Kibble, Phys. Rev. Lett. **13**, 585 (1964); T. W. B. Kibble, Conf. Proc. C **670828**, 277 (1967).
- [10] P. Langacker, arXiv:0901.0241 [hep-ph].
- [11] E. S. Abers and B. W. Lee, Phys. Rept. **9**, 1 (1973); and references therein.
- [12] T. W. B. Kibble, Conf. Proc. C **670828**, 277 (1967).
- [13] Y. Nambu, Phys. Rev. Lett. **4**, 380 (1960); Y. Nambu and G. Jona-Lasinio, Phys. Rev. **122**, 345 (1961); J. Goldstone, Nuovo Cim. **19**, 154 (1961); J. Goldstone, A. Salam and S. Weinberg, Phys. Rev. **127**, 965 (1962).
- [14] N. Cabibbo, Phys. Rev. Lett. **10**, 531 (1963); M. Kobayashi and T. Maskawa, Prog. Theor. Phys. **49**, 652 (1973).
- [15] For a historical review of QCD, see for example, D. J. Gross, Proc. Nat. Acad. Sci. **102**, 9099 (2005) [Int. J. Mod. Phys. A **20**, 5717 (2005)] [Rev. Mod. Phys. **77**, 837 (2005)]; For a modern review of QCD, see for example, G. F. Sterman, hep-ph/0412013.
- [16] For the original works, see for example, D. J. Gross and F. Wilczek, Phys. Rev. D **8**, 3633 (1973); D. J. Gross and F. Wilczek, Phys. Rev. D **9**, 980 (1974); H. D. Politzer, Phys. Rept. **14**, 129 (1974).
- [17] M. Gell-Mann, Phys. Rev. **125**, 1067 (1962).
- [18] C. T. Hill and E. H. Simmons, Phys. Rept. **381**, 235 (2003) [Erratum-ibid. **390**, 553 (2004)] [hep-ph/0203079].

- [19] For the original work of technicolor see, for example, L. Susskind, Phys. Rev. D **20**, 2619 (1979); S. Weinberg, Phys. Rev. D **19**, 1277 (1979).
- [20] S. P. Martin, In *Kane, G.L. (ed.): Perspectives on supersymmetry II* 1-153 [hep-ph/9709356].
- [21] H. K. Dreiner, H. E. Haber and S. P. Martin, Phys. Rept. **494**, 1 (2010) [arXiv:0812.1594 [hep-ph]].
- [22] S. R. Coleman and J. Mandula, Phys. Rev. **159**, 1251 (1967).
- [23] R. Haag, J. T. Lopuszanski and M. Sohnius, Nucl. Phys. B **88**, 257 (1975).
- [24] Y. A. Golfand and E. P. Likhtman, JETP Lett. **13**, 323 (1971) [Pisma Zh. Eksp. Teor. Fiz. **13**, 452 (1971)].
- [25] M. A. Luty, hep-th/0509029.
- [26] J. Wess and B. Zumino, Nucl. Phys. B **70**, 39 (1974).
- [27] L. Girardello and M. T. Grisaru, Nucl. Phys. B **194**, 65 (1982).
- [28] S. Dimopoulos and L. J. Hall, Phys. Lett. B **207**, 210 (1988).
- [29] H. Goldberg, Phys. Rev. Lett. **50**, 1419 (1983) [Erratum-ibid. **103**, 099905 (2009)]; J. R. Ellis, J. S. Hagelin, D. V. Nanopoulos, K. A. Olive and M. Srednicki, Nucl. Phys. B **238**, 453 (1984).
- [30] S. Dimopoulos and D. W. Sutter, Nucl. Phys. B **452**, 496 (1995) [hep-ph/9504415].

- [31] H. E. Haber and R. Hempfling, Phys. Rev. Lett. **66**, 1815 (1991); J. R. Ellis, G. Ridolfi and F. Zwirner, Phys. Lett. B **257**, 83 (1991); Y. Okada, M. Yamaguchi and T. Yanagida, Prog. Theor. Phys. **85**, 1 (1991).
- [32] S. Heinemeyer, W. Hollik and G. Weiglein, Phys. Rept. **425**, 265 (2006) [hep-ph/0412214].
- [33] G. L. Kane, C. F. Kolda and J. D. Wells, Phys. Rev. Lett. **70**, 2686 (1993) [hep-ph/9210242]; J. R. Espinosa and M. Quiros, Phys. Lett. B **302**, 51 (1993) [hep-ph/9212305]; E. Accomando *et al.*, hep-ph/0608079.
- [34] J. Hisano, T. Moroi, K. Tobe, M. Yamaguchi and T. Yanagida, Phys. Lett. B **357**, 579 (1995) [hep-ph/9501407].
- [35] M. L. Brooks *et al.* [MEGA Collaboration], Phys. Rev. Lett. **83**, 1521 (1999) [hep-ex/9905013]; M. Ahmed *et al.* [MEGA Collaboration], Phys. Rev. D **65**, 112002 (2002) [hep-ex/0111030].
- [36] M. Dine, A. E. Nelson, Y. Nir and Y. Shirman, Phys. Rev. D **53**, 2658 (1996) [hep-ph/9507378].
- [37] G. F. Giudice, M. A. Luty, H. Murayama and R. Rattazzi, JHEP **9812**, 027 (1998) [hep-ph/9810442]; L. Randall and R. Sundrum, Nucl. Phys. B **557**, 79 (1999) [hep-th/9810155].
- [38] J. Wess and J. Bagger, *Supersymmetry and Supergravity*, (Princeton Univ. Press, 1992); D. Bailin and A. Love, *Supersymmetric Gauge Field Theory and String Theory*, (Institute of Physics Publishing, 1994); S. Weinberg, *The Quantum Theory*

- of Fields, Vol. 3: Supersymmetry*, (Cambridge University Press, 2000); M. Drees, R. Godbole and P. Roy, *Theory and Phenomenology of Sparticles*, (World Scientific, 2004); H. Baer and X. Tata, *Weak Scale Supersymmetry*, (Cambridge University Press, 2006); J. Terning, *Modern Supersymmetry: Dynamics and Duality* (Oxford University Press, 2006); M. Dine, *Supersymmetry and String Theory: Beyond the Standard Model* (Cambridge University Press, 2007).
- [39] M. E. Peskin, “Supersymmetry in Elementary Particle Physics,” arXiv:0801.1928 [hep-ph]; M.A. Luty, “2004 TASI lectures on supersymmetry breaking,” [hep-th/0509029]; I. Aitchison, “Supersymmetry and the MSSM: an elementary introduction,” [hep-ph/0505105].
- [40] J. R. Ellis, S. Kelley and D. V. Nanopoulos, Phys. Lett. B **260**, 131 (1991); U. Amaldi, W. de Boer and H. Furstenau, Phys. Lett. B **260**, 447 (1991); P. Langacker and M. -x. Luo, Phys. Rev. D **44**, 817 (1991); C. Giunti, C. W. Kim and U. W. Lee, Mod. Phys. Lett. A **6**, 1745 (1991).
- [41] R. N. Mohapatra, *Unification And Supersymmetry. The Frontiers Of Quark - Lepton Physics* (Springer-Verlag, New York 1992); G. G. Ross, *Grand Unified Theories* (Benjamin-Cummings, 1984).
- [42] T. Han, “The ‘Top Priority’ at the LHC,” Int. J. Mod. Phys. A **23**, 4107 (2008) [arXiv:0804.3178 [hep-ph]].
- [43] Z. Dong, T. Han, M. -x. Huang and G. Shiu, JHEP **1009**, 048 (2010) [arXiv:1004.5441 [hep-ph]].

- [44] For a review of string constructions prior to the second string revolution, see, e.g., B. Schellekens, “Superstring construction,” *Amsterdam, Netherlands: North-Holland (1989) 514 p. (Current physics - sources and comments)*; K. R. Dienes, “String Theory and the Path to Unification: A Review of Recent Developments,” *Phys. Rept.* **287**, 447 (1997) [arXiv:hep-th/9602045]; F. Quevedo, “Lectures on superstring phenomenology,” [arXiv:hep-th/9603074]; Z. Kakushadze, G. Shiu, S. H. H. Tye and Y. Vtorov-Karevsky, “A review of three-family grand unified string models,” *Int. J. Mod. Phys. A* **13**, 2551 (1998) [arXiv:hep-th/9710149]; and references therein.
- [45] G. L. Kane, P. Kumar and J. Shao, *J. Phys. G* **34**, 1993 (2007) [arXiv:hep-ph/0610038]; G. L. Kane, P. Kumar and J. Shao, “Unravelling Strings at the LHC,” *Phys. Rev. D* **77**, 116005 (2008) [arXiv:0709.4259 [hep-ph]]; J. J. Heckman, G. L. Kane, J. Shao and C. Vafa, “The Footprint of F-theory at the LHC,” [arXiv:0903.3609 [hep-ph]].
- [46] L. Aparicio, D. G. Cerdeno and L. E. Ibanez, “Modulus-dominated SUSY-breaking soft terms in F-theory and their test at LHC,” *JHEP* **0807**, 099 (2008) [arXiv:0805.2943 [hep-ph]].
- [47] J. P. Conlon, C. H. Kom, K. Suruliz, B. C. Allanach and F. Quevedo, “Sparticle Spectra and LHC Signatures for Large Volume String Compactifications,” *JHEP* **0708**, 061 (2007) [arXiv:0704.3403 [hep-ph]].
- [48] N. Arkani-Hamed, S. Dimopoulos and G. R. Dvali, “The hierarchy problem and

- new dimensions at a millimeter,” *Phys. Lett. B* **429**, 263 (1998) [arXiv:hep-ph/9803315]; I. Antoniadis, N. Arkani-Hamed, S. Dimopoulos and G. R. Dvali, “New dimensions at a millimeter to a Fermi and superstrings at a TeV,” *Phys. Lett. B* **436**, 257 (1998) [arXiv:hep-ph/9804398].
- [49] G. Shiu and S. H. H. Tye, “TeV scale superstring and extra dimensions,” *Phys. Rev. D* **58**, 106007 (1998) [arXiv:hep-th/9805157].
- [50] I. Antoniadis, “A Possible new dimension at a few TeV,” *Phys. Lett. B* **246**, 377 (1990).
- [51] J. D. Lykken, “Weak scale superstrings,” *Phys. Rev. D* **54**, 3693 (1996) [arXiv:hep-th/9603133].
- [52] L. Randall and R. Sundrum, “A large mass hierarchy from a small extra dimension,” *Phys. Rev. Lett.* **83**, 3370 (1999) [arXiv:hep-ph/9905221]; “An alternative to compactification,” *Phys. Rev. Lett.* **83**, 4690 (1999) [arXiv:hep-th/9906064].
- [53] H. L. Verlinde, “Holography and compactification,” *Nucl. Phys. B* **580**, 264 (2000) [arXiv:hep-th/9906182].
- [54] K. Dasgupta, G. Rajesh and S. Sethi, “M theory, orientifolds and G-flux,” *JHEP* **9908**, 023 (1999) [arXiv:hep-th/9908088].
- [55] B. R. Greene, K. Schalm and G. Shiu, “Warped compactifications in M and F theory,” *Nucl. Phys. B* **584**, 480 (2000) [arXiv:hep-th/0004103].
- [56] S. B. Giddings, S. Kachru and J. Polchinski, “Hierarchies from fluxes in string compactifications,” *Phys. Rev. D* **66**, 106006 (2002) [arXiv:hep-th/0105097].

- [57] S. Kachru, R. Kallosh, A. Linde and S. P. Trivedi, “De Sitter vacua in string theory,” *Phys. Rev. D* **68**, 046005 (2003) [arXiv:hep-th/0301240].
- [58] G. Shiu, R. Shrock and S. H. H. Tye, “Collider signatures from the brane world,” *Phys. Lett. B* **458**, 274 (1999) [arXiv:hep-ph/9904262].
- [59] S. Cullen, M. Perelstein and M. E. Peskin, “TeV strings and collider probes of large extra dimensions,” *Phys. Rev. D* **62**, 055012 (2000) [arXiv:hep-ph/0001166].
- [60] P. Burikham, T. Figy and T. Han, “TeV-scale string resonances at hadron colliders,” *Phys. Rev. D* **71**, 016005 (2005) [Erratum-ibid. *D* **71**, 019905 (2005)] [arXiv:hep-ph/0411094].
- [61] D. Chialva, R. Iengo and J. G. Russo, “Cross sections for production of closed superstrings at high energy colliders in brane world models,” *Phys. Rev. D* **71**, 106009 (2005) [arXiv:hep-ph/0503125].
- [62] D. Lust, S. Stieberger and T. R. Taylor, “The LHC String Hunter’s Companion,” [arXiv:0807.3333 [hep-th]].
- [63] L. A. Anchordoqui, H. Goldberg, D. Lust, S. Nawata, S. Stieberger and T. R. Taylor, “Dijet signals for low mass strings at the LHC,” [arXiv:0808.0497 [hep-ph]].
- [64] L. A. Anchordoqui, H. Goldberg, D. Lust, S. Nawata, S. Stieberger and T. R. Taylor, “LHC Phenomenology for String Hunters,” [arXiv:0904.3547 [hep-ph]].
- [65] D. Lust, O. Schlotterer, S. Stieberger and T. R. Taylor, “The LHC String Hunter’s Companion (II): Five-Particle Amplitudes and Universal Properties,” *Nucl. Phys. B* **828**, 139 (2010) [arXiv:0908.0409 [hep-th]].

- [66] L. A. Anchordoqui, H. Goldberg, S. Nawata and T. R. Taylor, “Jet signals for low mass strings at the LHC,” *Phys. Rev. Lett.* **100**, 171603 (2008) [arXiv:0712.0386 [hep-ph]].
- [67] L. A. Anchordoqui, H. Goldberg, S. Nawata and T. R. Taylor, “Direct photons as probes of low mass strings at the LHC,” *Phys. Rev. D* **78**, 016005 (2008) [arXiv:0804.2013 [hep-ph]].
- [68] L. A. Anchordoqui, H. Goldberg and T. R. Taylor, “Decay widths of lowest massive Regge excitations of open strings,” [arXiv:0806.3420 [hep-ph]].
- [69] P. Meade and L. Randall, “Black Holes and Quantum Gravity at the LHC,” *JHEP* **0805**, 003 (2008) [arXiv:0708.3017 [hep-ph]].
- [70] B. Hassanain, J. March-Russell and J. G. Rosa, “On the possibility of light string resonances at the LHC and Tevatron from Randall-Sundrum throats,” [arXiv:0904.4108 [hep-ph]].
- [71] R. Blumenhagen, M. Cvetič, P. Langacker and G. Shiu, “Toward realistic intersecting D-brane models,” *Ann. Rev. Nucl. Part. Sci.* **55**, 71 (2005) [arXiv:hep-th/0502005].
- [72] R. Blumenhagen, B. Kors, D. Lust and S. Stieberger, “Four-dimensional String Compactifications with D-Branes, Orientifolds and Fluxes,” *Phys. Rept.* **445**, 1 (2007) [arXiv:hep-th/0610327].
- [73] F. Marchesano, “Progress in D-brane model building,” *Fortsch. Phys.* **55**, 491 (2007) [arXiv:hep-th/0702094].

- [74] D. Malyshev and H. Verlinde, “D-branes at Singularities and String Phenomenology,” Nucl. Phys. Proc. Suppl. **171**, 139 (2007) [arXiv:0711.2451 [hep-th]].
- [75] P. Burikham, T. Han, F. Hussain and D. W. McKay, “Bounds on four fermion contact interactions induced by string resonances,” Phys. Rev. D **69**, 095001 (2004) [arXiv:hep-ph/0309132].
- [76] I. I. Y. Bigi, Y. L. Dokshitzer, V. A. Khoze, J. H. Kuhn and P. M. Zerwas, “Production and Decay Properties of Ultraheavy Quarks,” Phys. Lett. B **181**, 157 (1986).
- [77] F. Cornet, J. I. Illana and M. Masip, “TeV strings and the neutrino nucleon cross section at ultra-high energies,” Phys. Rev. Lett. **86**, 4235 (2001) [arXiv:hep-ph/0102065].
- [78] J. J. Friess, T. Han and D. Hooper, “TeV string state excitation via high energy cosmic neutrinos,” Phys. Lett. B **547**, 31 (2002) [arXiv:hep-ph/0204112].
- [79] ATLAS Collaboration, ” Detector and Physics Performances Technical Design Report,” Vol.II, ATLAS TDR 14, CERN/LHCC 99-14; CMS Physics TDR, Volume II: CERN-LHCC-2006-021, 25 June 2006 As published in J. Phys. G: Nucl. Part. Phys. **34**, 995 (2006)
- [80] V. Barger, T. Han and D. G. E. Walker, “Top Quark Pairs at High Invariant Mass - A Model-Independent Discriminator of New Physics at the LHC,” Phys. Rev. Lett. **100**, 031801 (2008) [arXiv:hep-ph/0612016].

- [81] R. M. Godbole, S. D. Rindani, K. Rao, R. K. Singh, “Top polarization as a probe of new physics,” AIP Conf. Proc. **1200**, 682 (2010) [arXiv:0911.3622 [hep-ph]].
- [82] D. E. Kaplan, K. Rehermann, M. D. Schwartz and B. Tweedie, “Top-tagging: A Method for Identifying Boosted Hadronic Tops,” Phys. Rev. Lett. **101**, 142001 (2008) [arXiv:0806.0848v2[hep-ph]].
- [83] J. Thaler and L.-T. Wang, “Strategies to Identify Boosted Tops,” JHEP **0807**, 092 (2008) [arXiv:0806.0023v2[hep-ph]].
- [84] M. Reece and L. T. Wang, “Randall-Sundrum and Strings,” [arXiv:1003.5669 [hep-ph]].
- [85] M. Perelstein and A. Spray, “Tensor Reggeons from Warped Space at the LHC,” JHEP **0910**, 096 (2009) [arXiv:0907.3496 [hep-ph]].
- [86] G. Shiu, B. Underwood, K. M. Zurek and D. G. E. Walker, “Probing the Geometry of Warped String Compactifications at the LHC,” Phys. Rev. Lett. **100**, 031601 (2008) [arXiv:0705.4097 [hep-ph]].
- [87] P. McGuirk, G. Shiu and K. M. Zurek, “Phenomenology of Infrared Smooth Warped Extra Dimensions,” JHEP **0803**, 012 (2008) [arXiv:0712.2264 [hep-ph]].
- [88] F. Marchesano, P. McGuirk and G. Shiu, “Open String Wavefunctions in Warped Compactifications,” JHEP **0904**, 095 (2009) [arXiv:0812.2247 [hep-th]].
- [89] G. Shiu, G. Torroba, B. Underwood and M. R. Douglas, “Dynamics of Warped Flux Compactifications,” JHEP **0806**, 024 (2008) [arXiv:0803.3068 [hep-th]].

- [90] M. R. Douglas, “Effective potential and warp factor dynamics,” JHEP **1003**, 071 (2010) [arXiv:0911.3378 [hep-th]].
- [91] O. DeWolfe and S. B. Giddings, “Scales and hierarchies in warped compactifications and brane worlds,” Phys. Rev. D **67**, 066008 (2003) [arXiv:hep-th/0208123].
- [92] S. B. Giddings and A. Maharana, “Dynamics of warped compactifications and the shape of the warped landscape,” Phys. Rev. D **73**, 126003 (2006) [arXiv:hep-th/0507158].
- [93] C. P. Burgess, P. G. Camara, S. P. de Alwis, S. B. Giddings, A. Maharana, F. Quevedo and K. Suruliz, “Warped supersymmetry breaking,” JHEP **0804**, 053 (2008) [arXiv:hep-th/0610255].
- [94] Z. Dong, G. Durieux, J. -M. Gerard, T. Han and F. Maltoni, Phys. Rev. D **85**, 016006 (2012) [Phys. Rev. D **85**, 039907 (2012)] [arXiv:1107.3805 [hep-ph]].
- [95] G. ’t Hooft, Phys. Rev. Lett. **37**, 8 (1976).
- [96] S. Weinberg, Phys. Rev. D **26**, 287 (1982).
- [97] H. Georgi and S. L. Glashow, Phys. Rev. Lett. **32**, 438 (1974).
- [98] J. D. Bekenstein, Phys. Rev. D **5**, 1239 (1972).
- [99] A. D. Sakharov, JETP Lett. **5**, 27 (1967) [Pisma Zh. Eksp. Teor. Fiz. **5**, 36 (1967)].
- [100] K. Nakamura *et al.* [Particle Data Group Collaboration], J. Phys. G G **37**, 075021 (2010).

- [101] J. Andrea, B. Fuks and F. Maltoni, Phys. Rev. D **84**, 074025 (2011) [arXiv:1106.6199 [hep-ph]].
- [102] J. F. Kamenik and J. Zupan, Phys. Rev. D **84**, 111502 (2011) [arXiv:1107.0623 [hep-ph]].
- [103] S. Weinberg, Phys. Rev. Lett. **43**, 1566 (1979).
- [104] F. Wilczek and A. Zee, Phys. Rev. Lett. **43**, 1571 (1979).
- [105] L. F. Abbott and M. B. Wise, Phys. Rev. D **22**, 2208 (1980).
- [106] I. Dorsner and P. Fileviez Perez, Phys. Lett. B **625**, 88 (2005) [hep-ph/0410198].
- [107] A. Denner, H. Eck, O. Hahn and J. Kublbeck, Nucl. Phys. B **387**, 467 (1992).
- [108] J. Pumplin, D. R. Stump, J. Huston, H. L. Lai, P. M. Nadolsky and W. K. Tung, JHEP **0207**, 012 (2002) [hep-ph/0201195].
- [109] J. Alwall, M. Herquet, F. Maltoni, O. Mattelaer and T. Stelzer, JHEP **1106** (2011) 128 [arXiv:1106.0522 [hep-ph]].
- [110] N. D. Christensen and C. Duhr, Comput. Phys. Commun. **180** (2009) 1614 [arXiv:0806.4194 [hep-ph]].
- [111] T. Plehn, G. P. Salam and M. Spannowsky, Phys. Rev. Lett. **104**, 111801 (2010) [arXiv:0910.5472 [hep-ph]].
- [112] W. -S. Hou, M. Nagashima and A. Soddu, Phys. Rev. D **72**, 095001 (2005) [hep-ph/0509006].